พฤติกรรมของโครงสร้างท่าเรือภายใต้แรงสึนามิ

นายราโดสลอว์ โรเบิร์ต ลูบิคคี

วิทยานิพนธ์นี้เป็นส่วนหนึ่งของการศึกษาตามหลักสูตรปริญญาวิศวกรรมศาสตรมหาบัณฑิต
สาขาวิชาวิศวกรรมโยธา ภาควิชาวิศวกรรมโยธา
คณะวิศวกรรมศาสตร์ จุฬาลงกรณ์มหาวิทยาลัย
ปีการศึกษา 2558

Behavior of port structures under tsunami loading

Mr. Radoslaw Robert Lubiecki

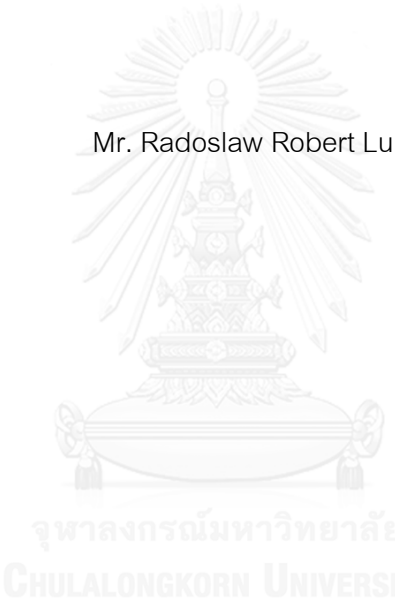

A Thesis Submitted in Partial Fulfillment of the Requirements

for the Degree of Master of Engineering Program in Civil Engineering

Department of Civil Engineering

Faculty of Engineering

Chulalongkorn University

Academic Year 2015

Thesis Title	Behavior of port structures under tsunami loading
By	Mr. Radoslaw Robert Lubiecki
Field of Study	Civil Engineering
Thesis Advisor	Associate ProfessorAnat Ruangrassamee, Ph.D.

Accepted by the Faculty of Engineering, Chulalongkorn University in Partial Fulfillment of the Requirements for the Master's Degree

.....Dean of the Faculty of Engineering

(ProfessorSupot Teachavorasinskun, Ph.D.)

THESIS COMMITTEE

.....Chairman

(Associate ProfessorTospol Pinkaew, Ph.D.)

.....Thesis Advisor

(Associate ProfessorAnat Ruangrassamee, Ph.D.)

.....Examiner

(Assistant ProfessorChatpan Chintanapakdee, Ph.D.)

.....External Examiner

(Piyawat Foytong, Ph.D.)

ราโดสลอว์ โรเบิร์ต ลูบิคคี : พฤติกรรมของโครงสร้างท่าเรือภายใต้แรงสึนามิ (Behavior of port structures under tsunami loading) อ.ที่ปรึกษาวิทยานิพนธ์หลัก: รศ. ดร. อาณัติ เรืองรัศมี, 97 หน้า.

ท่าเรือสำหรับ LPG และ LNG ประกอบด้วยแท่น ดอลฟิน และสะพานเชื่อม โดยโครงสร้างเหล่านี้จะตั้งอยู่ใกล้ชายฝั่งเพื่อรับเรือขนาดใหญ่ โครงสร้างนี้โดยส่วนใหญ่ไม่ได้มีสิ่งป้องกันสึนามิที่อาจเกิดขึ้น จากเหตุการณ์สึนามิในมหาสมุทรอินเดียในปี ค.ศ. 2004 ได้เกิดความเสียหายกับโครงสร้างในทะเลหลายแห่ง การศึกษาผลกระทบและวิธีการบรรเทาผลกระทบจึงเป็นสิ่งจำเป็น ในการศึกษานี้ได้ทำการวิเคราะห์ผลตอบสนองของโครงสร้างท่าเรือภายใต้แรงจากสึนามิ ในการวิเคราะห์ได้พิจารณาแรงอุทกพลวัตและแรงลอยตัวด้วยวิธียืดหยุ่นเชิงเส้น ความสูงและความเร็วของสึนามิได้มีการรวบรวมจากการศึกษาในอดีตเพื่อเลือกช่วงของค่าที่เหมาะสม โดยพิจารณาความสูง 1-3 เมตร และ ความเร็ว 1-3 m/s จากการวิเคราะห์ได้พิจารณาระยะเคลื่อนตัวด้านข้างและแรงภายในเสาเข็ม ผู้วิจัยได้ศึกษาผลของพารามิเตอร์ของโครงสร้างและสึนามิที่มีต่อพฤติกรรมของโครงสร้าง และได้ศึกษาผลของมุมเอียงของเสาเข็มตั้งแต่ 1:32 ถึง 1:3 โดยพบว่าเสาเข็มเอียงช่วยลดการเคลื่อนตัวด้านข้างและแรงดัดได้อย่างมีนัยสำคัญแต่ทำให้มีการเพิ่มขึ้นของแรงในแนวแกน

ภาควิชา วิศวกรรมโยธา ลายมือชื่อนิสิต .....

สาขาวิชา วิศวกรรมโยธา ลายมือชื่อ อ.ที่ปรึกษาหลัก .....

ปีการศึกษา 2558

5770527021 : MAJOR CIVIL ENGINEERING

KEYWORDS: PORT STRUCTURES / TSUNAMI / LOADING

RADOSLAW ROBERT LUBIECKI: Behavior of port structures under tsunami loading. ADVISOR: ASSOC. PROF.ANAT RUANGRASSAMEE, Ph.D., 97 pp.

LPG and LNG terminals consist of loading platform, dolphins, jetties and trestles. Since these structures are required to berth large vessels for loading and unloading of the cargo they are located in near shore area. Due to that often terminals or parts of it are constructed with limited or no protection against tsunamis. After the 2004 Indian Ocean tsunami, severe damage to marine structures has been observed in many affected areas. In order to better understand responses of port structures during tsunami, an analysis of the berthing dolphin, mooring dolphin and loading platform is conducted. Behavior of port structures under hydrodynamic drag forces and buoyant forces is analyzed using linear elastic models. Tsunami amplitude and current velocity are chosen based on previous simulations and observed data. Tsunami amplitude between 1-3m and tsunami velocity between 1-3 m/s are considered in the analysis. Top deck displacement and internal forces in piles are compared and discussed. Effects of the structural and tsunami parameters on structure behavior are reported. An effect of utilization of batter piles with rake from 1:32 to 1:3 is studied. It is observed that using batter piles reduces displacement and bending moment values, however increases axial forces. For the mooring dolphin with piles raked 1:4, reduction of displacement is equal to 82% and reduction of bending moment is equal to 60% of the values of structure supported only by vertical piles.

Department:	Civil Engineering	Student's Signature	.....
Field of Study:	Civil Engineering	Advisor's Signature	.....
Academic Year:	2015		

ACKNOWLEDGEMENTS

CONTENTS

Page

Page

Page

1. Introduction

1.1. Problem statement

A tsunami is a naturally occurring series of ocean waves resulting from a rapid, large-scale disturbance in a body of water. They cause severe destruction and loss of lives even at locations far from their source.

On 26 December 2004 an earthquake of magnitude Mw=9.0 struck near the Sumatra and generated a massive tsunami which affected countries such as: Indonesia, Thailand, India and Sri Lanka. This disaster killed over 230 000 people in 14 countries and inundated coastal regions with waves up to 30 meters. It resulted also in complete destruction of buildings, roads and marine structures.

It was one of the most tremendous in loss tsunami event in the history of humanity. However every year tsunamis occur around the world. With modern technology and early warning system it is much easier to save human lives. However there is also need to prevent damage to engineering structures and especially marine structures. Port structures are often facing open sea. Due to that they are vulnerable to damage caused by these extreme waves. In the recent years more researches and observations have been made in order to better understand the behavior of tsunami and more accurately estimate forces acting on the structures located in ports.

Figure 1.1 Damage to Khao Lak Harbor (Saatcioglu M. et al. 2006)

After the 2004 Indian Ocean Tsunami numerous port structures have been damaged or destroyed. Figure 1 and 2 presents Khao Lak Harbor and Nagapattinam

harbor, respectively. Most of the damage was caused by the water flowing around the structure and washing away soil under foundation.

Figure 1.2 (a) Damage to a wharf at the Nagapattinam harbor. (b) Base of an oil tank damaged by erosion; sandbags were temporarily placed to support the tank. (Makeshwari B. K. et al., 2006)

A bridge located in the harbor over the Palyar River was destroyed. Due to drag and uplift forces of tsunami wave all four spans of the bridge were washed away. Two of them were still missing at the time of survey.

Figure 1.3 Damaged Keelamanakudy Bridge on the Palyar River: (a) substructure of the bridge all four spans washed away; (b) a span that washed about 20 m away. (Makeshwari B. K. et al., 2006)

On Andaman Islands structures which were facing open sea at the time of the tsunami were damaged. Due to high lateral loading corresponding to earthquake and tsunami waves berthing jetty collapsed and during the time of the survey was completely under water. Additionally pounding damage caused by lateral displacement of the top deck of approach has been observed.

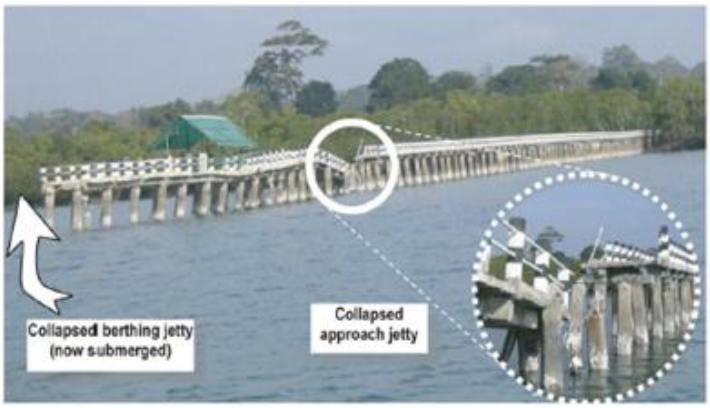

Figure 1.4 Gandhinagar jetty in North Andaman: Total collapse of the berthing jetty and partial collapse of the approach jetty, (Goutam Mondal, Durgesh C. Rai, 2006)

In Thailand, in the fishing port Phang-Nga in Ban Nam Kem Village a piled jetty structure in was severely damaged due to excessive uplift pressure. Main reason behind this damage is that uplift pressure was not considered during the design process. The most damaged were precast reinforced concrete slabs. Moreover extensive cracks formed due to the reversed moment and pull-out from support of slab members. Similar damage has been observed in the Khao Lak Harbor.

Figure 1.4 Damage to pier deck on Ban Num Kem Port, (a) joint failure, (b) failure of precast concrete slabs (Lukkunaprasit Panitan, and Ruangrassamee Anat ,2008)

Figure 1.5 Damage to precast slab strips of the concrete dock in Khao Lak Harbor

Most of these damages were observed after one tsunami event. There is insufficient number of research on near shore port structures such as jetties, wharfing dolphins and loading platforms. Recent events showed that these structures often take extreme damage and fails during the tsunami events. To prevent and reduce damage caused in the future, an understanding of port structures responses under tsunami loading is needed. In order to better understand the nature of loading acting on marine structures during tsunami an analysis is proposed in this study.

1.2. Objectives

Mooring dolphins, breasting dolphins and loading platform are often exposed to wave loading, however insufficient number of research has been done in that area. Therefore, objectives of this study are as:

- To study near shore structures behaviors and responses under tsunami loading.
- To numerically model the interaction between tsunami wave and near shore structures: platform and dolphins.
- To observe the performance of the structures with different configurations of batter and vertical piles.

1.3. Scope

Scope of this study is defined as below:

- analyzed structure are as follow: mooring dolphin, breasting dolphin and loading platform
- responses of port structures are analyzed and observed by static analysis of 3-dimensional linear elastic model using SAP2000
- tsunami amplitude and current velocity is based on an articles, no propagation of tsunami wave will be simulated

2. Literature review

2.1. Port structures

Port structures are a group of structures and facilities, which are built in the marine environment such as coastal areas. The name itself describes structures such as: jetties, wharves, dry docks, dolphins and quay walls. This research is focused only on the responses of mooring dolphin, breasting dolphin and loading platform. These structures are generally used in petroleum gas and liquid natural terminals. They are required to berth large vessels for loading and unloading of the cargo and are usually located in deep water with limited or no protection against waves and especially tsunamis..

2.1.1. Offshore jetties and loading platforms

An offshore jetty or pier is a dock structure that typically projects outward nearly perpendicular to the shoreline. It is a free-standing structure, connected at one end to the shore. It allows vessels to berth along both sides. Sometimes it may be constructed as T or L configuration.

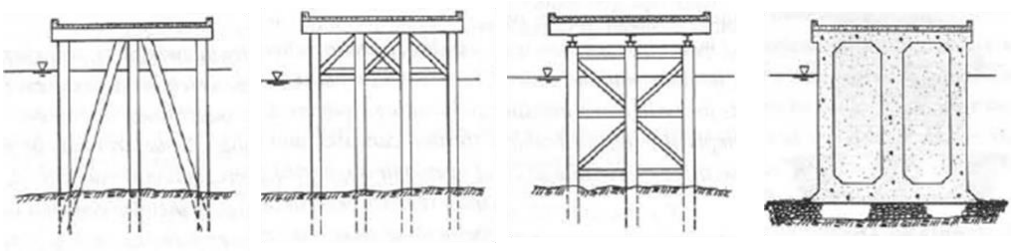

Figure 2.1- Different types of piers. From the left: batter pile, braced, jacket, concrete caisson (Gaythwaite John, 2004)

The most common construction consists of a pile foundation of timber, concrete or steel piles supporting a deck, made of timber or concrete. In order to resist lateral loads a deck may be designed in different ways, for example with the usage of batter piles or by being rigidly cross-braced.

Loading platform is a kind of jetty structure which supply conveyor equipment and hose towers for vessels, particularly at oil and bulk cargo terminal. These platforms are designed in the same way as pier or dolphins with the exception that lateral loads are typically lower. Since platform supports pipelines and conveyors it is crucial that movement of the structure does not produce excessive stresses in them. That is why platform structures should not be too flexible.

2.1.2. Dolphins

Name dolphins refer to solitary structures used primarily to accommodate the lateral forces associated with vessel berthing and mooring. This kind of structure is commonly used at the jetties, especially those at bulk handling terminals. Berthing or breasting dolphins are designed mainly to absorb the impact of berthing ships, while mooring dolphins are designed strictly to secure a vessel's mooring lines. Figure 2.2 presents localization of the dolphins along a jetty.

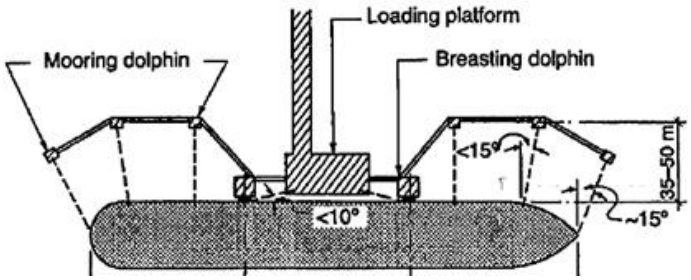

Figure 2.2- Location of dolphins along a loading platform (Thoresen Carl, 2003)

Dolphin structural types vary greatly with vessel size, water depth and water condition and range from simple timber pile clusters to deep water steel jacket structures. Dolphins are categorized by their structural stiffness into two groups: flexible and rigid. Typically both types of structure consist of group of piles, that's why the resistance to uplift caused by horizontal loading should receive particular attention. Flexible dolphin structure usually consists of a group of vertical piles built into a heavy concrete cap or a braced frame and deck. By the horizontal displacement of the pile heads, the flexible dolphin absorbs kinetic energy of the berthing vessel. Generally for flexible dolphins' piles one uses tubes made of high yield steel, which are suitable on account of energy absorbing properties and high strength.

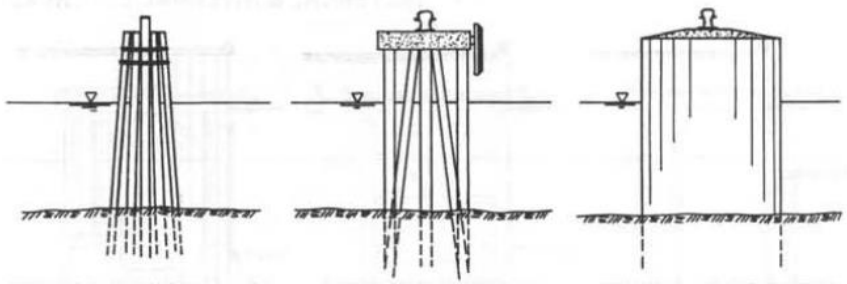

Figure 2.3 Dolphin structural types. From the left: timber pile cluster, concrete cap, cellular (Gaythwaite John, 2004)

Rigid dolphin structures may be either open-piled or solid construction. The most common type is a raking pile structure. For maximum efficiency rake of the piles should be as large as possible, without obstruction of the water passage. Some of the piles usually need to resist uplift forces. If it is not possible to achieve required resistance by traditional methods it is advised to install a rock anchor through the pile. Generally rigid dolphin structures are built into massive concrete cap, which is commonly 1.5-2.5m thick. It serves to ensure rigidity, disperse concentrated loads and reduce net uplift on the structure.

2.1.3. Piles foundation in port structures

Piles are deep foundation elements installed by driving or by drilling-and-grouting. Generally piles that are used under marine structures are subjected to high

lateral loads. For use as foundations in deep water, steel pipe sections are the most commonly used pile types.

In order to better resist lateral loads and reduce lateral movements of offshore structures batter piles or raked piles are employed. These piles usually are usually angled at ratio batter ranging from 1:12 to 1:3. Shallower batters are usually avoided because of the large bending stresses they induce. The main advantage of using batter piles is dramatic reduction in pier deflections. Research shows that even a relatively shallow batter of 1:12 may reduce overall deflections some 40% or more over only vertical piles.

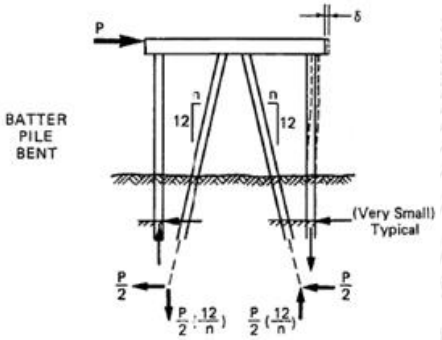

Figure 2.4- Pile bent configuration for resisting lateral loads (V.N.S. Murthy, 2007)

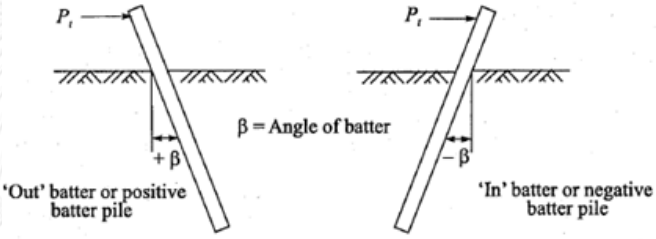

Figure 2.5 Types of batter piles (V.N.S. Murthy, 2007)

Generally batter piles are driven in opposite direction and coupled. This way when one pile acts in tension the other one acts in compression.

Disadvantage of using batter piles is that they are susceptible to down drag forces. Due to this and sloped pile configuration, large bending stresses may be introduced into the pile shaft.

2.2. Tsunami forces acting on port structures

Port structures are located in coastal area, often directly exposed to the open sea. Due to that they are the most susceptible to tsunami waves. It is difficult to predict the forces from the tsunami events, because of the random nature of that wave. Often port structures are first damaged by an earthquake and then completely destroyed by

the following tsunami. After tsunamis and earthquakes in 2004 and 2011 many researches and experiments has been conducted in order to improve the accuracy of evaluation of tsunami forces acting on port structures.

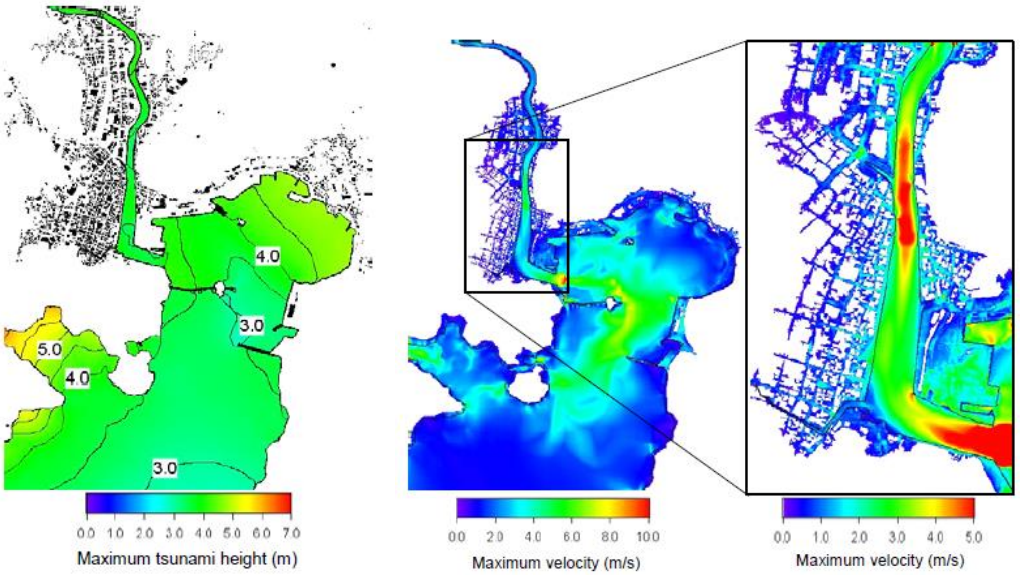

Figure 2.5 Numerical simulation of tsunami intrusion. (PIANC 2009)

Figure 2.5 shows the interaction between tsunami, harbor facilities and topography. The tsunami height near the breakwater zone was equal to about 3m. Since the entrance to the port is not narrow enough, the tsunami height is not reduced by the presence of breakwaters. The highest water level may be observed in areas surrounding quays and other harbor structures. This is due to the effect of wave reflection. It may be seen that behavior of wave depends on both the opening section of the breakwater and water area in the port. If a water area in port is small, water level raises quickly. If inundation exceeds the ground level of the port, it results in drifting and floating of vessels, tanks and containers. If the wave velocity is high it may cause severe damage since floating objects will induce additional impact forces. Total damage inflicted by tsunami wave greatly depends on the wave height. A 2m high wave may not cause any major disaster however wave height exceeding 8m becomes destructive.

In the Indonesia, the 2004 Sumatera Earthquake hit the worst Aceh area. Surveys conducted after the event showed that many buildings in that zone failed to meet the safety criteria against tsunamis and earthquake.

Ulee Lheue Port was one of the ports which were greatly damaged by the tsunami. Figure 2.6 shows the scale of damage caused to port by tsunami wave. It can be seen that parts of the dyke were destroyed by the impact of the wave. Tsunami inundated over 50% of the area and resulted in soil erosion during the event. Due to that many structures located in the port, settled.

Figure 2.9 Ulee Lheue Port - Photos of the port before and after the event (on the left before the earthquake, on the right after) (Mitigation of tsunami disasters in ports, PIANC 2009)

2.2.1. Observations and surveys of port damage caused by tsunami wave

Tomita T., et al. (2006) surveyed damage caused to the structures by the 2004 Indian Ocean Tsunami on the southwestern coast of Sri Lanka. At the Galle Port tsunami inundation height was estimated to be around 6 m, based on the watermarks found on the exterior walls of port office building. The quay located at the port suffered damage caused by hydrostatic uplift and drag forces as shown in the figure 2.10.

Figure 2.10 Damage to the quay in the innermost area of the Galle Port. (Tomita T., et al. 2006)

Makeshwari B. K. et al. (2006) studied structures in Tami Nadu, India after 2004 Indian Ocean Tsunami. Harbor structures in the city of Nagapatinam experienced severe damage. Tsunami run up in that city was in the range of 10-12 m. cylindrical oil

tank suffered exposure of foundation by soil erosion. Keelamanakudy Bridge over the Palyar River was destroyed. All four spans of the bridge were washed away. Of span was washed away 20 meters, second one 50 meters. While spans where washed away and separated from the pile foundation, the substructure suffered no significant damage. Observation showed that bearing failure caused span displacements.

Damage to jetty of Colachal harbor was not observed. Some soil around the foundation were scoured, however not excessive amount. Authors compared jetty structure with previously noted bridge structure. It appears that jetty superstructure and substructure were integrated which resulted in resisting tsunami fluid forces.

Figure 2.11 (a) Substructure of the jetty at Colachal harbor, in Kanyakumari; the jetty remained intact. (b) Close-up of the jetty foundation, which was resting on piles. (Makeshwari B. K. et al., 2006)

Lukkunaprasit and Ruangrassamee (2008) conducted a survey on building damage in Thailand in the 2004 Indian Ocean tsunami. A piled jetty structure in fishing port Phang-Nga in Ban Nam Kem Village was severely damaged due to excessive uplift pressure. Since uplift pressure was not considered during the design the beam-column-joint were partly destroyed.

The most damaged were precast reinforced concrete slabs. Huge amount of water caused an extreme uplift pressure for which the deck hasn't been designed. Moreover extensive cracks formed due to the reversed moment and pull-out from support of slab members.

Figure 2.12Damage to pier deck on Ban Num Kem Port, (a) joint failure, (b) failure of precast concrete slabs (Lukkunaprasit Panitan, and Ruangrassamee Anat ,2008)

PIANC (2009) noted that during the 2004 Sumatra earthquake and tsunami, despite the fact that the Ulee Lheue Port was severely damaged dolphins for power generator barge hasn't been damaged, even though the barge itself has been displaced to a distance about 3 km.

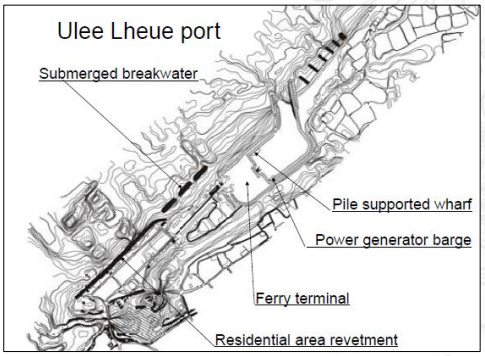

Figure 2.13 Plan of Ulee Lheue Port (PIANC 2009)

Figure 2.14 - Dolphins at Ulee Lheue (PIANC 2009)

Observation of damages after the tsunami showed that pile-deck structures such as dolphins, wharves and ferry terminal were more resistant to tsunami related damage than other structure. Most damage was caused by the drifting object's impact forces and scouring.

2.3. Tsunami flow velocity and amplitude

Since run-up height, inundation height and tsunami forces are related to tsunami flow velocity it is one of the most important parameters of the tsunami wave. Many researches and surveys have been conducted to accurately calculate the tsunami

forces and flow velocity. Most of the current data comes from numerical simulations and experiments.

2.3.1. Theory

Shen and Meyer (1963) based on Ho and Meyer (1962) research provided an exact solution for the run up of incident bore. Assumptions for this solution are as following: beach with uniform slope, fully nonlinear shallow-water-wave theory and one-dimensional problem. Then maximum flow velocity may at the leading bore can be calculated by:

$$u = \sqrt{2gx \tan \alpha}$$

Where:

α – beach slope

g – gravitational acceleration

x - the distance from the maximum run-up location to the location of interest

Yeh (2007) further studied above equation. His research provided data that this equation may be used to obtain upper-limit range of the flow velocity for all incident tsunami forms. Since beach slope is seldom uniform he proposed an improved equation, which is the function of the ground elevation, instead of distance as follows:

$$u_{max} = \sqrt{2gR(1 - \frac{z}{R})}$$

Where:

R - ground elevation at the maximum penetration of tsunami run-up, measured from the initial shoreline

z - ground elevation of the location of interest, measured from the initial shoreline level

Additionally, based on Peregrine and Williams (2001) equation for the temporal and spatial variations in fluid velocity and flow depth of the incident bore run-up in the vicinity of the leading run-up tip, Yeh (2007) proposed new equation with different scaling as follows:

$$\eta = \frac{1}{36\tau}(2\sqrt{2}\tau - \tau^2 - 2\xi)^2$$

And:

$$\nu = \frac{1}{3\tau}(\tau - \sqrt{2}\tau^2 + \sqrt{2}\xi)$$

Where:

$$\eta = \frac{d}{R}; \nu = \frac{u}{\sqrt{2gR}}; \tau = t\,tan\,\alpha\sqrt{\frac{g}{R}}; \xi = \frac{z}{R}$$

d – water depth,

R – ground elevation at the maximum penetration of tsunami run-up, measured from the initial shoreline,

u – flow velocity

g – gravitational acceleration

α – beach slope,

t – time: 0 when the bore passes at the initial shoreline

z – ground elevation of the location of interest, measured from the initial shoreline

It has been proved many times that for all types of tsunami formations, for the same configuration bore formation will yield fastest flow velocity. That's why above equations can be used for estimation of maximum flow velocity at a location of interest for a given flow depth. By combining equations and eliminating τ, figure 2.14 can be obtained.

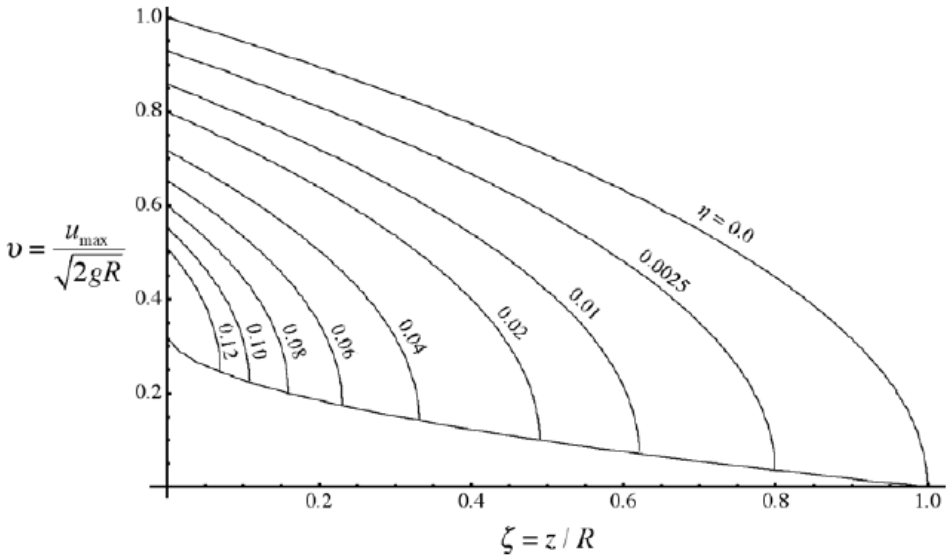

Figure 2.14 - Maximum flow velocity of depth, d, at the ground elevation, z, and maximum run-up elevation, R. The bottom curve represents the lower limit of maximum flow velocity. (Yeh,2007)

The curve on the bottom represents lower limit of maximum flow velocity for a given depth, d. However since this figure show results for a uniform incident bore and local inundation depth of other tsunami forms usually exceeds that of bore run-up, the maximum flow velocity is generally lower than that presented by the limit curve.

Matsutomi and Okamoto (2010) proposed the equation based on relationship between inundation flow velocity and inundation depth. In their report they have collected data from past event. Based on this data the estimation for tsunami flow velocity was made using Bernoulli's theorem. Additionally to check the accuracy of the obtained results an experiment on inundations flow velocity has been conducted. Tsunami flow velocities were calculated using following equation:

$$u = \sqrt{2g(h_f - h_r)}$$

Where:

g- gravitational acceleration

h_f- inundation depths at the front of the structure

h_r-inundation depths at the back of the structure

Proposed tsunami velocity ranges from $0.7\sqrt{gh_r)}$ to $2.0\sqrt{gh_r)}$. Figure 2.1.1 presents these velocities, where R is a tsunami height or a nearest tsunami run-up height from the sea level.

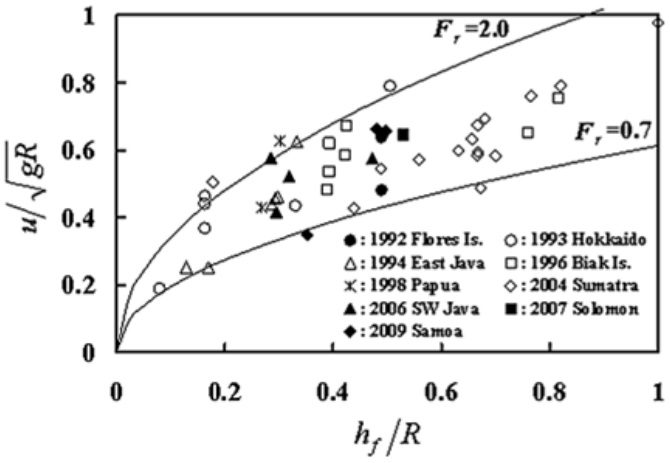

Figure 2.17 - Relationship between nondimensionalized inundation depth and inundation flow for the case used with inundation depth used on the back side (Matsutomi and Okamoto, 2010)

2.3.2. Observation

Tsutsumi A. et al (2002) studied the tsunami flow velocity after Southwest Hokkaido earthquake on July 12,1993. The survey was conducted at Aonae on the southern end of Okurishi Island, Japan. Then the flow velocity was estimated based on the forces exerted on damaged structures along the coast. In order to predict the forces induced by current Morison's equation was used. Total moment of tsunami force MT exerted on a pole was given by:

$$M_2 = \sin^2\theta \frac{\rho}{2} C_D' u^2 h_2 A$$

Where:

θ – angle between the vertical pole and base of stairs

ρ – fluid density

C_D' - drag coefficient

u – flow velocity along horizontal axis

h_2 – height of the center of the plate

A – area of horizontal plate of unit length (2m)

An experiment has been conducted in order to obtain the yield stress of iron handrail and bent iron guardrail. The results in the strength tests indicated that maximum tsunami velocity for the tsunami arriving from the northeast direction was in the range of 10 - 18m/s.

EERI Special Earthquake Report (2011) presents results of tsunami flow velocities in Sendai, during the 2011 Tohoku earthquake and tsunami. Since it happened during the daylight it was captured on video by numerous sources. This provided an unprecedented opportunity to analyze tsunami flow conditions using video and field evidence, such as video footage from helicopter. Research team was able to calculate the tsunami flow traveling up the Natori River south of Sendai. This is however in-land tsunami flow speed.

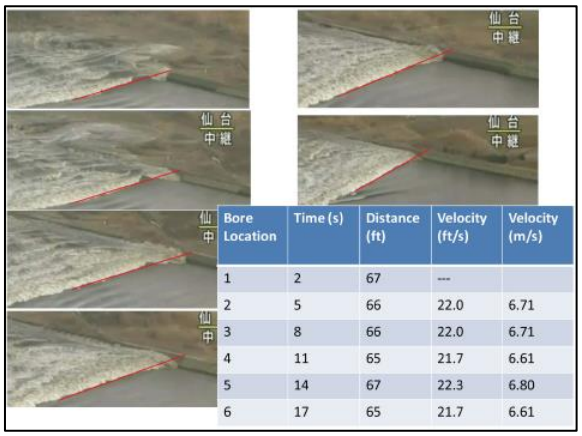

Bore Location	Time (s)	Distance (ft)	Velocity (ft/s)	Velocity (m/s)
1	2	67	---	
2	5	66	22.0	6.71
3	8	66	22.0	6.71
4	11	65	21.7	6.61
5	14	67	22.3	6.80
6	17	65	21.7	6.61

Figure 2.18 - Analysis of river bore velocity (EERI Special Earthquake Report , 2011)

Result showed that generally flow velocities, that damaged engineered structures varied from 5 to 8 m/s. The average velocities were 6.7 m/s for bore in the Natori River and 6.3 m/s for the case on a farmland. The tsunami inundation depth for the river was observed to be around 1.2m. Its flow velocity in term of the inundation depth is 1.94 gh .

Lynett et al. (2014) gathered surveys in order to obtain data from observation and then based on it modeled current induced by the 2011 Tohoku and 2004 Indian Ocean tsunami. Observations showed that even remote tsunamis may induce strong current. In the Port of Salalah in Oman after 2004 Indian Ocean Tsunami numerical simulations based on the damages in port have been researched. Results showed that current flow velocity in the harbor was between 4-5m/s, while maximum tsunami elevation was around 1.5 m. After earthquake in Chile in February 2010 current speed up to 8 m/s in docks in San Diego, Catalina Island, Ventura, and Santa Cruz have been observed and recorded. After the Tohoku tsunami current speed at was estimated at inner harbor of Crescent City in California, USA. Tsunami flow velocity was estimated to be in the range of 2.6 - 5.1m/s, depending on the location in the harbor. In New Zealand at the Port of Tauranga in the Bay of Plenty during the same tsunami event recorded tsunami flow velocity was exceeding 2.3m/s.

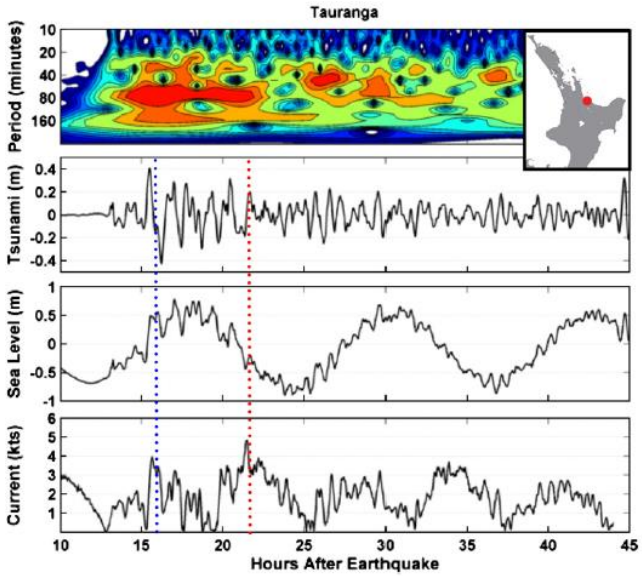

Figure 2.19 - Measured current speed, water level and spectral content from the Tohoku tsunami at Tauranga Harbour, New Zealand. (Lynett et al. (2014)

2.3.3. Simulation

Ruangrassamee and Saelem (2009) conducted a simulation of earthquake and tsunami generated in the Manila Trench. It has been shown that earthquake in that area can create tsunami which will be a serious threat to Thailand, southern part of Vietnam and Cambodia. Simulation covered three cases of earthquake magnitude of 8.0, 8.5, and 9.0. The Gulf of Thailand was only slightly affected by the currents generated in the Manila trench. Maximum current velocity for Gulf of Thailand is 0.27 m/s at a sea depth of 16m, while in the middle of the gulf the velocity was about 0.1 m/s. Obtained tsunami amplitude and current velocity were greatest in the direction towards the Philippines and Vietnam as shown on the figure below.

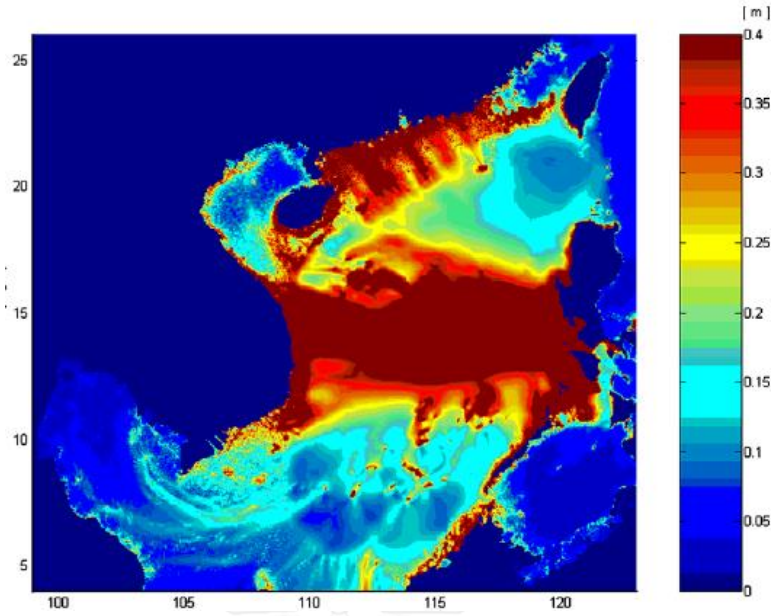

Fig 2.20 – Distribution of tsunami amplitudes in the South China Sea for Case 3 (Ruangrassamee and Saelem, 2009)

M.H. Dao et al. (2009) studied various tsunami scenarios in South China Sea with application of TUNAMI-N2-NUS model. Tsunamis were generated by a rupture along Manila Trench. Figure below presents peak height of the first wave for different cases of slip scale. Based on the earthquake magnitude and location of the port tsunami amplitude was in the range of 0.4m-3.1m.

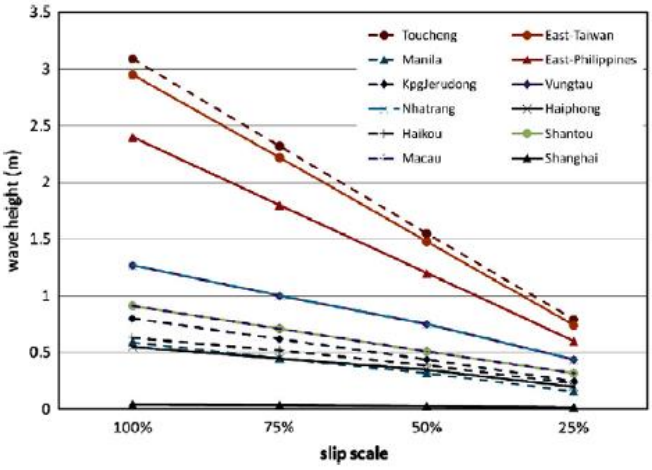

Figure 2.21 Plot of the first wave peak height at observation points versus different slip magnitude of the rupture (M.H. Dao et al. (2009))

Lynett et al. (2014) modeled tsunami acting on the harbor area of Crescent City, CA. In the study they took into account information about current induced by 2010 and 2011 tsunamis as well as model tsunamis generated by hypothetical large earthquake.

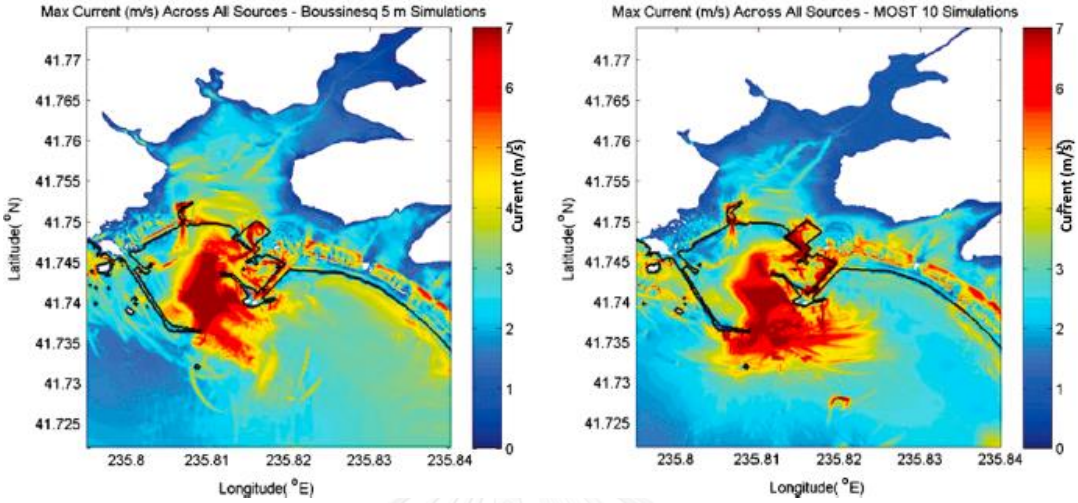

Figure 2.22 Maximum speed predicted across a range of different tsunami sources, Left: COULWAVE model,; Right: MOST model (Lynett et al. (2014)

Majority of the hydrodynamic parameters resulted from application of the "Method of Splitting Tsunami". In order to compare results from different sources second model using a high-order Boussinesq-type COULWAVE was employed. Comparison of obtained data with digitized video data showed that generally results from Boussinesq model were more accurate. Maximum current velocity was close to 4m/s while average current speed was between 1-3 m/s. For the MOST model maximum tsunami flow was exceeding 6m/s, and the average speed was between 2-4 m/s.

Mikami and Takabatake (2014) evaluated tsunami risk along the Vietnamese Coast. Simulated earthquakes of magnitudes between Mw=8.3-8.7 created tsunami waves in the range of 0.5m to 2.5m depending on the location. The distribution of the maximum amplitude is shown in figure 1. Largest amplitude was mainly observed in the direction toward the western coast of Luzon Island and the middle part of the Vietnamese coast. Southern and northern have experienced smaller tsunami amplitudes.

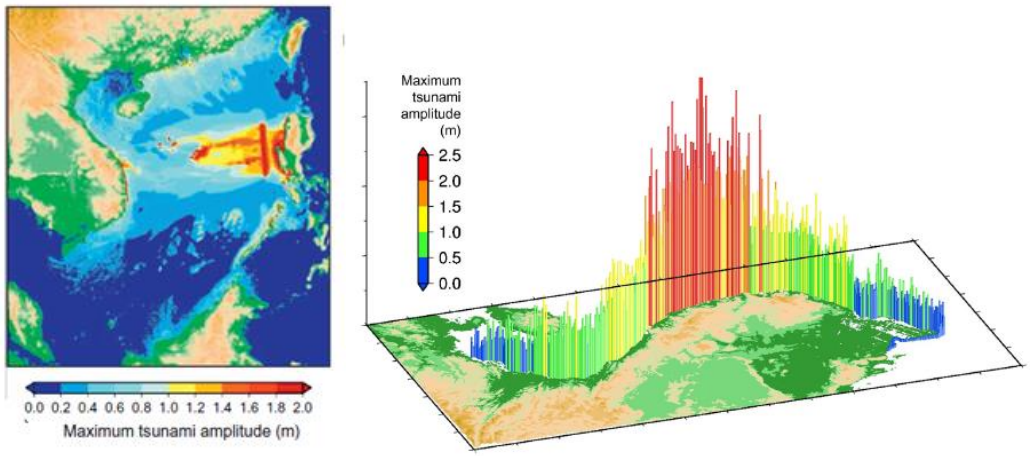

Figure 2.22 - Distributions of the maximum tsunami amplitude (Mikami and Takabatake, 2014)

Muhari et al. (2015) researched tsunami hazards in ports, based on the simulation of 2011 Great East Japan Tsunami. Selected ports were located in the southern part in Honshu Island in Japan to be modeled, were structures were not severely damaged by tsunami. Simulated tsunami run-ups were mainly consistent with the observed data as shown in figure below.

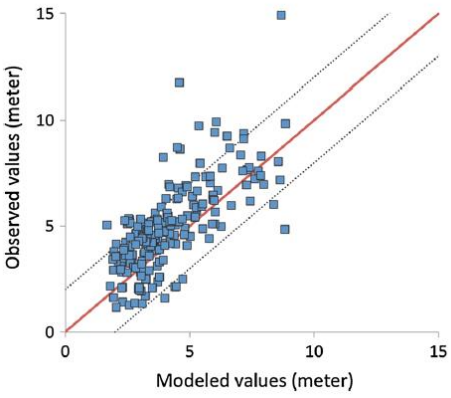

Figure 2.23 The comparison between the observed and simulated tsunami run-ups at the ports (Muhari et al. (2015))

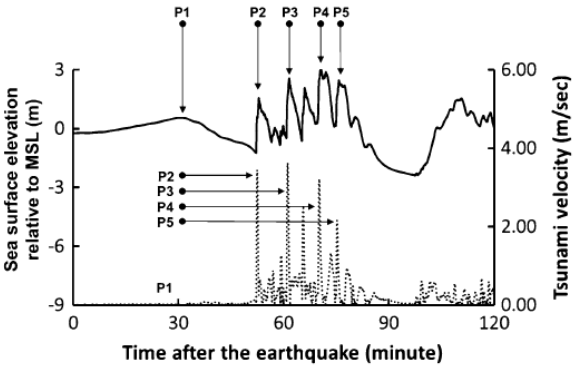

Figure 2.24 Values of simulated tsunami heights (solid line) and tsunami velocities (dashed line) at one of the observation points. (Muhari et al. (2015))

Tsunami current velocity and amplitude were checked for each point from 38 ports. The average height of the first to the fifth peaks was 2.71, 3.75, 3.91, 3.93, and 3.94 m, respectively. For the tsunami current velocity, the average values of the first five peaks were equal to 2.29, 3.12, 3.36, 3.45, and 3.45 m/s.

2.4. Tsunami forces

After tremendous damage caused by December 26, 2004 Indian Ocean Tsunami and March 11, 2011 Tohoku Japan Tsunami updated edition of Guidelines for Design of Structures for Vertical Evacuation from Tsunamis has been released. Since then it is one of the most comprehensive book on this matter. Due to that tsunami forces in this paper will be calculated according to guidelines described in FEMA P-646 and British Standard.

2.4.1. Theory

Hydrostatic forces act on a structure when slowly moving or standing water encounters a building on its way. It occurs due to an imbalanced pressure caused by different levels of water depth located on the opposite sites of a structural element. The direction of these forces is always perpendicular to the surface of the construction. These forces are often responsible for failure of the long structures such as breakwaters or seawalls. Since in this study structures does not consist of wall like components this forces are relatively small and are not considered in the analysis.

Hydrodynamic forces occur when water flows at high velocity around structure and structural components. Due to that they may act on a structure as a whole or only on particular element. Fluid density, flow velocity and structural geometry have great influence on the intensity. They are also known as drag forces, since they are combination of the lateral forces caused by the pressure forces from the moving mass of water and the friction forces generated as the water flows around the structure or component. During the tsunami event these forces are often responsible for overturning of structural components such as concrete blocks of the breakwaters but also whole building such as houses. Hydrodynamic forces can be computed using following formula:

$$F_d = \frac{1}{2}\rho_s C_d B (hu^2)_{max}$$

ρ_s – fluid density (with sediment)

C_d – drag coefficient

B – breadth of the structure in the plane normal to the direction of flow

hu^2 - momentum flux per unit mass per unit width

Impulsive forces are caused by the leading edge of a surge of water impacting a structure. Laboratory data show no significant initial impact force in dry-bed surges, but an “overshoot” in force was observed in bores that occur when the site is initially flooded. The maximum overshoot is approximately 1.5 times the subsequent hydrodynamic force. If the run-up zone is flooded by an earlier tsunami wave, subsequent waves could impact buildings in the form of a bore. For safety measures FEMA P-646 (2000) recommends evaluating impulsive forces as 1.5 times the hydrodynamic forces.

Debris impact forces occurs when tsunami wave cause waterborne debris (e.g. boats, vehicles, shipping containers) to float and go with the water flow. Floating debris may inflict severe damage or no damage at all. Unfortunately, it is really difficult to estimate the force accurately. Unlike other tsunami induced forces, debris impact forces act locally on a single member of the structure. Since the probability of the two or more simultaneous debris strikes is low it is usually ignored during design process. Another load associated with debris is damming force. It occurs when debris is accumulated and the surface on which a hydrodynamic force acts is increased by the breadth of the debris dam. Due to this the value of the hydrodynamic force increases. Since analyzed structures are located in the near shore area, probability of occurring of debris impact forces is exceptionally low, thus these forces are not considered as relevant for simulation.

Buoyant or vertical hydrostatic act on a structure or structural element when it is submerged in water and volume of the water is displaced. The total buoyant force equals the weight of water displaced. Buoyant forces on components must be resisted by the weight of the component and any opposing forces resisting flotation. Buoyant forces are a concern for structures that have little resistance to upward forces like basements or swimming pools. For a watertight structure FEMA P-646 (2012) recommend using equation below:

$$F_b = \rho_s g V$$

Where:

ρ_s- fluid density including sediment

g – gravitational acceleration

V – volume of water displaced by the building

Uplift forces act on building that are submerged by tsunami inundation. While submerged additional uplift forces are applied to floor levels of a building. Structures located in coastal areas should be designed that way, that in addition to standard design for gravity loads, their floors must also be designed to resist uplift due to buoyancy and hydrodynamic forces. When computing the buoyant forces on a floor slab, consideration must be given to the potential for increased buoyancy due to the additional volume of water displaced by air trapped below the floor framing system. Analyzed structures does not consist of floors and are not watertight, thus this kind of uplift force is not considered in the analysis.

During the tsunami event often buildings got partially or totally submerged. During the drawdown, when the wave is moving back, water may retain on the top of elated floors. This water will apply additional gravity loads, which sometimes may exceed the loads for which the floor was originally designed. The depth of water retained, h_r, will depend on the maximum inundation depth at the site, h_{max}, and the lateral strength of the wall system at the elevated floor. Generally the rate of the drawdown is rapid. Due to that upper levels are more exposed to this additional gravity load on the floor system. This load is often relatively high for structures located in land, however are almost nonexistent in near shore area.

2.4.2. Experiments on tsunami force

Iemura H. et al. (2007) conducted survey and experiment on Ulee Lheue Bridge located near the north coast of Banda Aceh. Due to damage, girders were displaced; however the bridge was still functional. Tsunami flow depth in that zone was observed to

be around 12m. The main problem of this experiment was to study the force created by the extreme wave, especially those forces connected with flow of the wave: drag forces and floating debris forces. Forces were calculated for the drag coefficient Cd=1.0

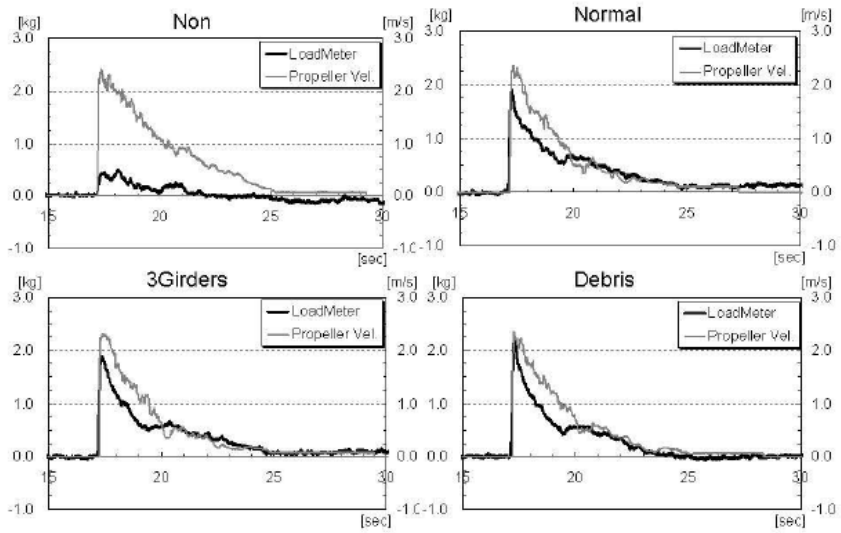

Figure 2.25 - Velocity and force time history for tsunami level 3 (Iemura H. et al. (2007))

Experiment results showed that tsunami force acting at the bridge started with a large spike and then gradually reduce to the lower one. It can be observed that maximum force and maximum velocity occurred simultaneously.

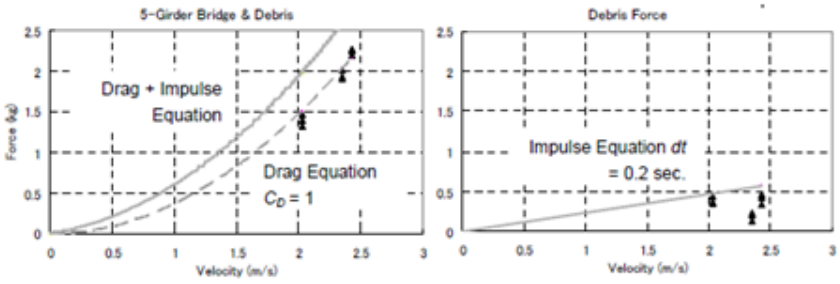

Figure 2.26 Correlation between maximum force and maximum velocity (Iemura H. et al. (2007))

Robertson L.H. et al. (2008) conducted an experiment to obtain fluid forces of a bore impacting a wall/floor system. Used system is similar to a deck of a loading platform supported on vertical piles. They collected data on fluid forces acting on

structural elements, water flow velocities, run-up and inundation height and energy dissipation. Main focus of the study was on the measurement of uplift forces. Experiment was conducted in a Tsunami Wave Basin. Water channel parameters: 48.8m length, 26.5m width and 2.1m height. Maximum water depth: 1.3m. Experiment involved a 1:15 beach slope and a flat section over which the water propagates. Beach slope ends 1 m above basin bottom. The solitary wave height was chosen to be 0.2m, 0.4m and 0.6m.

Figure 2.27 shows the relation between initial wave height and bore height, and figure 2.28 presents the relation between initial wave height and bore velocity. It may be observed that higher initial wave height results in higher bore height and bore velocity.

Table 2.1 - Laboratory bore characteristics (Robertson L.H. et al, 2008)

Still water depth on reef (cm)	Solitary Wave Height (cm)	Bore Height H_b (cm)	Bore Velocity V_b (cm/s)	Froude Number
0	20	6	191	2.49
	40	13.1	310	2.73
	60	16.6	375	2.94
10	20	8.1	193	2.17
	40	14.8	220	1.82
	60	19.9	299	2.14

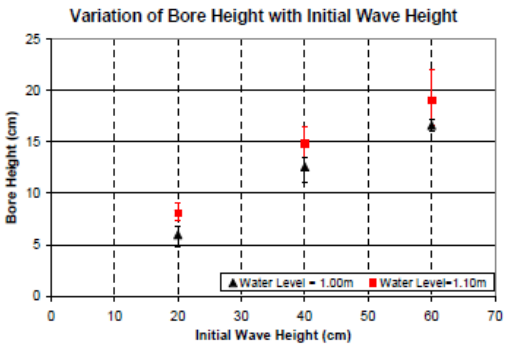

Figure 2.27 - Variation of bore height with wave height (Robertson L.H. et al., 2008)

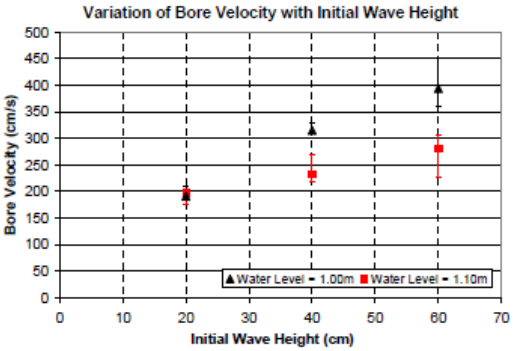

Figure 2.28 - Variation of bore velocity with wave height (Robertson L.H. et al., 2008)

Figures 2.29 and 2.30 shows the time history of the pressure acting on the soffit of the model floor slab. What can be clearly observed is a sudden load spike followed by rapid decrease to a slightly fluctuating residual uplift. For the first case, when the water level is equal to 1.0m and the reef under the slab is dry the impulsive load has a duration order of 0.05 to 0.1, while the residual uplift varies from 15 to 30 percent of the peak uplift pressure. The maximum uplift pressures are observed by the 40 cm and 60 cm solitary waves. Both of this waves had bores heights exceeding the 10 cm height of the model slab soffit. Highest uplift pressures ranged from 10 to 17 kPa.

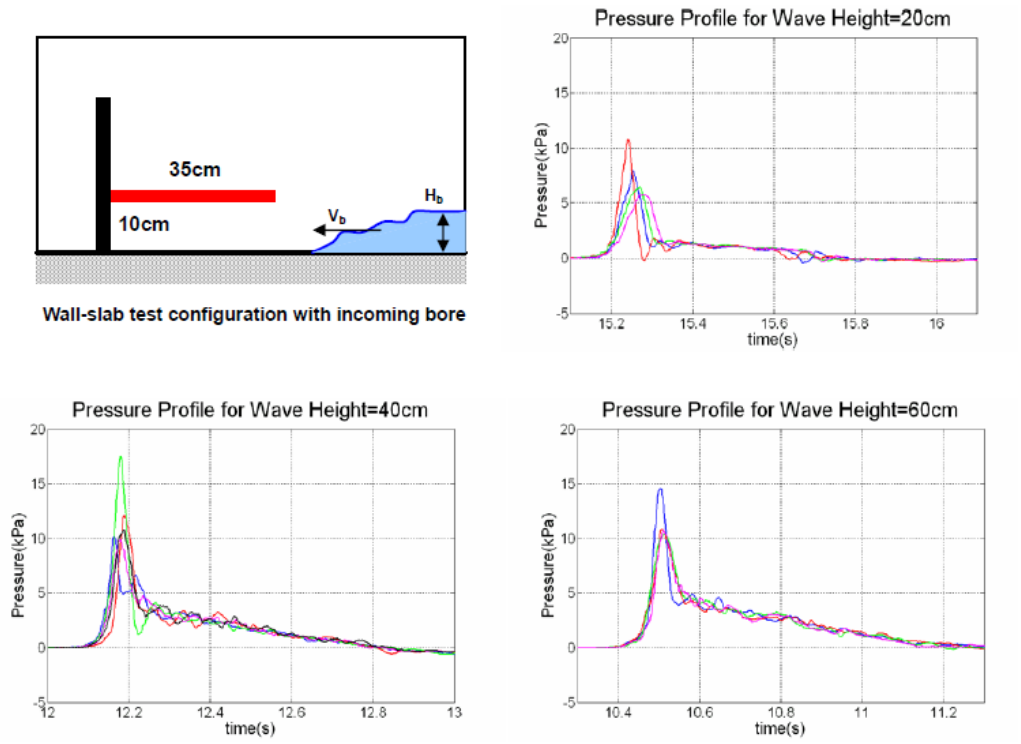

Figure 2.29 Uplift pressure on floor slab for bores caused by 20, 40 and 60 cm solitary waves with no water on reef (Robertson L.H. et al., 2008)

For the 20 cm wave heigth, pressured varied from 6 to 11 kPa. For the second scenario, water level of 1.1m and reef with 10 cm standing water the impulsive load has a duration order of 0.06 to 0.15, while the residual uplift varies significantly for different wave heights. For this case there is a noticeably variability in the peak values of uplift pressures for identical waves. These values range from 3 to 7.5 kPa. The maximum uplift is obtained when the bore depth is close to the clear height below the slab. Moreover

the study extended the results, and proposed a scaling of experimental results to prototype conditions.

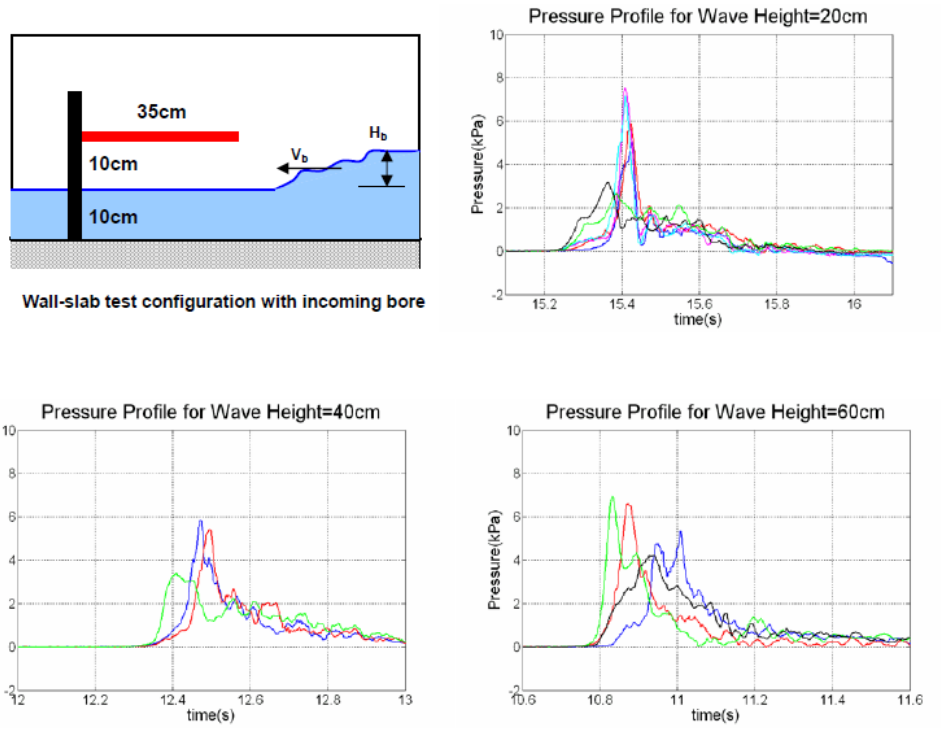

Figure 2.30- Uplift pressure on floor slab for bores caused by 20, 40 and 60 cm solitary waves with 10 cm water on reef (Robertson L.H. et al., 2008)

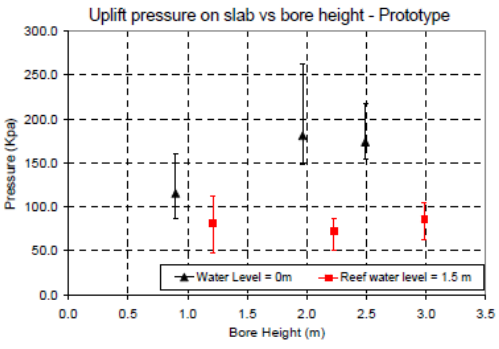

Figure 2.31- Model: Relation between uplift pressure and bore height (Robertson L.H. et al., 2008)

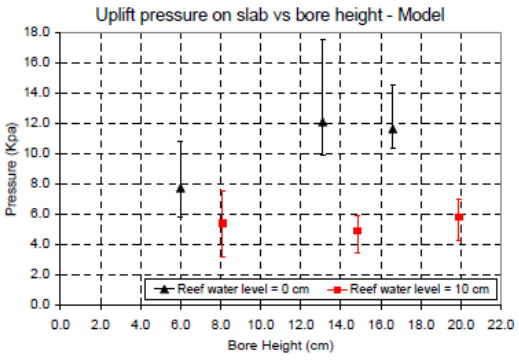

Figure 2.32 - Prototype: Relation between uplift pressure and bore height (Robertson L.H. et al., 2008)

Figure 2.31 and 2.32 shows the peak uplift pressure values for model and prototype, respectively. It may be observed that scaling of pressures would result in significant forces for a typical floor system. A 20 cm thick concrete slab has dead weight

of 4.8 kPa, while typical live loads range from 2.5 to 12 kPa. Scaled uplift impulsive upward loads caused by the tsunami would result in uplift failure of the system. This could be an answer to many failures of floor and deck slab failures occurred during the Indian Ocean Tsunami of 2004.

Lau T.L. et al. (2010) in order to obtain more accurate data on tsunami forces acting on bridges conducted a wave flume experiments on two types of bridges: with solid parapets and with perforated ones. Figure below presents the parameters of both models:

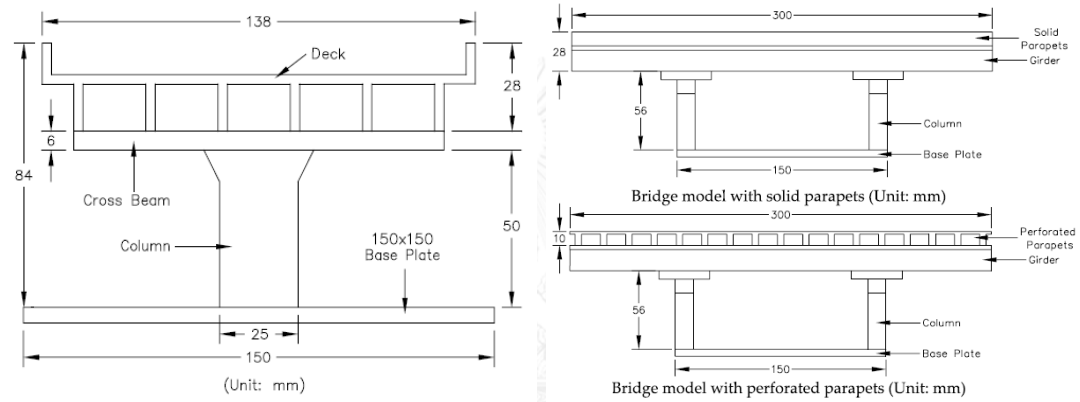

Figure 2.33 Parameters of model bridges (Lau T.L. et al., 2010)

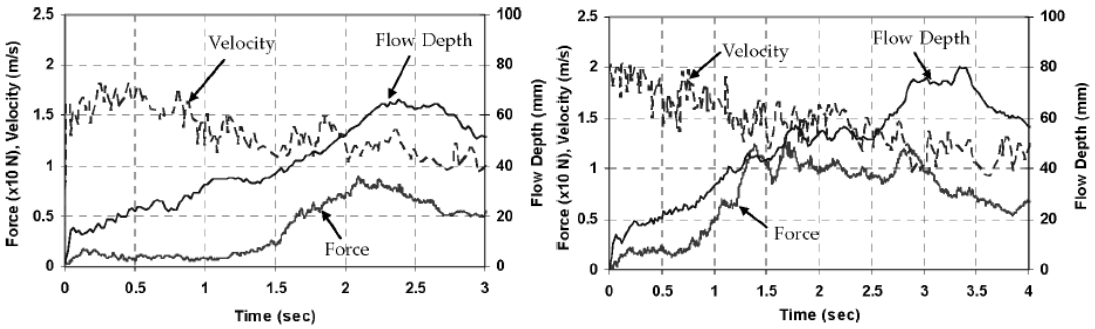

Figure 2.34 Correlation among flow velocity, flow depth and total wave force on the bridge deck with solid parapets at 65mm (left) and 80mm (right) nominal wave heights. (Lau T.L. et al., 2010)

Figure 2.45 shows time-histories of flow depth and flow velocities. This figure presents also total horizontal wave force on the deck. It can be clearly seen that velocity is highest on the beginning and then it decreases over time. Flow depth and wave force increases over time however reach peak values at different times. Simulated wave reaches peak velocity of about 2.5 $\sqrt{gh}$.

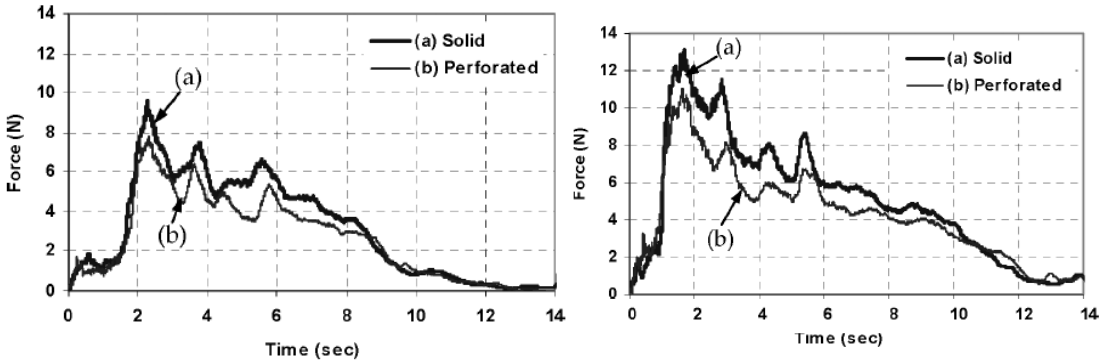

Figure 2.35 Average force time-histories for 65mm (left) and 80mm (right) nominal wave heights. (Lau T.L. et al., 2010)

Study concluded that perforation in bridge parapets reduce the overall tsunami forces acting on the bridge. Figure 2.46 presents average time-history results for the force acting on the bridge. Apart from maximum force that acted on a strucutre within relatively short period, forces which acted after may still severely damage the construction. Generally bridge with perforation in parapaters suffered less damage due to horizontal force than bridges with solid parapets.

2.5. Influence of earthquake forces on port structures

2.5.1. Observation on port damage

Goutam Mondal and Durgesh C. Rai (2006) surveyed the damage caused in Andaman Islands to jetties after 2004 Sumatra earthquake and tsunami. During the event most damage to the jetties and coastal structures were caused due to the earthquake forces since majority of these buildings where shielded by small islands and mangrove forest. However those jetties facing the open sea experienced damage due to tsunami.

Due to complexity of soil-structure interaction, authors grouped geotechnical damage applied to the jetties into 3 groups. First type of damage which was common for jetties in an area of Andaman Islands is pounding damage. Pounding occurs when there is not sufficient space between pier segments and lateral displacements cannot be accommodated. Usually small space between segments is provided only to reduce damage resulting due to shrinkage or creep however during earthquake it is not enough.

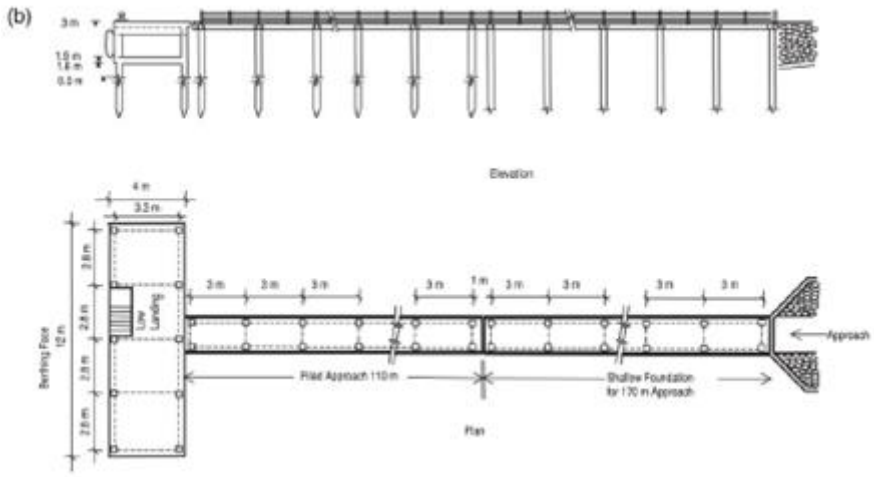

Figure 2.36 Gandhinagar jetty in North Andaman: (b) Elevation and plan. (Goutam Mondal, Durgesh C. Rai, 2006)

Pounding damage has been observed at berthing jetty in Mayabandar and Sagar Dweep (Fig 2.1.10-4). It is clear that these structures were not designed for sustaining earthquake induced forces and displacements. To prevent or minimize such damage authors recommend use of energy dissipation devices or allowing sufficient space between the plates.

Figure 2.37 Pounding damage to jetty at Sagar Dweep. (Goutam Mondal, Durgesh C. Rai, 2006)

Figure 2.38 Damage in short-piles of the approach jetty at Mayabandar Harbour in Middle Andaman Islands. (Goutam Mondal, Durgesh C. Rai, 2006)

| du

usually located away from the shore in orde

It is connected to the shore by an approach jetty. An approach jetty is a long structure, usually embedded in a sloping ground. Due to that the length of the unsupported length of piles varies. Shorter piles have bigger stiffness and take more shear forces during an

earthquake. The common mistake during designing such pier is assumption that every pile takeS the same amount of shear force. It is advised to design shorter piles for withstanding large amount of shear damage, because they may lead to the failure of the whole structure during the event of earthquake. This kind of damage was observed in the piles of the jetty at Mayabandar. Little or no damage was observed in the relatively longer piles while the approach slab fell due to the failure of shorter slabs.

Third kind of damages caused to the jetties is damage due to improper design and/or poor maintenance. Since piles of the jetties are partly submerged in saline water, they are exposed to environmental related damage. Special care should be taken to prevent the corrosion of the iron reinforcement. At Rangat Bay harbor corroded reinforcement led to severe damage of the piles in the jetty. Sufficient protection against the saline water would prevent or minimize the damage caused to piles.

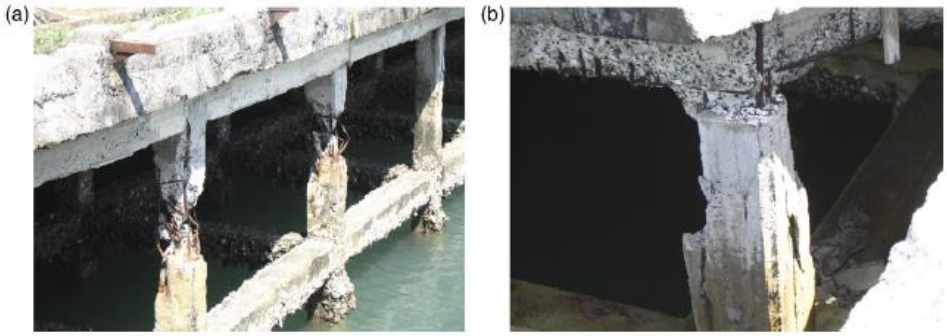

Figure 2.39 - Rangat Bay Harbour at Middle Andaman: (a) Damaged columns of approach jetty (b) Damaged beams and piles. (Goutam Mondal, Durgesh C. Rai, 2006)

Tobita T., et al. (2006) surveyed damage to geotechnical works in Banda Aceh and Meulaboh due 2004 Great Sumatra Earthquake. The region of Banda Aceh suffered critical damage. The coastlines receded several hundred meters after tsunami. It was caused by scouring effect of tsunami force and soil liquefaction due to earthquake. House located at fishery port of Ulee Lheue were completely swept away. Significant damage was also found on the left bank of the river channel. Levee's body expanded in the transverse direction due to loss of bearing capacity with liquefaction.

In the city of Meulaboh houses were totally destroyed and only debris remained. Researched team reported also damage to a jetty. Floor slabs of a pile supporting a passenger jetty collapsed into the sea, and only piles were left.

Figure 2.40 Collapsed floor slab of passenger jetty at a ferry port in Ujoung Kalang, Meulaboh. (Tobita T., et al. (2006)

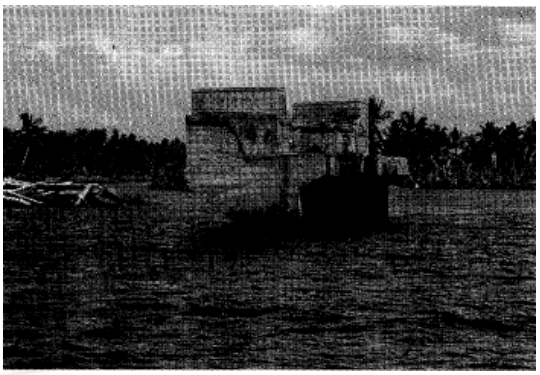

Figure 2.41 Bridge abutment of collapsed steel truss bridge in Kuala Bubon (Tobita T., et al. (2006))

In the city of Meulaboh the 60m steel truss bridge at the river of Bubon river was destroyed. Girders fell into the water and only two bridge abutments were left. Tsunami force was responsible for this failure however abutments and access roads collapsed as a result of strong earthquake.

2.5.2. Performance of the structures with batter piles

Utilization of batter piles in the jetty structures have been used for a long time in order to due to resist high lateral loading resulting from winds, waves and impacts. Using of batter piles concentrates the horizontal force onto a few members that act mainly in compression and possess limited ductility. During seismic events it is more beneficial to avoid that situation and distribute the loading. However often it is not possible due to the magnitude of berthing loads and required limited lateral displacement. In this chapter role of batter piles is described, both beneficial and detrimental.

Gerolymos et al. (2008) gathered data on the role of inclined piles in structures. During 1989 Loma Prieta Earthquake of magnitude Mw=6.8 prestressed concrete batter piles of the wharf in the Port of Oakland failed in tension at the pile-deck connection. Vertical piles were mostly undamaged. Investigation showed that the reason for that failure was due to insufficient reinforcement in the top of the piles and poor design of the pile-deck connection.

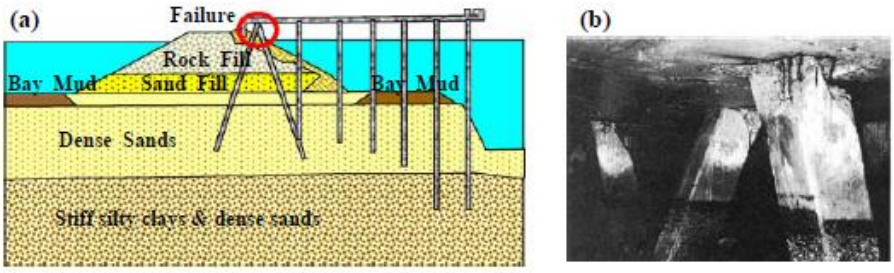

Figure 2.42 7th Street terminal, Oakland, after the Loma Prieta earthquake: (a) cross section, (b) damage to batter piles

One of the very few quay-walls which survived the 1995 Kobe earthquake in the harbor of Kobe was a composite wall supported by batter piles. Utilization of inclined piles was the reason of why the wharf withstood the seismic forces and was only slightly displaced. A similar structure located nearby but supported only by vertical piles was completely destroyed, with displacement of over 3m.

Another documented example of satisfactory response of batter pile supported structure is the case of the pier of the Landing Road Bridge in New Zealand after 1987 Edgecumbe Earthquake. Due to employment of the raked piles structure had necessary lateral stiffness required for withstanding large lateral ground movement resulting from the liquefaction of sandy layer.

Brunet S. et al (2012) conducted a survey on a seismic performance of ports in the Southern Chile after February 27, 2010, Maule earthquake. Most of the observed piers experienced damage in battered piles. The reason for that is battered piles are significantly stiffer laterally than vertical piles and attract larger earthquake forces. Piles battered in the transverse direction of the last 96m of the Huachipato pier were cut at joints with the deck. Vertical piles and longitudinal battered piles did not suffered structural damage. An explanation for that is natural torsion in connection with poor design of pile-deck joint.

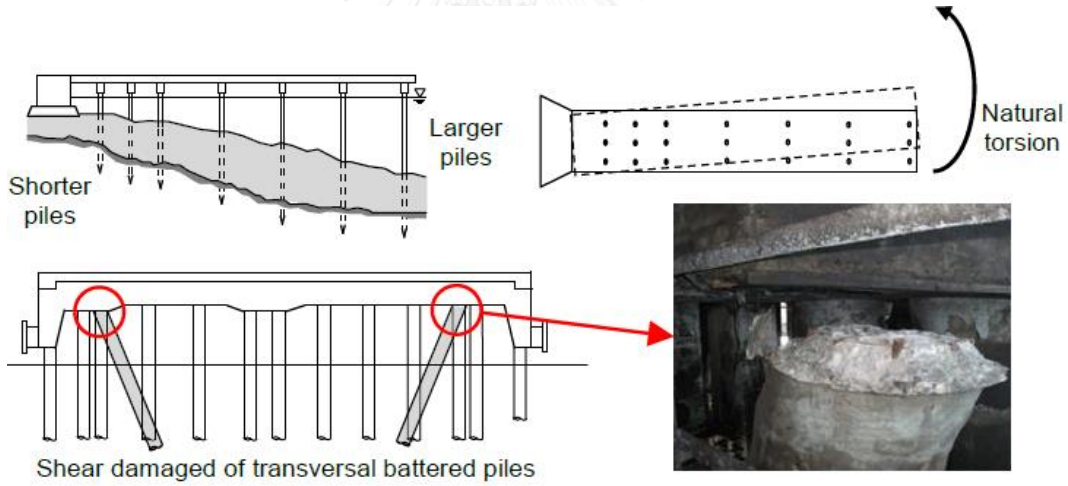

Figure 2.43 Shear damage in transversal battered piles due natural torsion at Huachipato Pier (Brunet S. et al (2012)

Gerolymos et al. (2008) conducted a numerical analysis of the implication of raked piles. Study concluded that using of batter piles in a group increases lateral stiffness and reduces displacements during earthquakes

Giannakou A. et al (2010) continued the research. More cases have been studied. Results in the study were presents in terms of ratios of response of the batter piles system with respect to corresponding system consisting of vertical piles only. Results concluded that for purely kinematic response, batter piles experience larger

bending moments than vertical piles. Moreover they experience significantly larger axial forces for all 4 cases of idealized soil profiles.

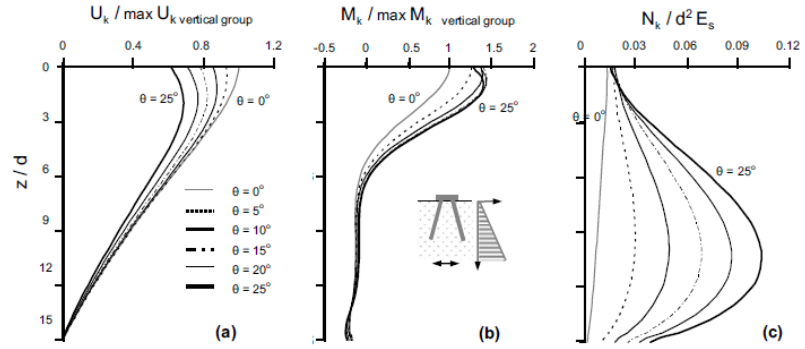

Figure 2.44 Kinematic response of rigidly capped two-pile group: distributions of a horizontal displacement relative to the displacement of the pile tip for various pile inclination angles (Giannakou A. et al (2010)

For a total response of the system, that is kinematic and inertia forces employment of batter piles was beneficial. For short structures, batter piles developed smaller bending moments than vertical piles. Additionally they were able to sustain larger axial forces than vertical group. Reasons for that are as follow: inertia forces induce a dynamic shear force. In vertical piles this force is resisted by lateral loads, but in batter piles it loads axially and laterally. -kinematic loading produces larger head moment in batter piles.

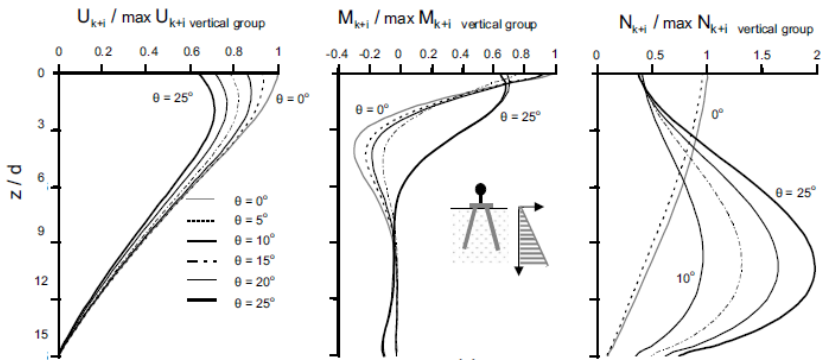

Figure 2.45 Total kinematic+inertial response: distributions of horizontal displacement, bending moment, and axial force along the pile supporting a short superstructure (Giannakou A. et al (2010)

3. Methodology

This chapter covers methodology proposed for the analysis of port structures under tsunami loadings. Technical papers and reports were reviewed in details in previous chapter, however this sections covers most important and relevant details considering proposed methodology. A flowchart of proposed way is presented below.

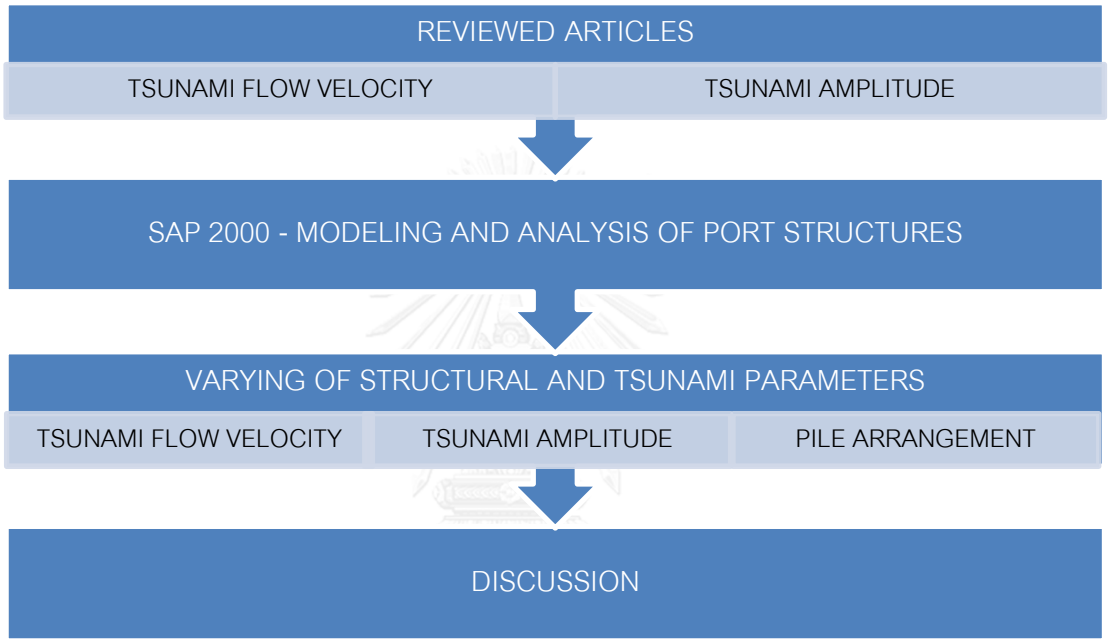

Three types of marine structures are analyzed: berthing dolphin, mooring dolphin and loading platform. Since these structures are required to berth large vessels for loading and unloading of the cargo they are located in deep water. Due to that often they are constructed with limited or no protection against waves and especially tsunamis.

Generally piles of these structures are subjected to high lateral loads. In order to resist lateral loads batter piles in configuration with vertical piles are employed. Different piles configuration are considered in order to analyze differences in responses.

3.1. Details of the port structures

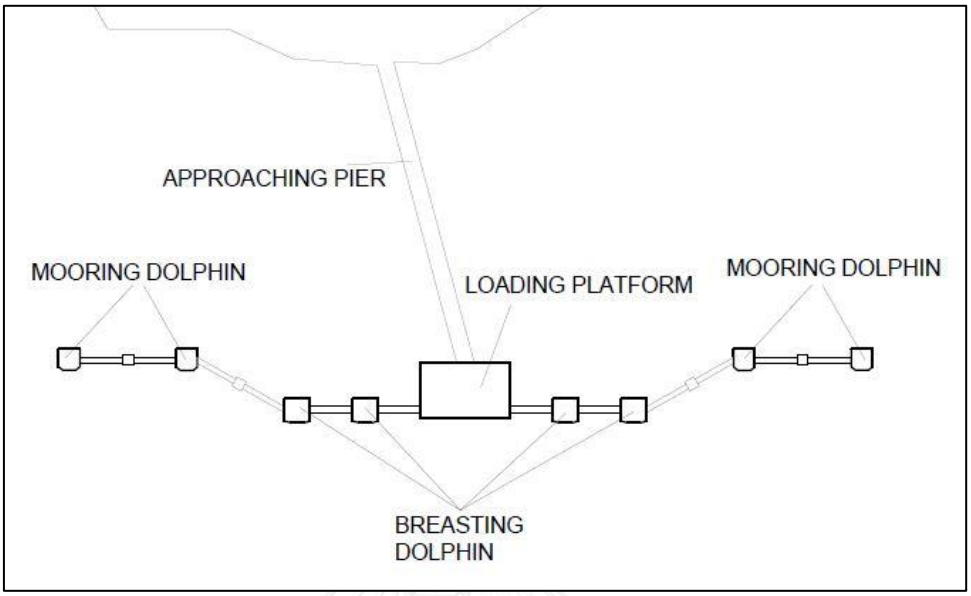

Figure 3.1 - Typical layout of LPG terminal

All port structures consist of a concrete deck supported by steel piles. The level of the top deck is same for all structures and is located +4.8mMSL. The water depth at the analyzed structures is -14.7 mMSL. Steel piles with diameter equal to 1m and wall thickness equal to 0.0025m are employed in every structure.

Deck of the first structure, loading platform, is a rectangular with sides equal to 26.0x42.0m. Concrete slab thickness is equal to 0.25m. The cross section of the beam is a rectangular 1.5x1.5m. Length of the pile, measured from the bottom of the deck to the seabed is equal to 17.75m. Figure 3.2 presents dimensions of the deck of the loading platform. Second structure, mooring dolphin, is presented in Figure 3.3. It consists of a concrete deck with dimensions 10x10x3m supported by 12 steel piles arranged in radial symmetry. All piles are raked in order to better resist lateral loading. Last structure, breasting dolphin, consists of a 12x11.5m concrete deck of 3.5m thickness supported on 16 steel piles of 1m diameter. Both vertical and raked piles are used in order to minimize displacement caused by berthing vessels. Figure 3.4 presents a structure of breasting dolphin used in analysis.

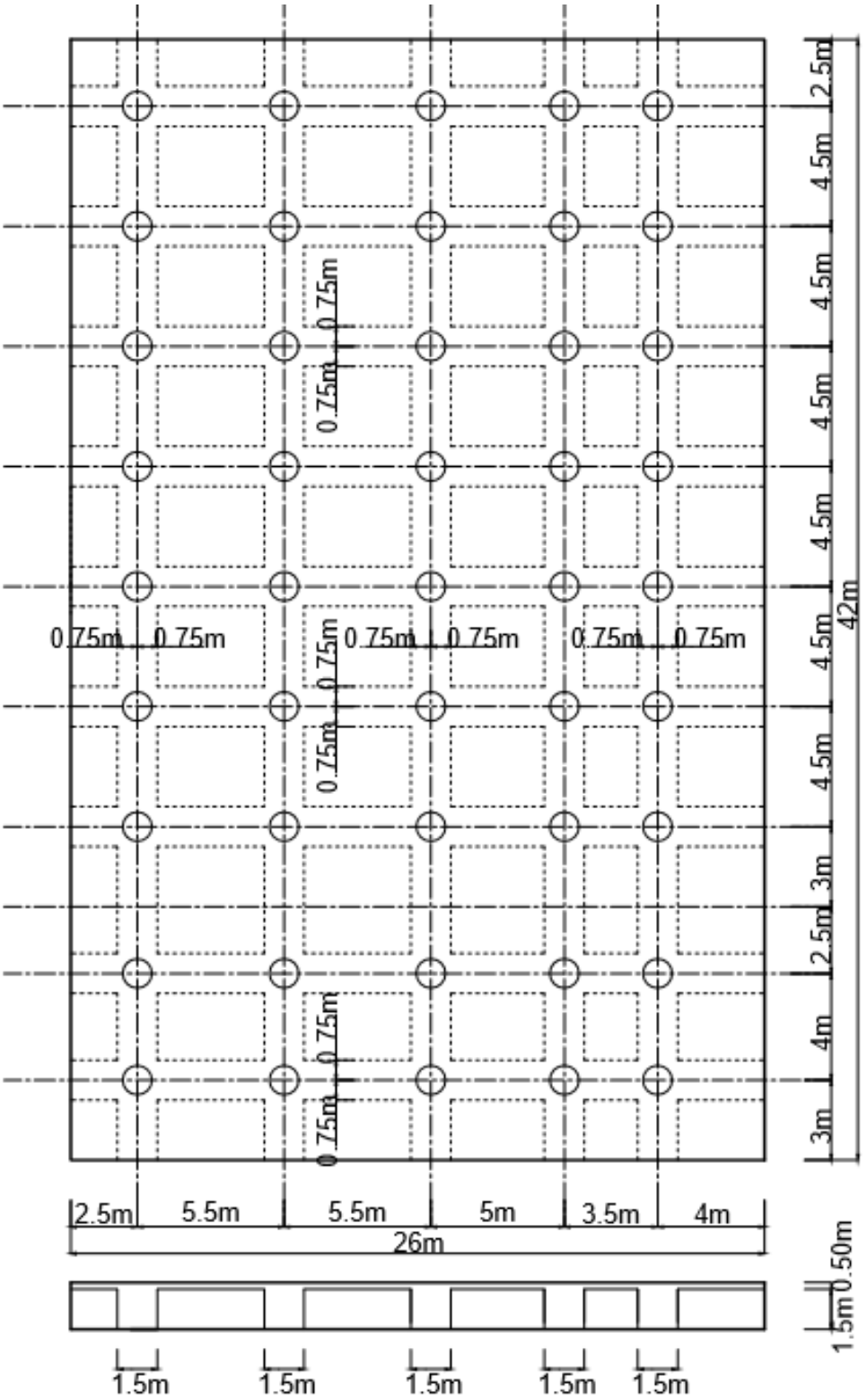

Figure 3.2 - Dimensions of loading platform

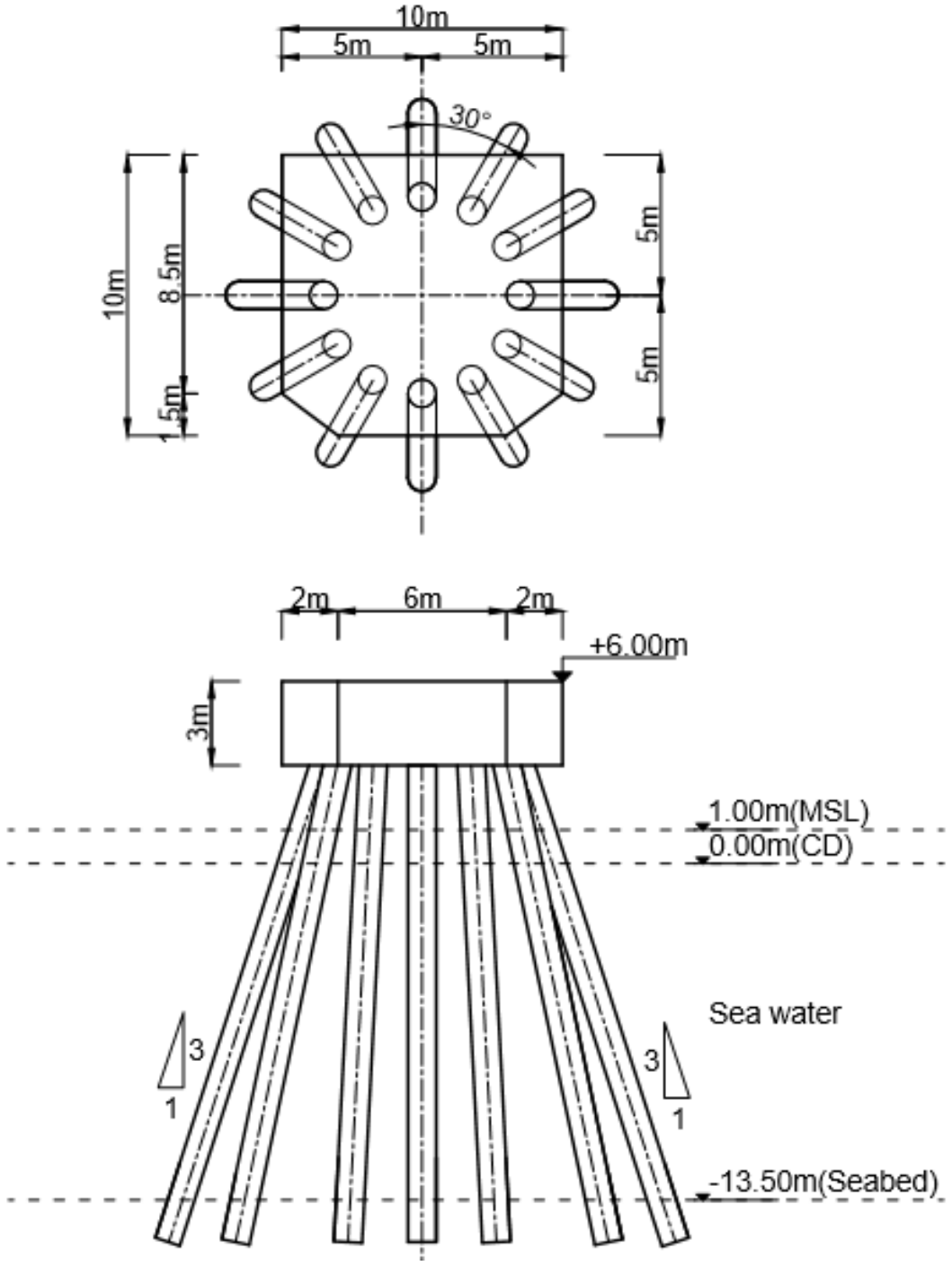

Figure 3.3 - Dimensions of mooring dolphin

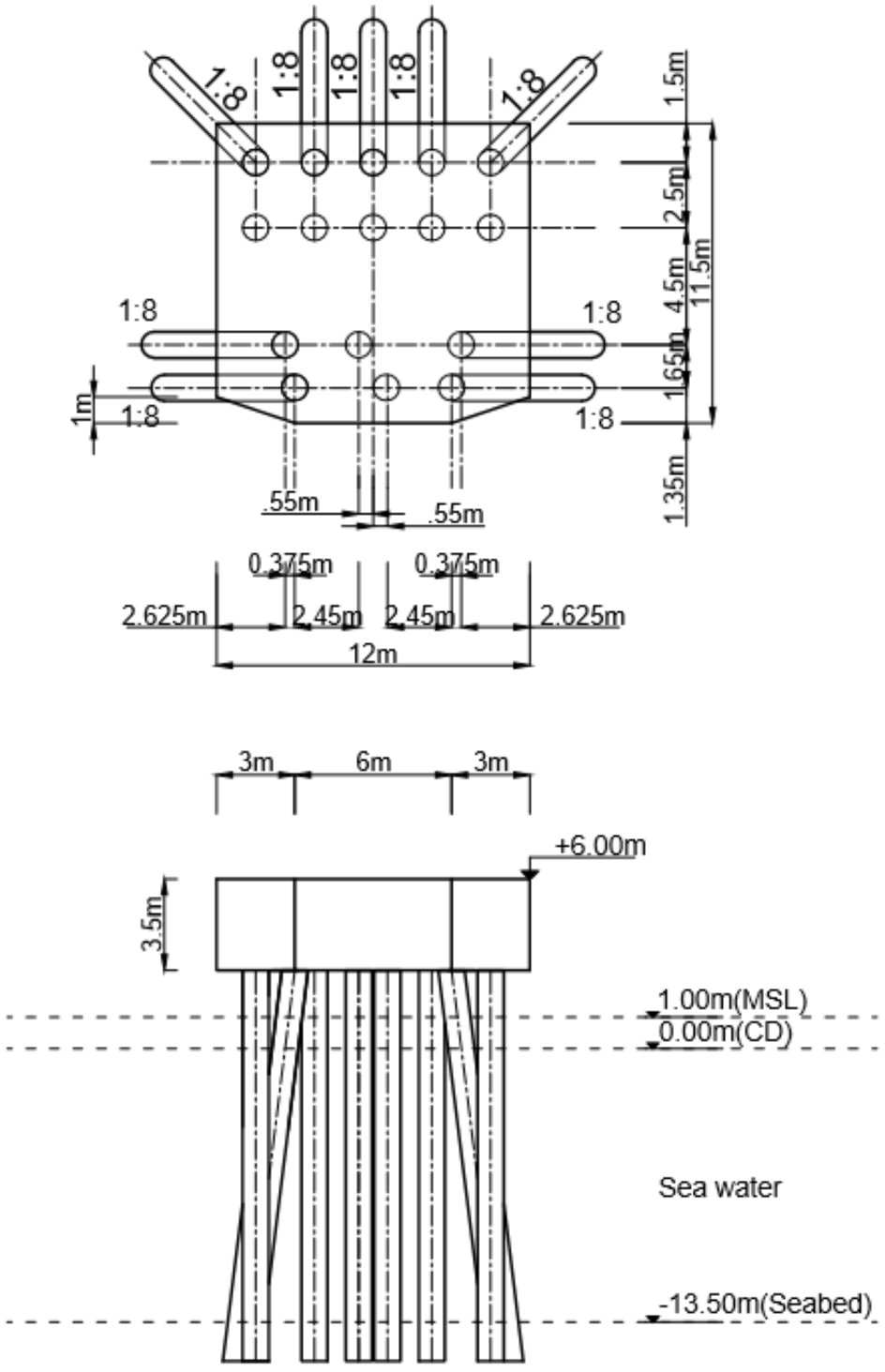

Figure 3.4 - Dimensions of breasting dolphin

3.2. Tsunami current velocity

Tsunami flow velocity is considered based on results from numerical simulations and observation of the reviewed articles. Since structures are located in near shore area appropriate range of tsunami flow velocity is considered.

Table 3.1 Tsunami flow velocity from reviewed literature

PAPER	TYPE OF RESEARCH	EVENT	LOCATION	TSUNAMI FLOW VELOCITY
TSUTSUMI ET AL. (2002)	OBSERVATION AND EXPERIMENT	SOUTHWEST HOKKAIDO EARTHQUAKE, 1993	AONEA, JAPAN	8-12m/s
MATSUTOMI ET AL. (2005)	OBSERVATION	INDIAN OCEAN TSUNAMI, 2004	PORT OF ULEE LHEUE, INDONESIA	~7m/s
RUANGRASSAMEE AND SAELEM (2009)	SIMULATION	MANILA TRENCH EARTHQUAKE	GULF OF THAILAND	0.1-0.4m/s
EERI SPECIAL EARTH. REPORT (2011)	OBSERVATION	TOHOKU EARTHQUAKE, 2011	SENDAI, JAPAN	5-8m/s
LYNETT ET AL. (2012)	OBSERVATION AND SIMULATION	TOHOKU EARTHQUAKE, 2011	PUERTO AYORA, GALAPAGOS ISLANDS	1-2m/s
LYNETT ET AL. (2014)	OBSERVATION	INDIAN OCEAN TSUNAMI, 2004	PORT OF SALALAH, OMAN	4-5m/s
	OBSERVATION	CHILE EARTHQUAKE, 2010	SAN DIEGO, CATALINA ISLAND, SANTA CRUZ	~8m/s
	OBSERVATION	TOHOKU EARTHQUAKE, 2011	CRESCENT CITY, USA	2.6-5.1m/s
	OBSERVATION	TOHOKU EARTHQUAKE, 2011	PORT OF TAURANGA, NEW ZEALAND	>2.3m/s
	SIMULATION	CASCADIA SUBDUCTION ZONE	CRESCENT CITY, USA	1-4m/s
MUHARI ET AL. (2015)	OBSERVATION SIMULATION	TOHOKU EARTHQUAKE, 2011	SOUTH OF HONSHU ISLAND, JAPAN	2.29-3.45m/s

Tsunami current velocities simulated or observed in ports and harbors are highlighted. These velocities are the most appropriate for this study due to similar sea depths. Different simulations are to be employed however fluid velocities will be in the range of above values.

3.3. Tsunami amplitude

Tsunami amplitudes are chosen in the same way tsunami flow velocities have been chosen since no simulation of wave propagation will be employed. Information on wave amplitude is scarce. Table 3.2 presents values obtained from the reviewed literature.

Table 3.2 Tsunami flow velocity from reviewed literature

PAPER	TYPE OF RESEARCH	EVENT	LOCATION	TSUNAMI AMPLITUDE
ROBERTSON L.H. ET AL. (2008)	EXPERIMENT	-	TSUNAMI WAVE BASIN	1.22m
M.H DAO ET AL. (2009)	SIMULATION	MANILA TRENCH EARTHQUAKE	TOUCHENG, TAIWAN	2.32m
			EAST PHILIPPINES	1.8m
			MACAU	0.71m
			SHANTOU, CHINA	1.53m
LYNETT ET AL. (2012)	OBSERVATION AND SIMULATION	TOHOKU EARTHQUAKE, 2011	PUERTO AYORA, SANTA CRUZ, GALAPAGOS ISLANDS	2-4m
MIKAMI AND TAKABATAKE (2014)	SIMULATION	MANILA TRENCH EARTHQUAKE	VIETNAMESE COAST	0.5-2.5m
LYNETT ET AL. (2014)	OBSERVATION	INDIAN OCEAN TSUNAMI, 2004	PORT OF SALALAH, OMAN	1.5m
MUHARI ET AL. (2015)	OBSERVATION SIMULATION	TOHOKU EARTHQUAKE, 2011	SOUTH OF HONSHU ISLAND, JAPAN	2.71-3.94m

Most of the obtained data considers tsunami amplitude on land or while hitting the coastline. Highlighted values consider amplitude simulated or measured directly in port. In the simulation different values are considered, however in the range stated in the table.

3.4. Tsunami forces

Tsunami acting on marine structures causes different forces. This study focuses mainly on uplift and drag forces, since these forces are major factor impacting displacement of top decks.

3.4.1. Drag forces

Drag forces are calculated following recommendation from British Standard, BS 6349-1:2000, and FEMA P-646. Generally drag forces can be divided as those acting on piles and those acting on deck of the structures. Drag force acting at the centroid of the area normal to the flow can be calculated using expression:

$$F_D = \frac{1}{2}(C_D \rho V^2 A_n)$$

Where:

ρ_s – seawater density

C_d – dimensionless time-averaged drag force coefficient

V – tsunami current velocity

A_n – area normal to flow

Drag force coefficient depends on various parameters such as: structure shape and tsunami flow direction. While calculating drag force acting on circular pile, FEMA P-646 recommends assuming C_d=1.2. For larger obstructions, like dolphin deck, it is advised to estimate drag coefficient considering: the ratio of the width of the element, w, to the submerged height of the element, h, Drag coefficients recommended by manual are indicated in Table 3.3.

Table 3.3 - Drag coefficients larger obstruction

W / h	Drag coefficient C_d
1-12	1.25
13-20	1.3
21-32	1.4
33-40	1.5
41-80	1.75
81-120	1.8
>120	2

3.4.2. Uplift forces

As defined by Robertson et al. (2007), hydrostatic uplift (F_u) is a combination of buoyancy due to submersion in water and the effect of air trapped below a structural element". For conservative approach, full submergence in water should be taken into account since it happens at one time during tsunami event. Then total uplift on the deck can be evaluated by:

$$F_U = F_b - F_w$$

Where:

F_b – buoyancy force

F_w – weight of the structure

Uplift forces acting on the analyzed structures are calculated assuming that uplift forces are hydrostatic and uniformly distributed. These forces can be calculated using expression:

$$F_b = \rho_s g V$$

Where:

ρ_s – seawater density V – volume of the submerged part of the structure

g – gravitational acceleration

3.5. Analysis

3.5.1. Structural model

Structural models of mooring dolphin, breasting dolphin and loading platform are analyzed using SAP2000 software.

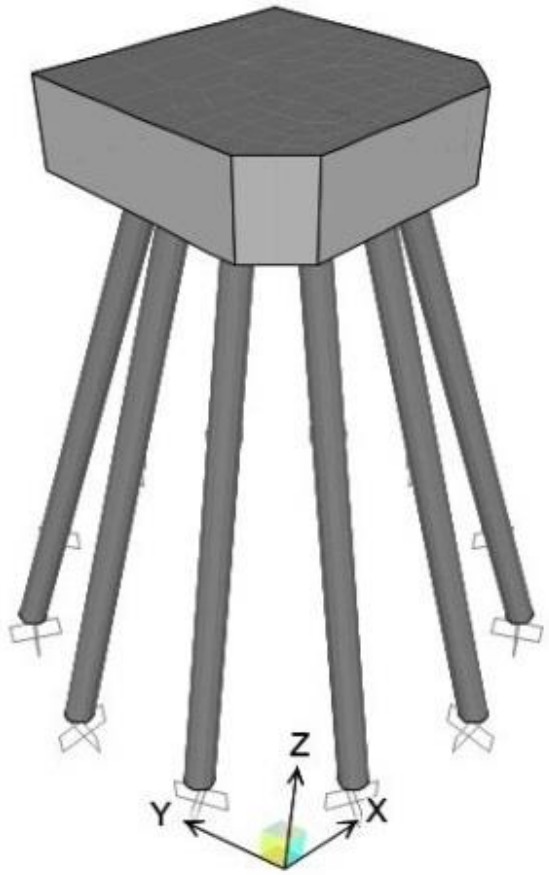

Figure 2.5 -Mooring dolphin modeled in SAP2000

All of the structures are analyzed using linear static analysis. Structures are modeled using 3-dimensional linear elastic model. This kind of modeling in simple way represents the structure behavior and is appropriate while analyzing displacement and forces. Analyzed models consist of concrete decks and steel piles. Parameters of used materials are described in Table 3.4.

Table 3.4 Types of materials used in the model

Type of material	Mass (t/m^3)	Weight (kN/m^3)	Young's Modulus (GPa)	Behavior
Concrete	2.407	23.6	25	linear elastic
Steel	7.850	76.9	200	linear elastic

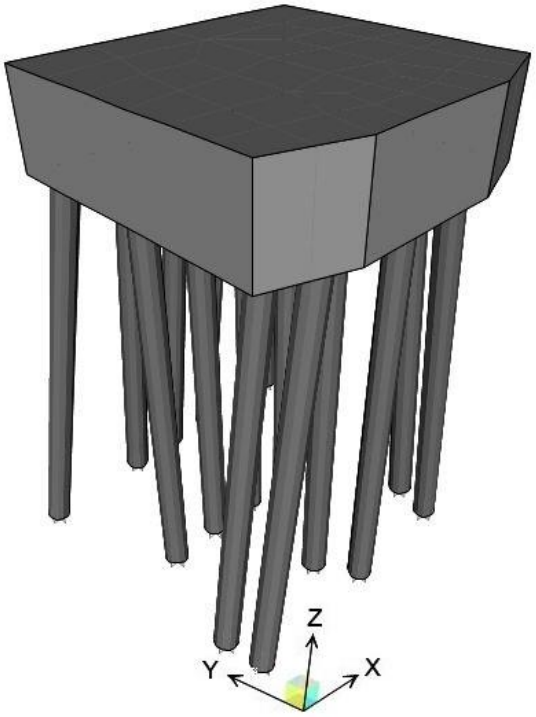

Fig.3.6. Breasting dolphin modeled in SAP2000

Table 3.4 Types of element used in the model

Structure	Element	Modeled element	Material
Loading platform	Slab	Thin shell element	Concrete
	Beams	Frame element	Concrete
	Piles	Frame element	Steel
Mooring dolphin	Deck	Solid Element	Concrete
	Piles	Frame element	Steel
Breasting dolphin	Deck	Solid Element	Concrete
	Piles	Frame element	Steel

Decks of dolphins are modeled using solid elements while loading platform slab are modeled using shell elements. Beams of the loading platform and piles are modeled using frame elements.

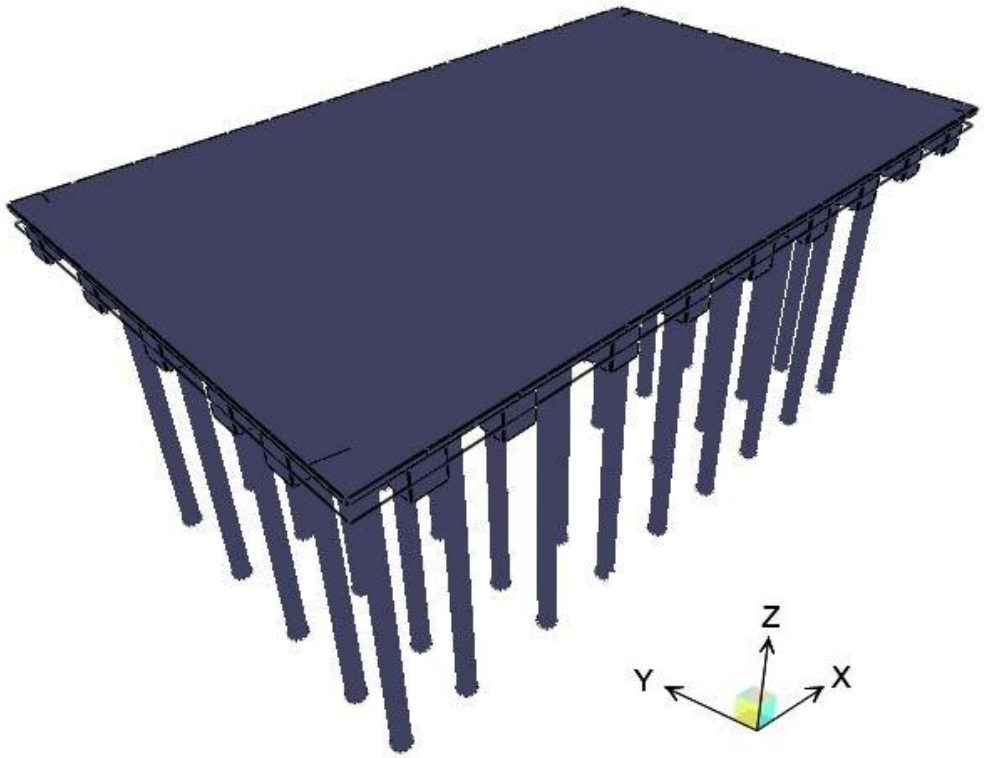

Fig.3.7. Loading platform modeled in SAP2000

3.5.2. Analytical parameters

During the analysis global coordinate system is considered as shown in Figure 5. All results including displacement of the deck are presented according to this system.

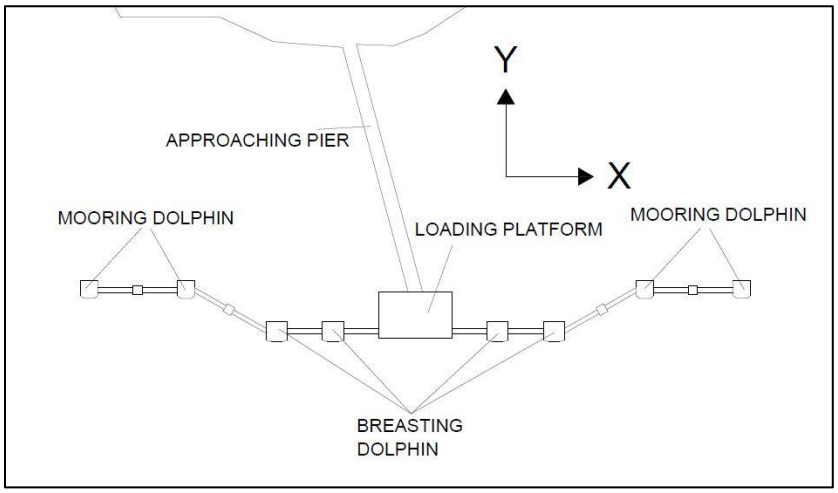

Figure 3.8 Coordinate system

. In the analysis parameters are varied. Water Level is used as parameter describing what part of structure experiences forces caused by tsunami wave. This parameter is a sum of Tide Level and Tsunami Amplitude and is measured from the Mean Sea Level or Chart Datum.

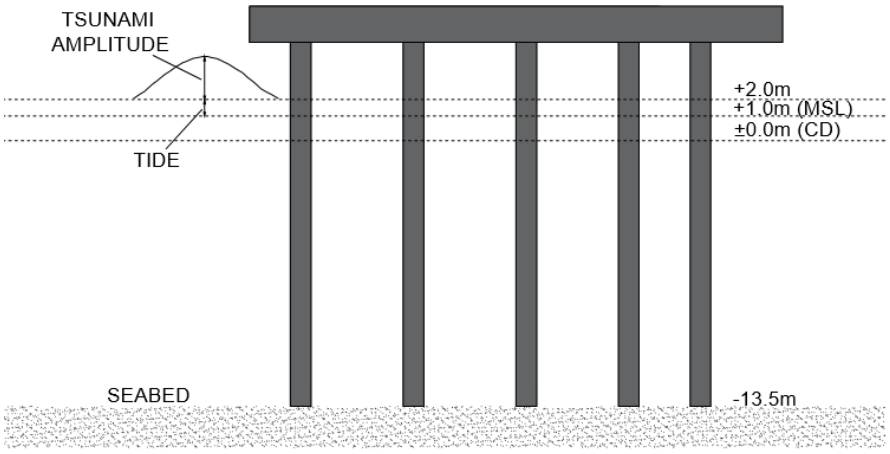

Figure 3.9 - Calculation of Water Level above MSL - Example

Figure 3.9 presents an example of calculating Water Level above MSL equal to 3.0m. In a given example it is assumed that Tide Level is +1.0m. Table 3.5 presents all cases of analyzed Tide Level and Tsunami amplitude, their summation and considered Water Levels above MSL and conversion to Water Level above CD.

Table 3.5 - Considered cases of Water Level

Tide Level [m]		Tsunami amplitude [m]		Water Level above MSL [m]		Water Level above CD [m]
0	+	1	=	1	=	2
0.5		1.5		1.5		2.5
1.0		2		2.0		3
1.5		2.5		2.5		3.5
2.0		3		3		4
				3.5		4.5
				4		5
				4.5		5.5
				5		6

Apart from the varying of tide level and tsunami amplitude, changing of tsunami flow velocity and tsunami flow direction is considered. In order to achieve continuous results for all analysis firstly flow direction is fixed. Then for specific flow velocity all tsunami height is analyzed, after analyses are finished, all calculation is repeated for next velocity. When analyses are complete for all flow velocities, tsunami flow direction is changed. Two cases of tsunami flow direction are considered. Following global coordinates system described in Fig. 3.8, they are: tsunami flow along axis X and tsunami flow along axis Y. Considered tsunami flow velocities are listed in Table 3.6.

Table 3.6 - Considered tsunami flow velocities

Tsunami flow velocity	1 m/s	2 m/s	3 m/s

4. Analysis

4.1. Loading cases

Depending on the analyzed tsunami amplitude and tide level different forces of different values acts on the marine structure. In some cases water level is not significant. In those cases it is assumed that uplift pressure acting on the decks of the structures

does not occur since the tsunami crest is below the deck soffit. In the case of tsunami of higher amplitudes uplift forces have to be considered. While tsunami does not cause uplift forces in some cases, it always results in drag forces acting on the piles. Tables 4.1, 4.2, and 4.3 present which forces are acting on structure, depending on the considered Water Level above CD.

Table 4.1- Loading platform loading cases

Deck Thickness [m]	1.75			Top Deck Level:		6.0
Water Level above CD [m]	Submerged depth [m]	Drag forces acting on piles	Drag forces acting on beams	Drag forces acting on slab	Uplift forces acting on beams	Uplift forces acting on slab
2	0.00	X				
2.5	0.00	X				
3	0.00	X				
3.5	0.00	X				
4	0.00	X				
4.5	-0.25	X	X		X	
5	-0.75	X	X		X	
5.5	-1.25	X	X		X	
6	-1.75	X	X	X	X	X

Table 4.2- Mooring dolphin loading cases

Deck Thickness	3		Top Deck Level:		6.0
Water Level above CD [m]	Submerged depth [m]	Drag forces acting on piles	Drag forces acting on deck	Uplift forces acting on deck	Overtopping
2	0.0	X			No
2.5	0.0	X			No
3	0.0	X	X	X	No
3.5	-0.5	X	X	X	No
4	-1.0	X	X	X	No
4.5	-1.5	X	X	X	No
5	-2.0	X	X	X	No
5.5	-2.5	X	X	X	No
6	-3.0	X	X	X	Yes

Table 4.3- Breasting dolphin loading cases

Deck Thickness	3.5		Top Deck Level:		6.0
Water Level above CD [m]	Submerged depth [m]	Drag forces acting on piles	Drag forces acting on deck	Uplift forces acting on deck	Overtopping
2	0.0	X			No
2.5	0.0	X			No
3	-0.5	X	X	X	No
3.5	-1.0	X	X	X	No
4	-1.5	X	X	X	No
4.5	-2.0	X	X	X	No
5	-2.5	X	X	X	No
5.5	-3.0	X	X	X	No
6	-3.5	X	X	X	Yes

4.2. Piles configuration

In this research soil-structure interaction is simplified. In linear analysis, common design practice is to use a point of fixity approach which idealizes the soil-pile system. By assuming a point of fixity, the pile can be analyzed as a cantilever structure with appropriate boundary conditions and external loadings. The calculated depth to fixity is a function of the soil properties, pile width, lateral loadings and pile head boundary conditions. The pile moment and deflection can be determined using structural analysis techniques.

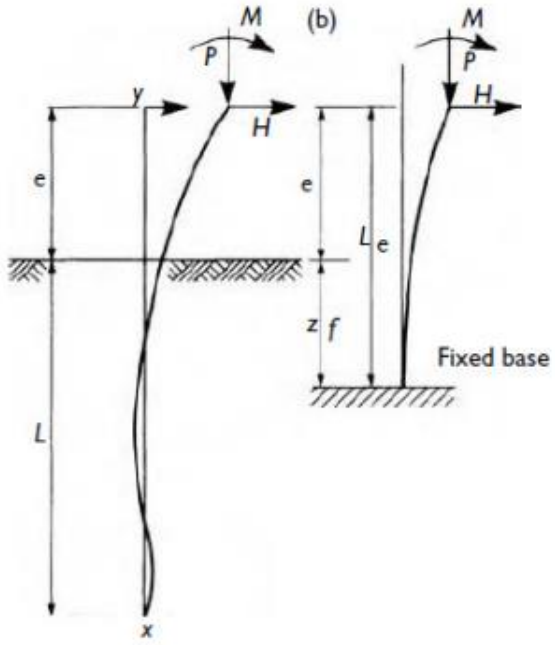

Figure 4.1 - Point of fixity concept

Depth to the pile of fixity can be calculated by expression:

$$z_f = 1.4R$$

Where:

$R = \sqrt[4]{\frac{EI}{KB}}$ – stiffness factor

Coefficient of subgrade reaction, K can be calculated using equation:

$$K = k_s \cdot B \cdot \Delta L$$

Where:

$k_s = 67\frac{S_u}{B}$, B – breadth of the pile, S_u – undrained shear strength

This research considers two types of seabed, made of rock and made of clay. Calculations of the point of fixity are presented in tables below:

Table 4.4 Pile parameters

d [m]	1
t [m]	0.0025
EI [kN/m^2]	194880

Table 4.5 Calculation of the point of fixity

SOIL PROFILE	ROCK	CLAY
S_u [kN/m^2]	-	2.20
k_s [kN/m^3]	-	147.40
ΔL [m]	-	1.00
K [kN/m]	-	147.40
R [m]	-	6.03
1.4 R [m]	-	8.44
Used depth to point of fixity [m]	0.00	8.50

Table 4.6 Effective pile length

	LOADING PLATFORM	MOORING DOLPHIN	BREASTING DOLPHIN
ROCK	17.75	16.5	16
CLAY	26.25	25.00	24.50

In this study influence of pile configuration on marine structure is considered. The influence of rake angle on the structure is discussed. Additionally influence of pile configuration with utilization of both raked and vertical piles is considered. Figure 4.2 presents the concept of using batter piles and rake angle. It shows loading platform with modified configuration, where battered piles angled at ratio 1:4 are employed on the perimeter is considered.

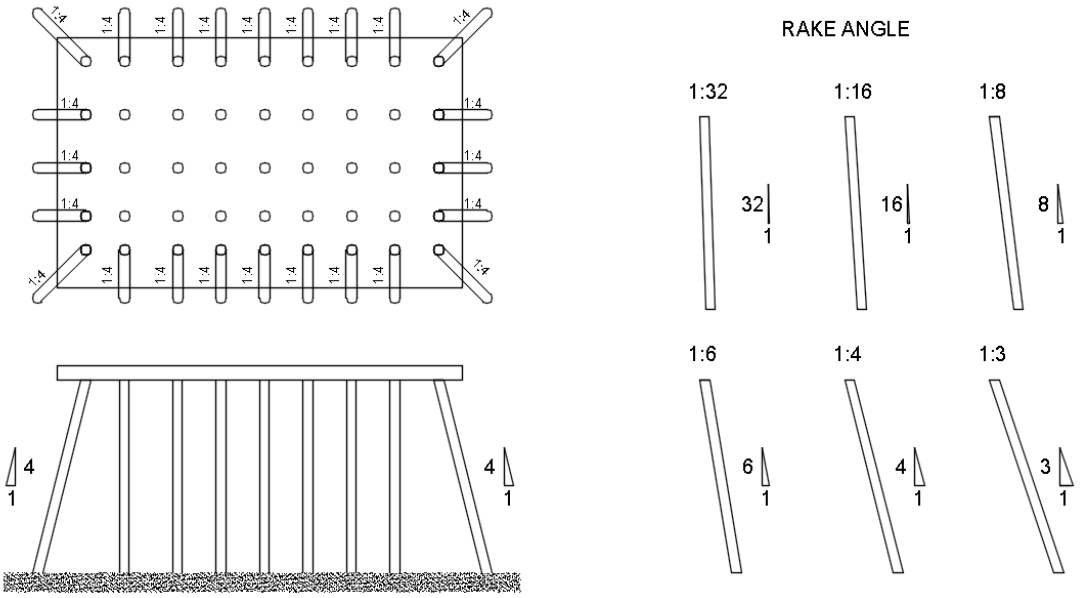

Figure 4.2 - Loading platform with raked piles

5. Results and discussion

The goal of this research is to study behavior of port structures under tsunami loadings with focus on displacement of the top deck due to drag forces. To achieve it, different cases of drag forces acting on as well piles as decks were analyzed. This chapter concentrates on influence of parameters on the maximum top deck displacement. All presented water levels are water levels above the CD level.

5.1. Behavior of port structured under tsunami loading.

The goal of this research is to study behavior of port structures under tsunami loadings with focus on displacement of the top deck due to drag forces. In order to achieve it, different cases of drag forces acting on as well piles as decks were analyzed. This chapter concentrates on influence of parameters, both tsunami and structural, on the maximum top deck displacement. These parameters include tsunami flow velocity, tsunami amplitude, water level and pile configuration with utilization of both vertical and batter piles. All presented water levels are water levels above the CD level.

Figures present bending moment diagrams and displacement of top deck under various tsunami conditions. Bending moments are assumed as on figure 5.1

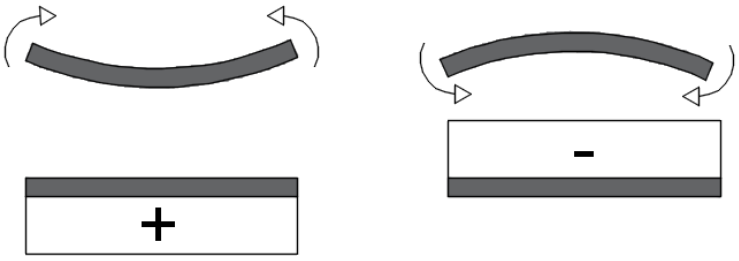

Figure 5.1 - Left: Positive bending moment, Right: Negative bending moment

5.1.1. Loading platform

All piles supporting the deck are vertical. Bending moment distribution is almost identical for every pile. Differences between the values are negligible. Bending moment is negative in the support and positive in the pile-deck connection. The displacement of the deck is higher than in other structures and it is equal to 40.2mm. Axial forces are similar in every pile. It can be noticed that all piles act in compression.

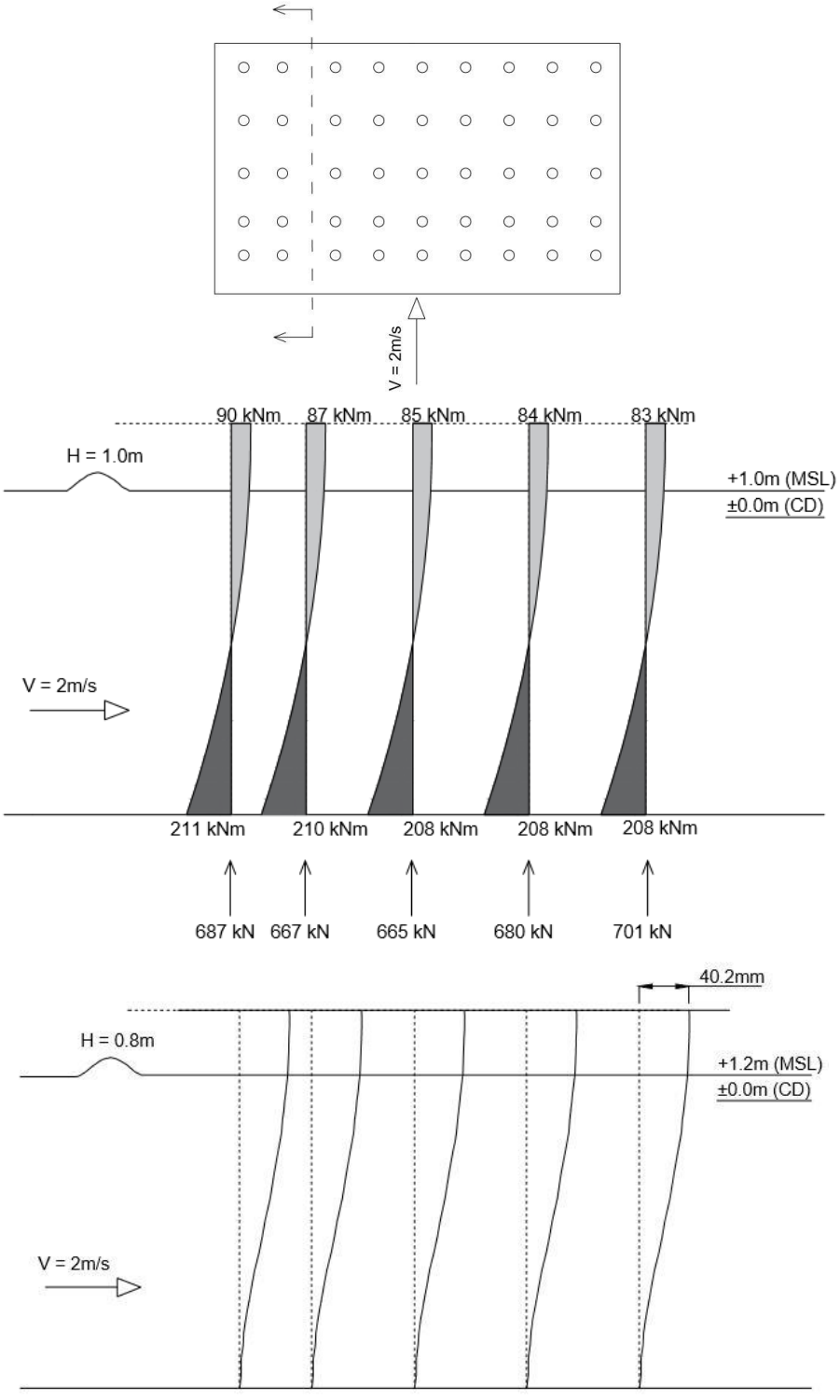

Figure 5.2 –Behavior of loading platform under tsunami loading. Top: cut location, Middle: bending moment distribution, Bottom: displacement

5.1.2. Breasting dolphin

In the structure of breasting dolphin, two kinds of piles are analyzed: vertical piles and batter piles perpendicular to the tsunami flow direction.

Looking at the bending moment diagram, it can be noticed that structure is very rigid, similar to mooring dolphin. Higher bending moment is reached in the deck and lower in the support. Axial force distribution is different than in mooring dolphin. All piles experience compression. Axial force in vertical piles is higher than in batter piles.

It can be noticed, that despite tsunami flowing in toward the structure, breasting dolphin deflects towards the wave. In fact under self-weight structure of breasting dolphin deflects significantly. For a case without any wave, top deck of the structure moves 28.5mm in direction opposite to the axis Y. Figure 5.4 presents displacement in direction opposite to the axis Y equal to 10.4mm. It can be concluded, that in fact under the drag forces exerted by tsunami flow equal to 2m/s, the structure of breasting dolphin deflected along the flow of the wave and absolute displacement due to tsunami wave is equal to 18.5mm.

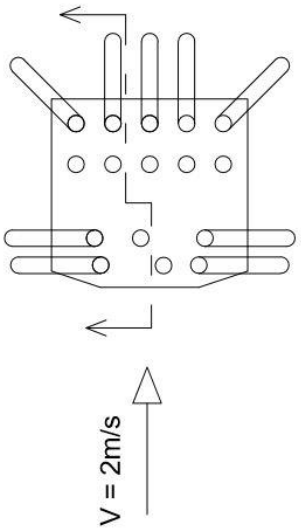

Figure 5.3 - Breasting dolphin cut location

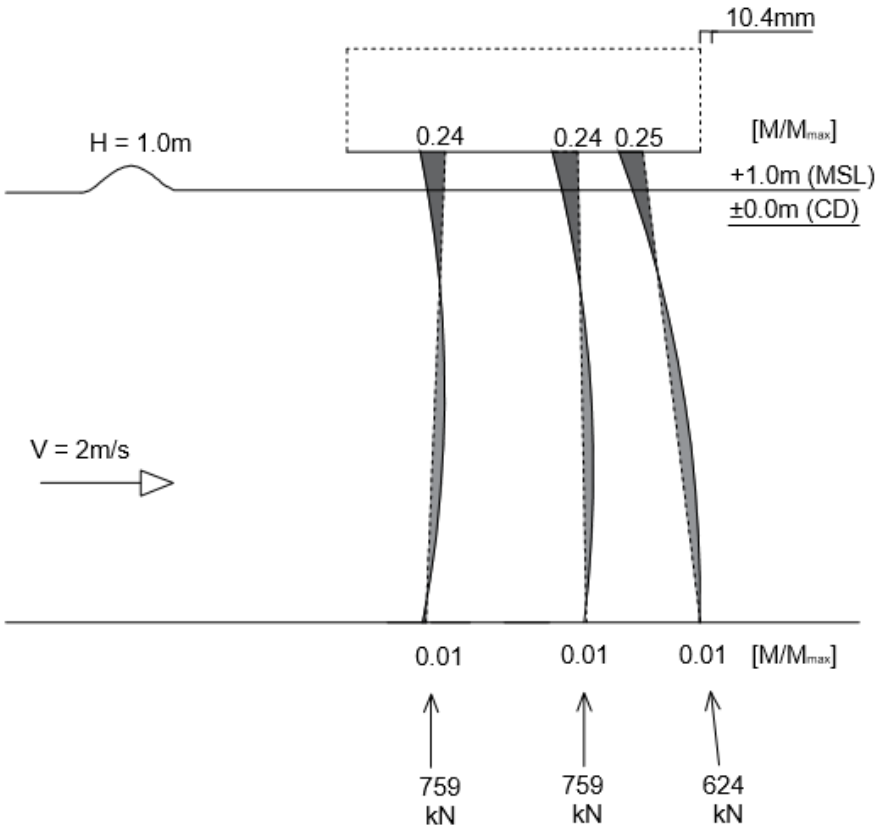

Figure 5.4 –Behavior of breasting under tsunami loading

5.2. Effect of rake angle

5.2.1. Mooring dolphin

Mooring dolphin is a structure generally supported only by batter piles. In this structure piles are employed in radial symmetry. Due to that, an influence of rake angle on behavior of the structure is studied. Different rake angle are considered in the analysis. First, for better comparison, a structure supported only by vertical piles is modeled. Internal forces and displacements are calculated. Then instead of vertical piles batter piles with ratio 1:8 are employed. Simulation is then repeated for different ratios: 1:6, 1:4 and 1:3. Tsunami and wave parameters are the same for all cases:

- Wave height = 1.0m
- Tsunami amplitude = 1.0m
- Tsunami flow velocity = 2m/s

Figures 5.6 to 5.12 present bending moment diagram and axial force distribution of mooring dolphins. While considering bending moment, piles may be divided into three groups: pile perpendicular to the wave flow, piles driven along the wave flow, and other piles. When the angle between the pile and the wave flow increases, absolute value of the bending moment also increases and reaches maximum for pile perpendicular to the wave flow. A noticeable symmetry in the bending moment diagram can be observed.

For higher rakes structure starts to become very rigid. Because of that, bending moment diagrams of the piles resemble the shape of the diagram of a beam fixed at both ends. This behavior can be observed for rake 1:4 and 1:3. Increasing the rake further increases this behavior.

While considering axial forces, it can be noticed that all piles are in compression. Piles located on the edge of the structure, where the wave hits first experience lower axial forces. Compression gradually increases for piles located further from the edge and reaches maximum in pile, which is hit last by the wave.

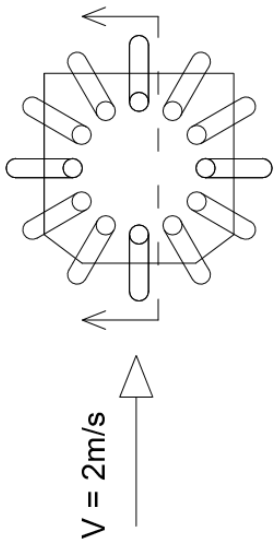

Figure 5.5 – Mooring dolphin cut location

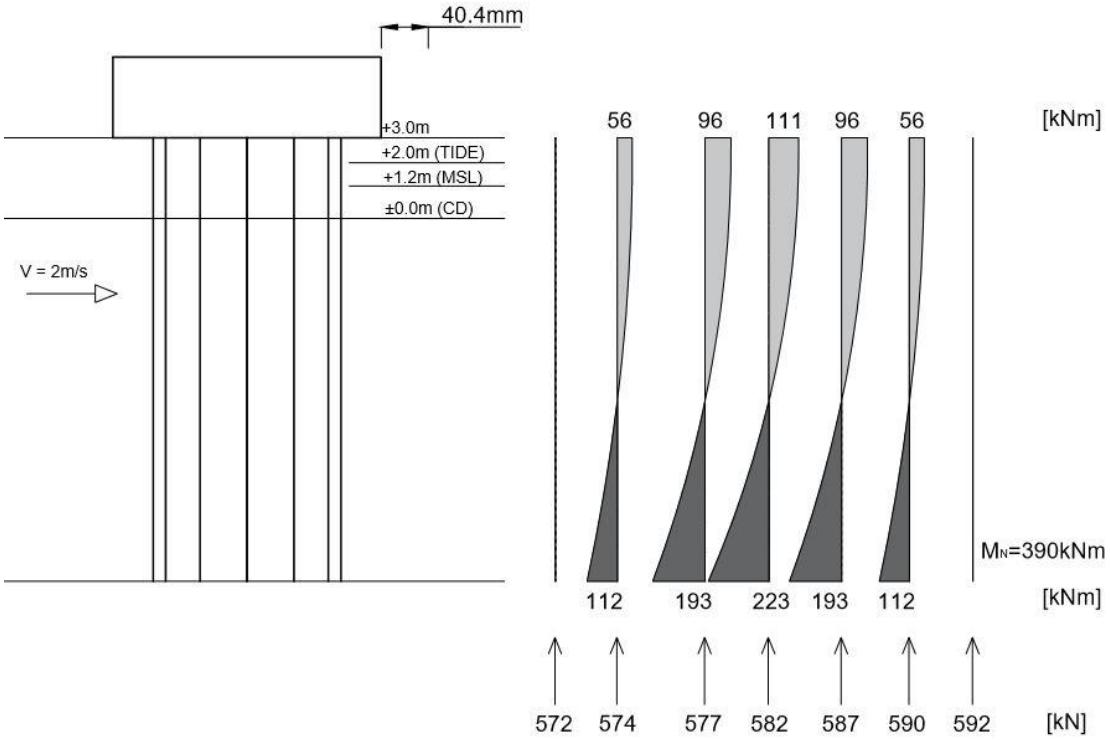

Figure 5.6 - Behavior of mooring dolphin supported by vertical piles

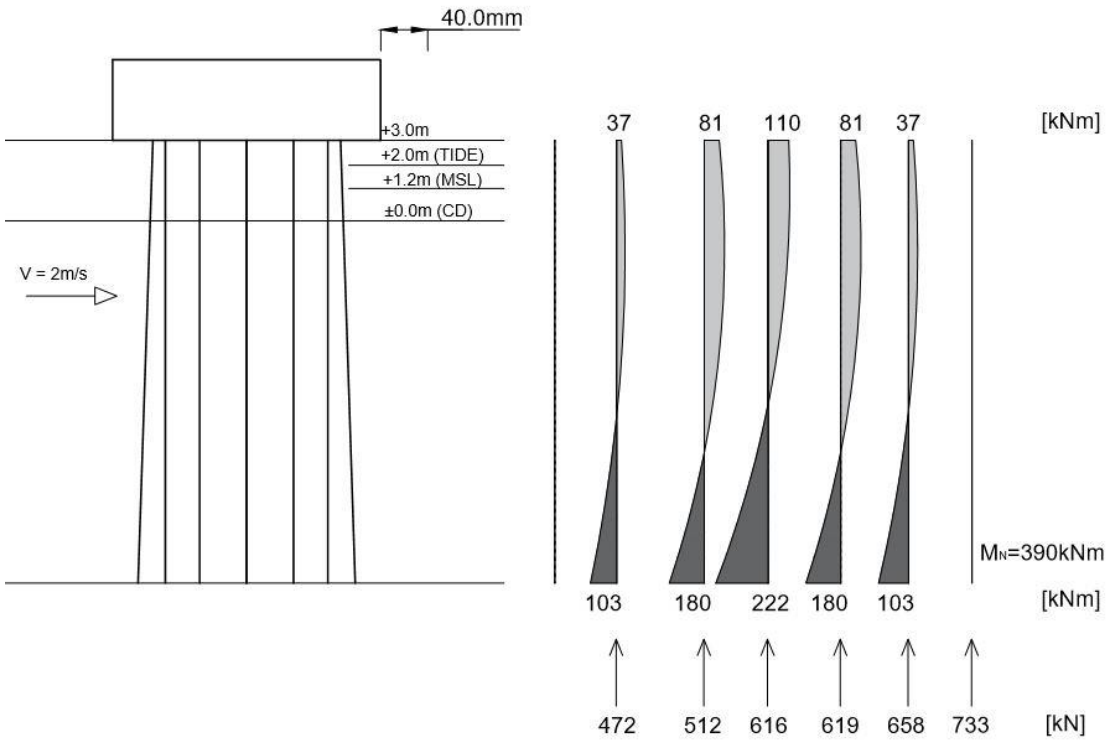

Figure 5.7 - Behavior of mooring dolphin supported by batter piles with rake 1:32

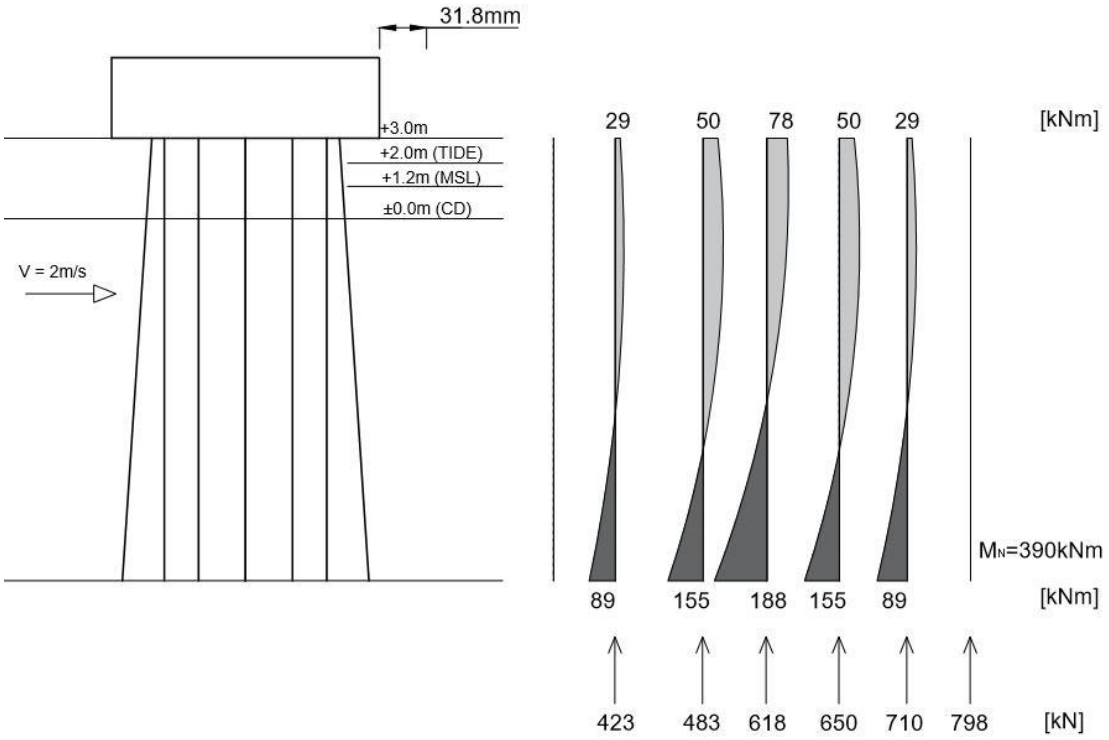

Figure 5.8 - Behavior of mooring dolphin supported by batter piles with rake 1:16

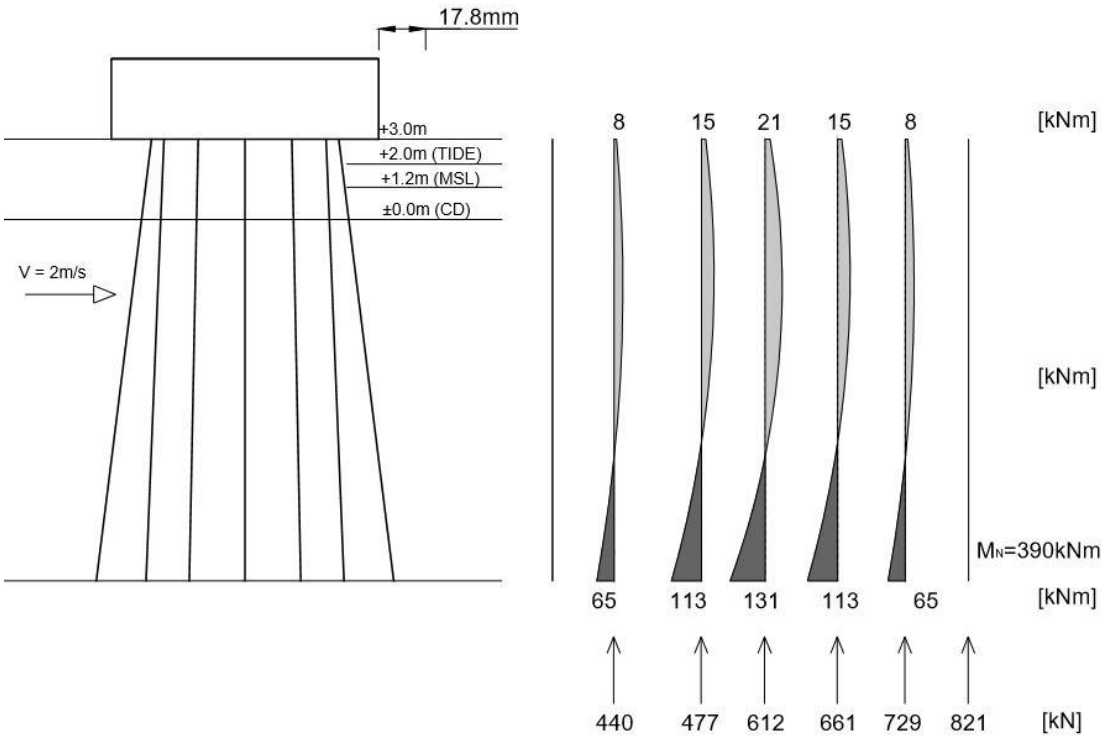

Figure 5.9 - Behavior of mooring dolphin supported by batter piles with rake 1:8

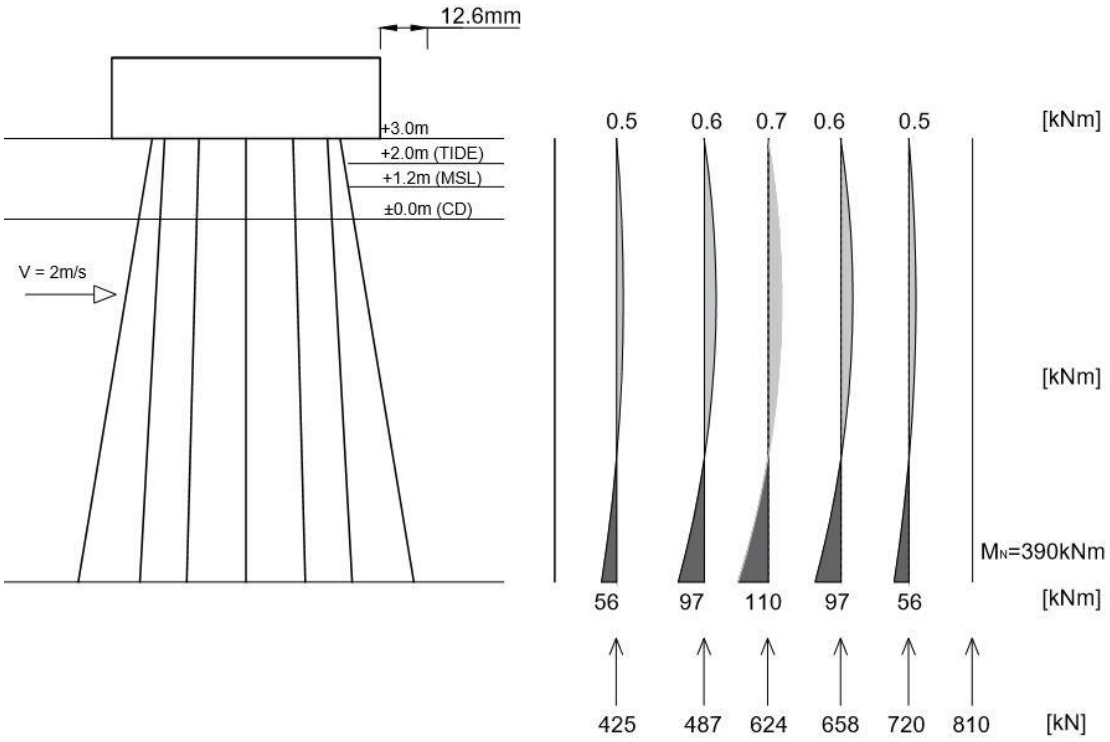

Figure 5.10 - Behavior of mooring dolphin supported by batter piles with batter rake 1:6

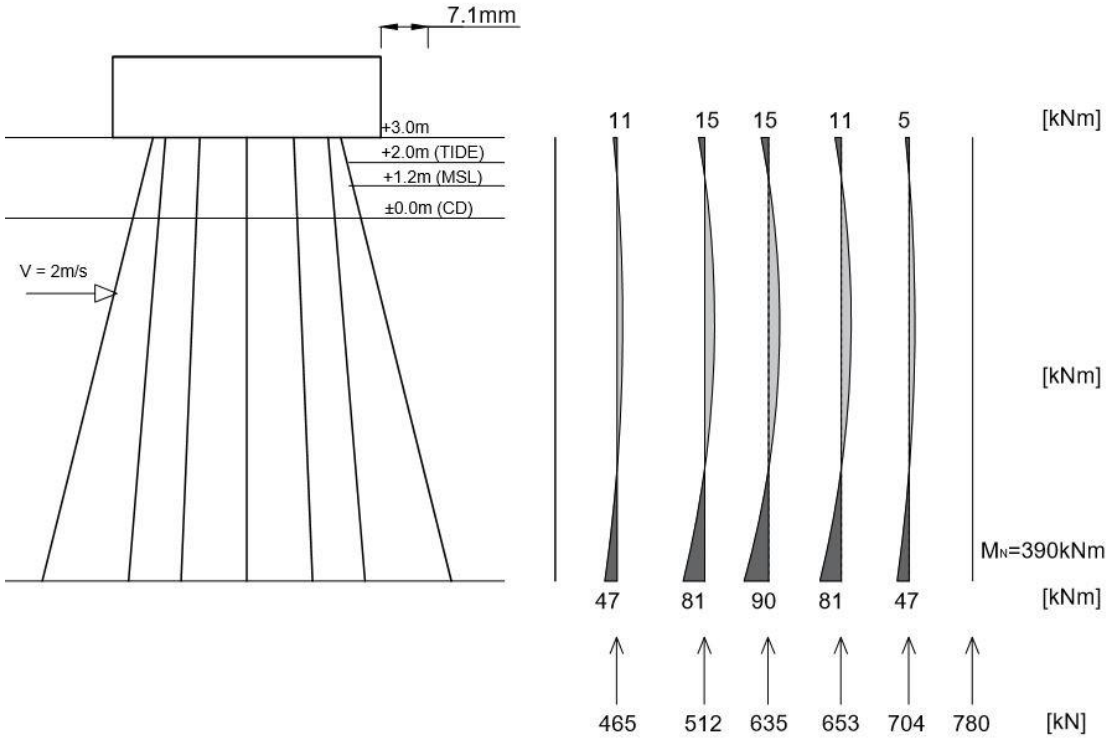

Figure 5.11 - Behavior of mooring dolphin supported by batter piles with batter rake 1:4

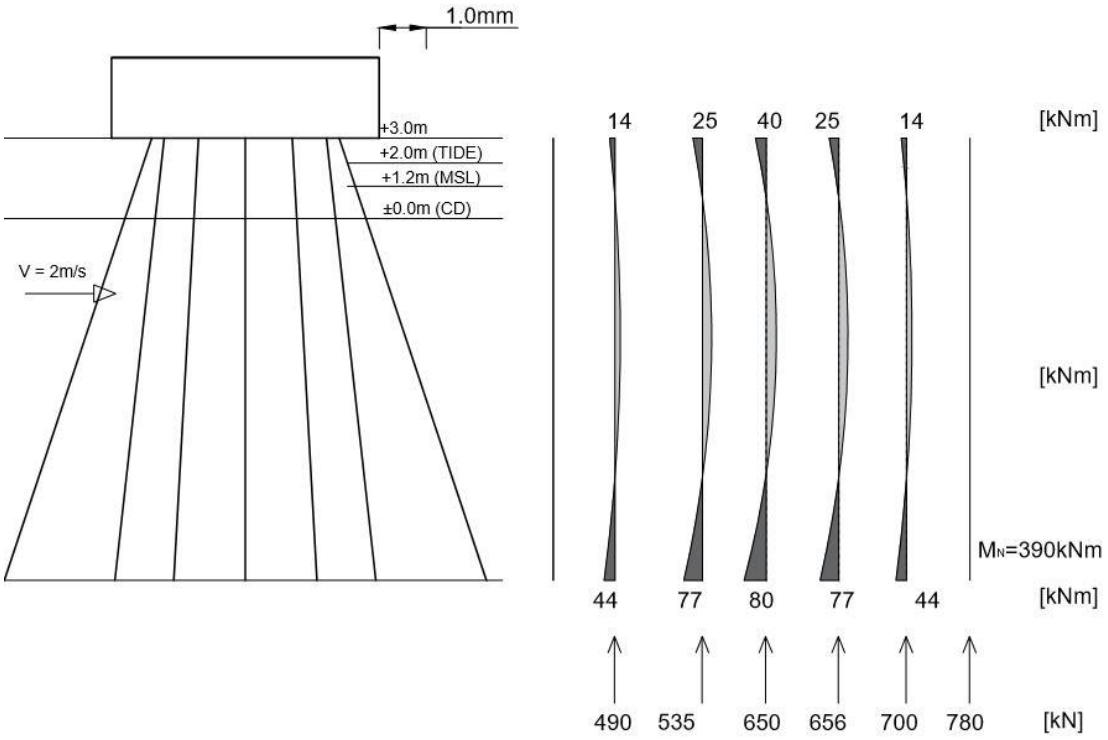

Figure 5.12 - Behavior of mooring dolphin supported by batter piles with batter rake 1:3

Table 5.1 – Axial force distribution in piles

Axial force [kN]							
Pile	-	Rake					
		1:32	1:16	1:8	1:6	1:4	1:3
1	-572.7	-472.7	-421.7	-411.9	-427.1	-461.6	-491.6
2	-574.0	-472.7	-421.7	-411.9	-427.1	-461.6	-491.6
3	-574.0	-499.6	-435.4	-422.7	-441.5	-483.5	-519.4
4	-577.5	-512.0	-482.9	-478.6	-488.9	-512.7	-535.6
5	-577.5	-512.0	-482.9	-478.6	-488.9	-512.7	-535.6
6	-582.3	-616.7	-617.5	-621.1	-624.8	-635.2	-649.4
7	-582.3	-616.7	-617.5	-621.1	-624.8	-635.2	-649.4
8	-587.2	-619.4	-650.0	-660.9	-657.5	-652.6	-655.9
9	-587.2	-619.4	-650.0	-660.9	-657.5	-652.6	-655.9
10	-590.7	-658.7	-711.2	-727.7	-719.2	-703.8	-699.9
11	-590.7	-658.7	-711.2	-727.7	-719.2	-703.8	-699.9
12	-592.0	-733.7	-799.6	-819.5	-808.1	-786.8	-779.4
Σ	-6988.0	-6992.288	-7001.486	-7042.8	-7084.4	-7202.1	-7363.6

It can be observed that increasing the rake increases the axial forces in the piles as showed in table 5.1. Highlighted are piles presented on the figures.

However the advantage of using batter piles is dramatic reduction in bending moment and displacement of the deck. It can be seen that for the case of mooring dolphin supported by batter piles with rake 1:3, maximum bending moment is reduced by 63% and displacement is reduced by 98%.

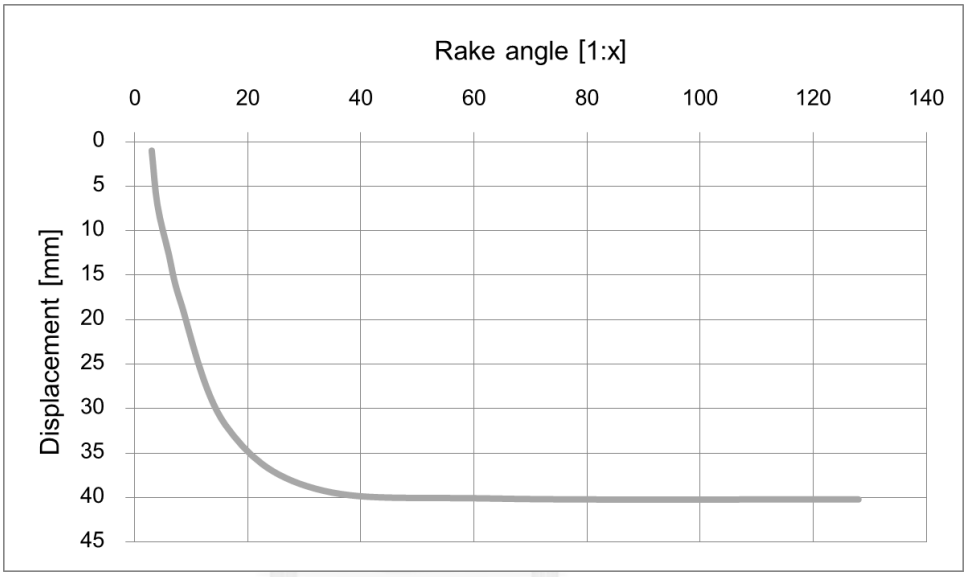

Figure 5.13 - Effect of rake angle on displacement on the structure

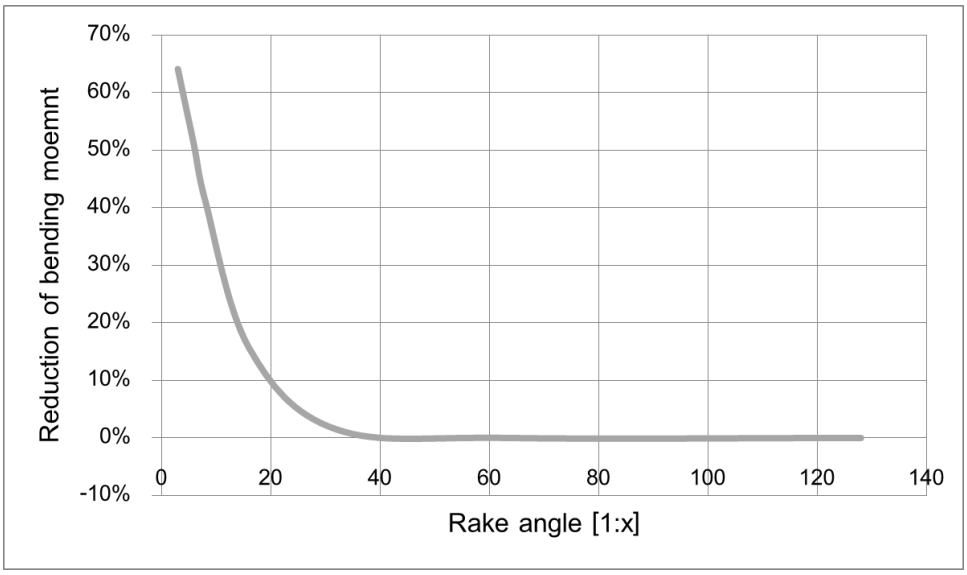

Figure 5.14 - Effect of rake angle on reduction of bending moment

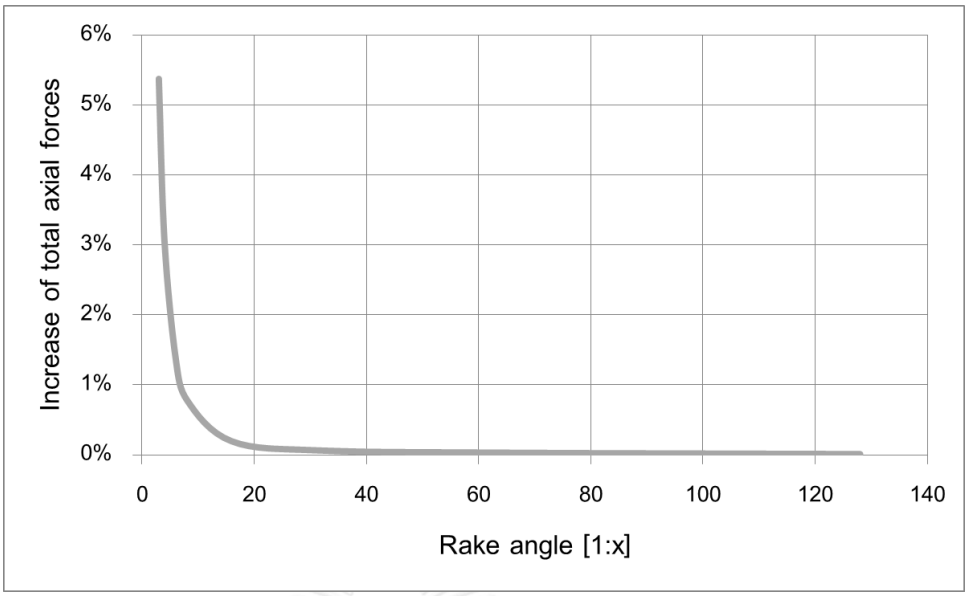

Figure 5.15 - Effect of rake angle on increase of total axial forces

Figures 5.13 5.14 and 5.15 present the effects of rake angle on the behavior of the structure. It can be observed that for rake higher than 1:20 the reduction effect dramatically increases. It should be noted, that the cost is increase in axial force. For the case of rakes from 1:8 to 1:3 an increase of maximum axial force is higher than 30%.

5.2.2. Loading platform with modified configuration

In this chapter effect of batter piles on the behavior of loading platform is studied. Batter piles are employed on the perimeter of the structure as presented in figure 5.8. Rake angle is varied in the analysis. Results for batter piles raked 1:8, 1:6 and 1:4 are reported. Tsunami and wave parameters are the same for all cases:

- Wave height = 1.0m
- Tsunami amplitude = 1.0m
- Tsunami flow velocity = 2m/s

Within one case, all piles experience similar bending moment in the support and in the pile-deck connection. Maximum values are reached in the batter piles which are first hit by the incoming wave. Piles located further from the wave experience lower bending moments. Distribution of axial force is different than for mooring dolphin. Maximum compressive force is experienced in the second pile.

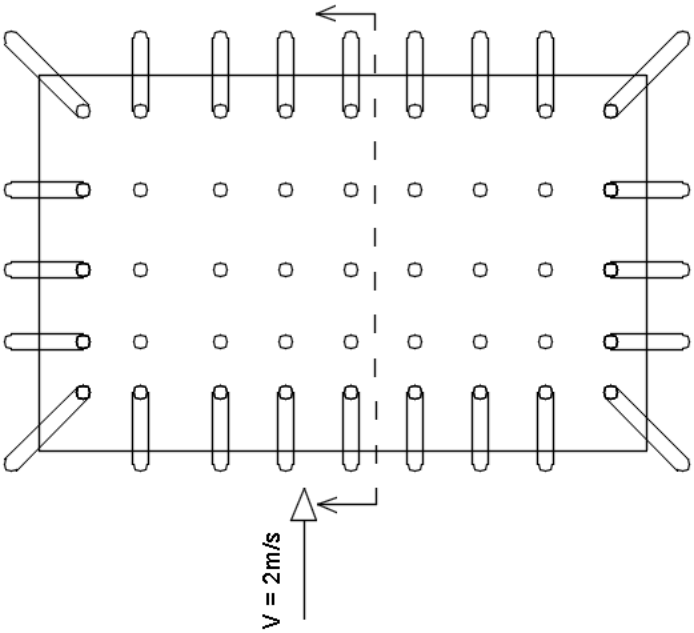

Figure 5.16 – Loading platform with batter piles cut location

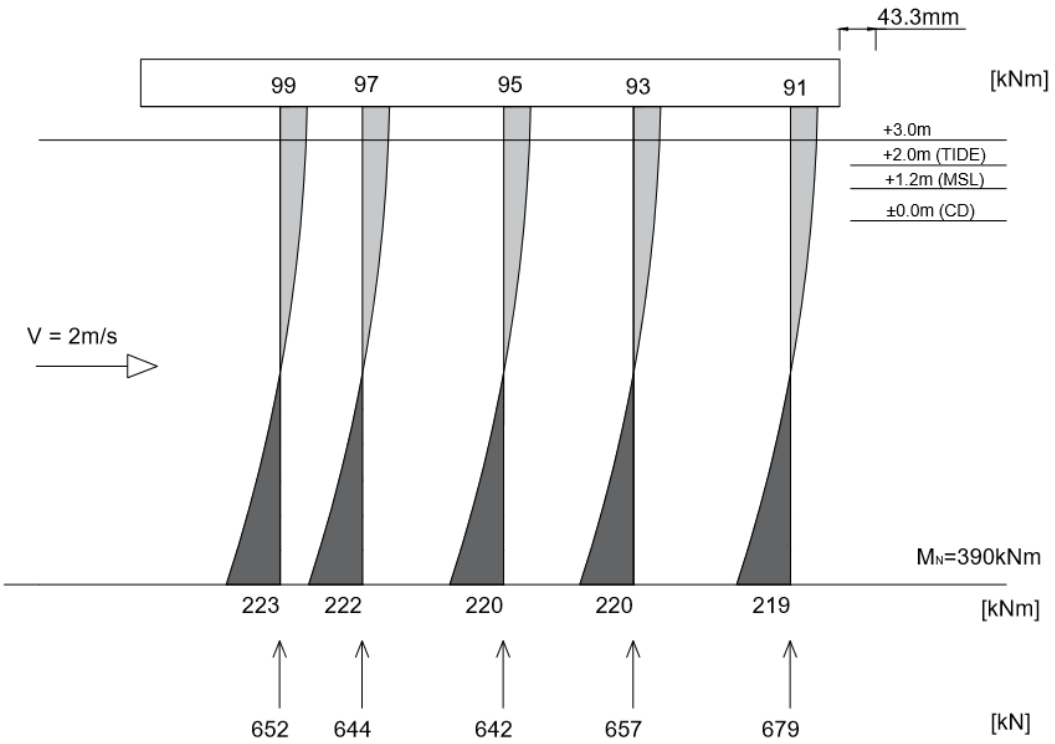

Figure 5.17 – Loading platform supported by vertical piles

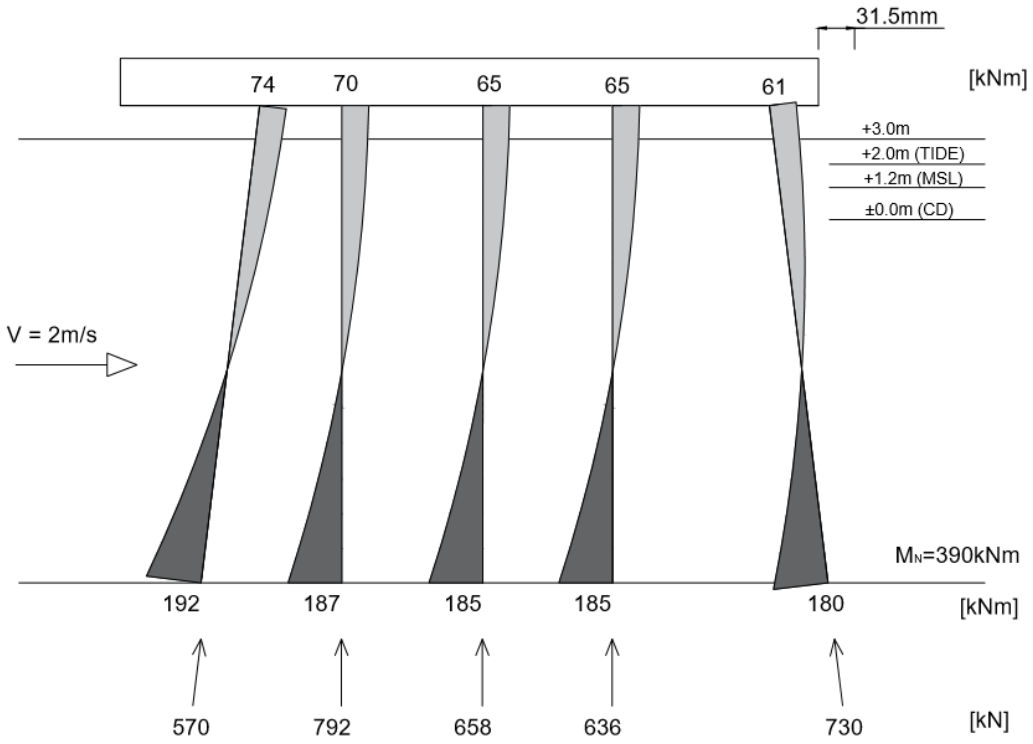

Figure 5.18 – Loading platform with batter piles raked 1:8

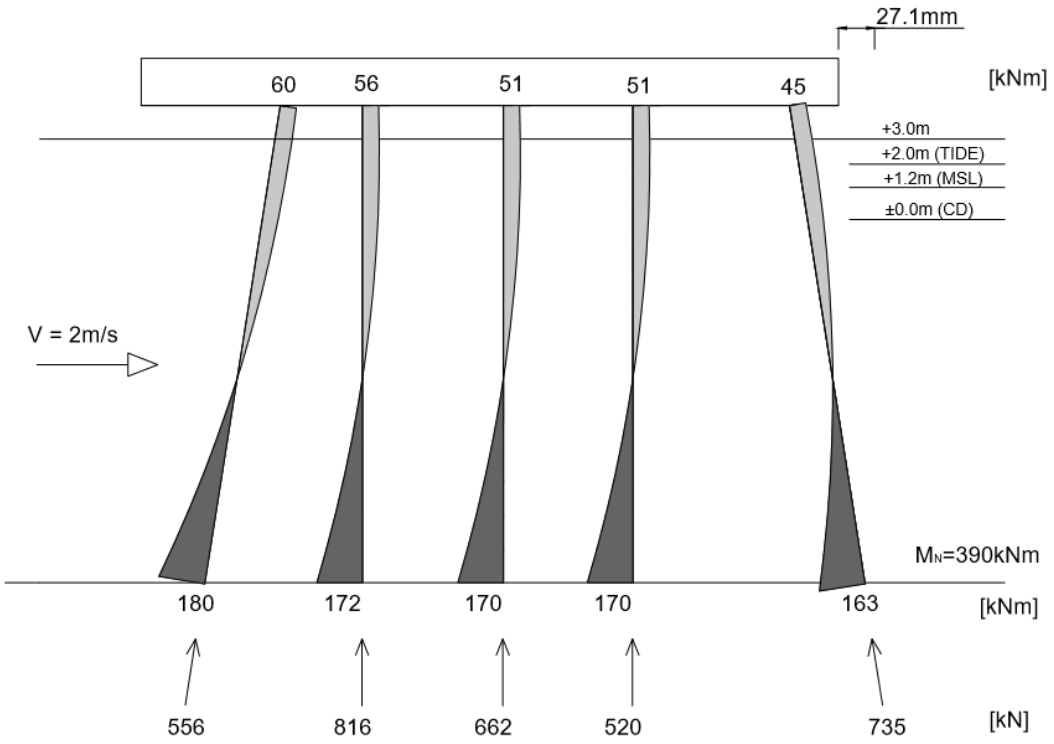

Figure 5.19 – Loading platform with batter piles raked 1:6

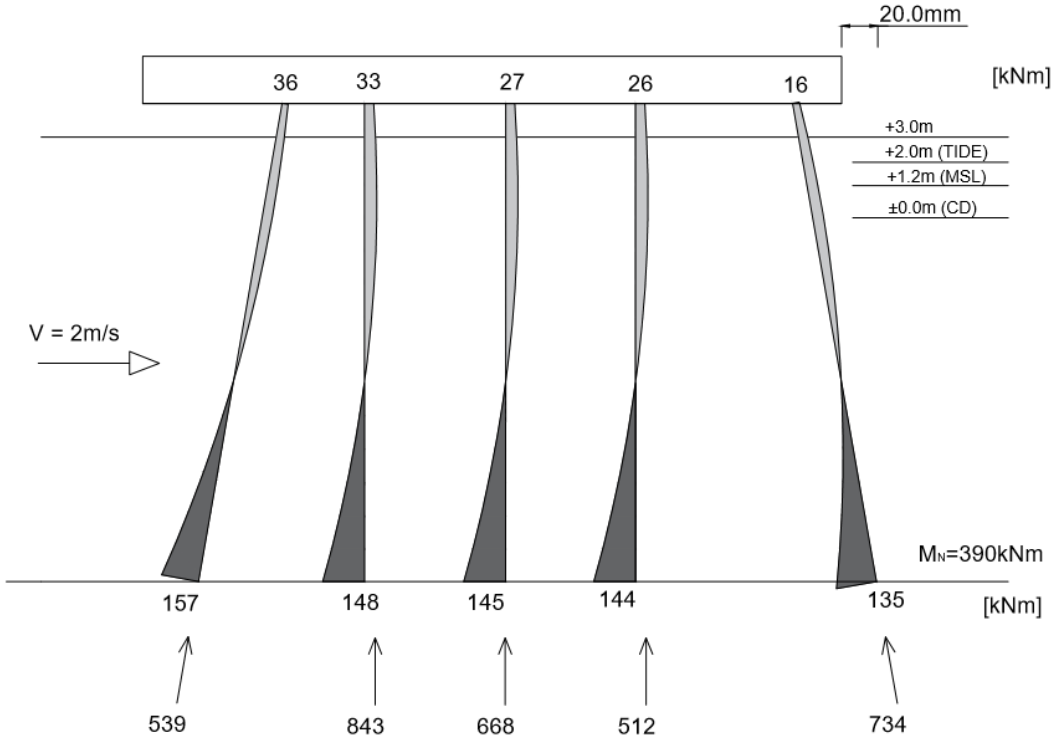

Figure 5.20 – Loading platform with batter piles raked 1:4

By comparing behavior of loading platform supported only by vertical piles and loading platform with pile configuration of both kind few conclusion can be made. Structure with batter piles experience lower displacement and bending moment values. However maximum axial forces increases. Table 5.3 presents effect of the rake angle.

Table 5.3 Effect of the rake angle on behavior of loading platform

Rake	Displacement [mm]	Reduction
Vertical piles	43.3	0%
8:1	31.5	27%
6:1	27.1	37%
4:1	20	54%
Rake	Maximum bending moment [kNm]	Reduction
Vertical piles	223	0%
8:1	192	14%
6:1	180	19%
4:1	157	30%
Rake	Maximum axial force [kN]	Increase
Vertical piles	-644	0%
8:1	-792	23%
6:1	-816	27%
4:1	-843	31%

5.3. Effect of point of fixity

In this research two types of seabed are considered: rock and clay. Type of seabed influence the effective pile length. Point of fixity for piles of structures founded on rock is on the seabed. For structures founded on the clay point of fixity for piles is located 8.5m below the seabed.

Figures 5.21 and 5.22 present structure of mooring dolphin with batter piles raked 1:4 fixed at seabed and 8.5m below the seabed respectively. It can be observed that for piles fixed below the seabed displacement is bigger by more than 100%. Bending moment values in the support increased by approximately 40%, however bending moment in the deck increased by more than 110%. Structure seems to be “locked”, because the bending moment diagram resembles the bending moment diagram of a beam fixed at both ends. Axial forces decreased in all piles.

Figures 5.23 and 5.24 present loading platform with batter piles raked 1:4 employed on the perimeter fixed at seabed and 8.5m below the seabed respectively. It can be observed that for piles fixed below the seabed displacement almost 3 times bigger. Bending moment values in the support increased by approximately 40%, however bending moment in the deck decreased by about 60%. Maximum axial forces increased and minimum axial forces decreased.

Soil condition is a factor which influences the point of fixity for piles and thus the effective pile lengths. As expected longer piles experienced higher deflection and bending moments in the support. An increase in the bending moment was approximately equal to 40% for two structures. For mooring dolphin axial forces decreased, however for loading platform both increase and decrease was observed.

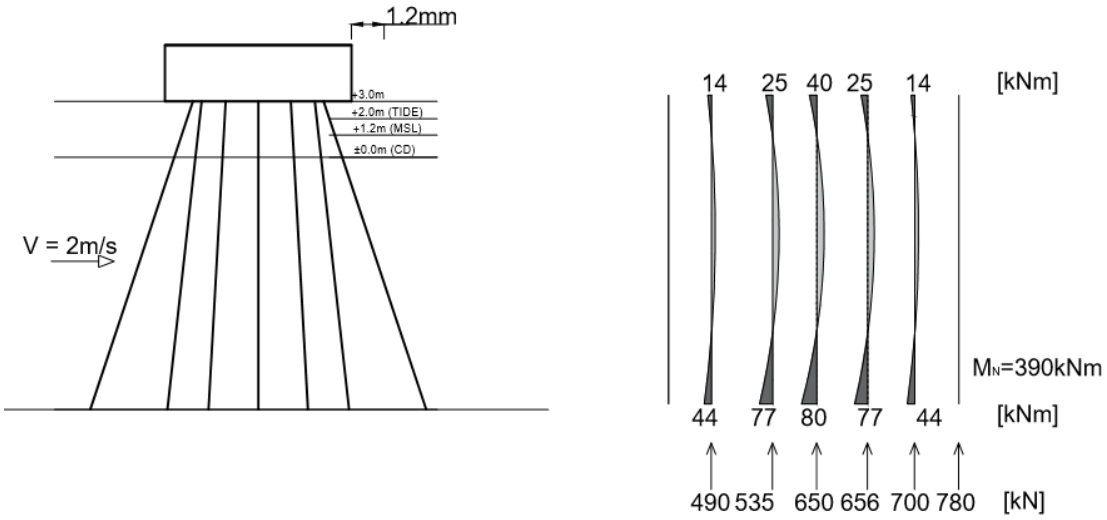

Figure 5.21 - Mooring dolphin with piles at seabed

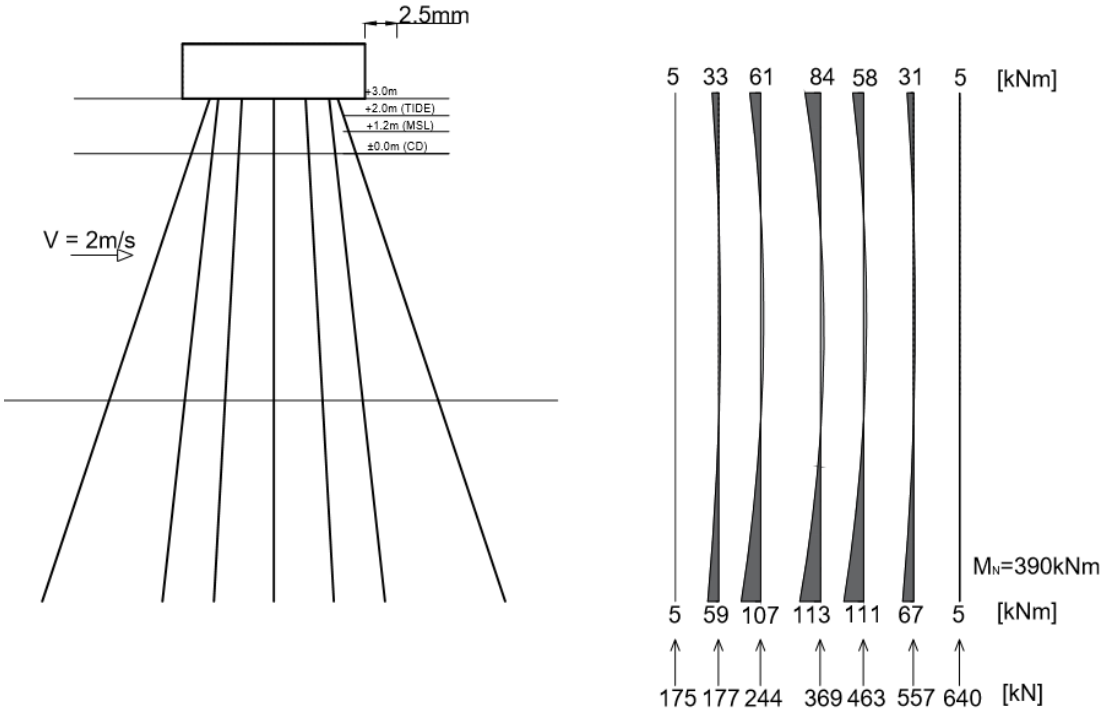

Figure 5.22 - Mooring dolphin with below the seabed

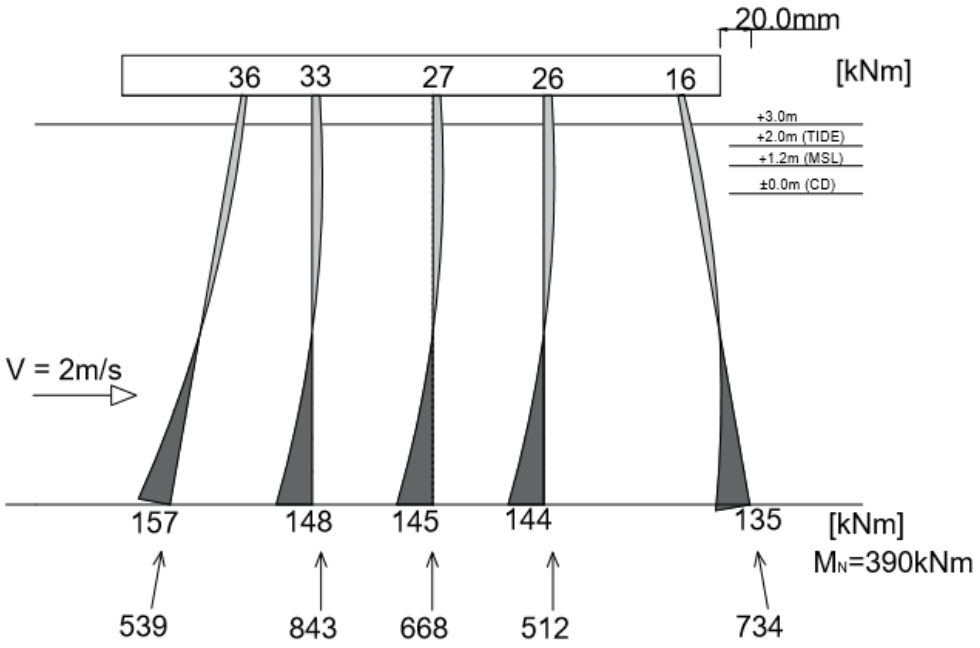

Figure 5.23 – Loading platform with piles fixed at seabed

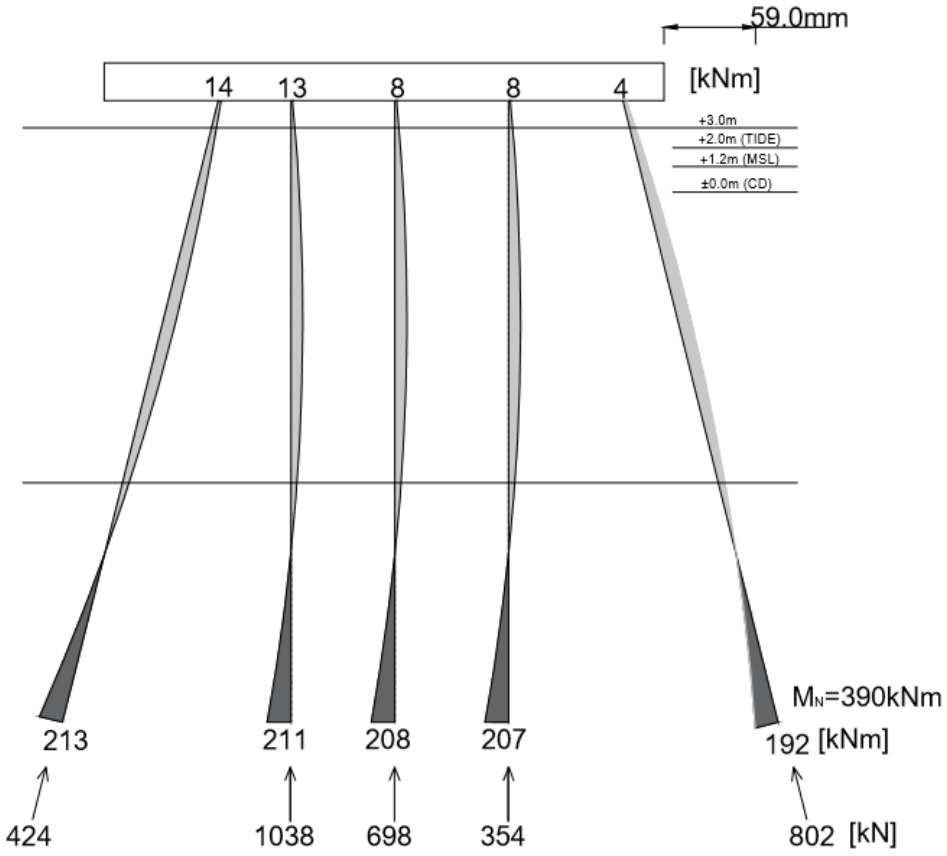

Figure 5.24 – Loading platform with piles fixed below seabed

5.4. Maximum top deck displacement along Y axis

Results discussed in this paragraph were measured for the tsunami of flow direction along axis Y. Generally analyzed port structures are parts of LNG terminal, located near shore, parallel to the seashore. In these cases waves flowing from the direction of open sea, along axis Y, are the most common. Since flow direction is assumed to be along axis Y, only maximum displacements along axis Y are shown. Two cases of seabed are considered. In the first case, piles are fixed at seabed, -13.5m. In the second case piles are fixed below the seabed, at previously calculated point of fixity equal to -22.0m.

On figures, by dashed line a lateral drift equal to $\frac{h}{100}$ and $\frac{h}{200}$ has been showed in order to visualize the magnitude of the displacement. In both cases h states for total height of the structure. For structures with rock seabed, the total height is equal to 19.5m thus the values are equal to 195mm and 97.5mm, respectively. For structures with piles founded on clay the total height of the structure is equal to 28m, and lateral drift values are equal to 280mm and 140mm.

Recommendations for limit displacement are as follow: for mooring dolphin 5% of pile diameter, for breasting dolphin up to 50% of pile diameter (rigid breasting dolphin may damage the boat), for loading platform displacement higher than h/100 may damage the equipment

5.4.1. Mooring Dolphin

For the structure of mooring dolphin, calculated point of fixity is 8.5m below the seabed. This leads to piles fixed at -22.0m and the total length of the pile equal to 26.4m. For the piles fixed at seabed, length is equal to 17.4m. It can be observed that even for longer piles displacements are negligible. The reason behind this is the pile configuration. All piles are battered at 3:1 ratio and employed in radial symmetry. The

effect of such configuration is that displacements are equal, independent of the wave flow direction.

Figure 5.25 presents maximum top deck displacement for considered cases. For piles fixed at seabed, maximum top deck displacement calculated for water level of 6.0m above MSL is equal to 13.7mm. For piles fixed below the seabed this value increases to 28.3mm

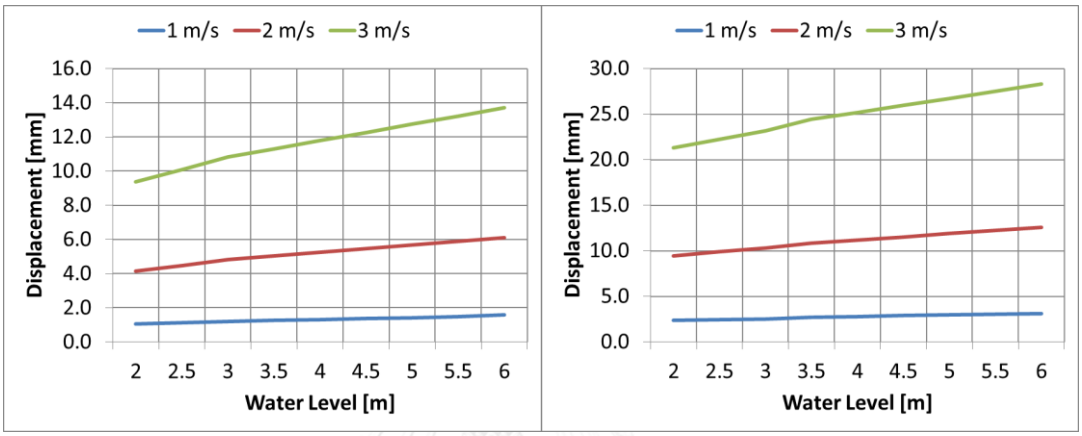

Figure 5.25 - Mooring dolphin - Maximum top deck displacement along axis Y for different velocities. Left: for piles fixed at seabed, Right:: for piles fixed at calculated fixity point below the seabed

5.4.2. Breasting Dolphin

For the structure of breasting dolphin, calculated point of fixity is 8.5m below the seabed. This leads to piles fixed at -22.0mMSL and the total length of the pile equal to 24.2m. For the piles fixed at seabed, length is equal to 16.1m.

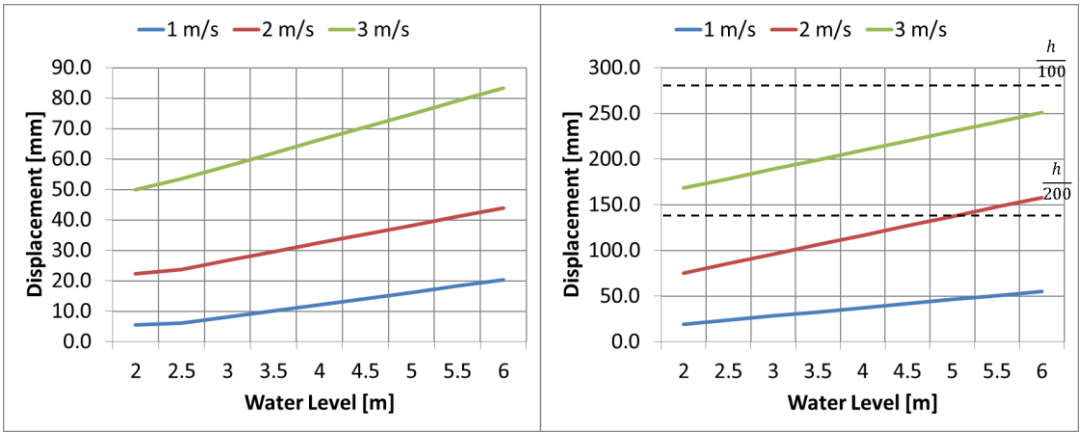

Figure 5.26 - Breasting dolphin - Maximum top deck displacement along axis Y for different velocities. Left: for piles fixed at seabed, Right: for piles fixed at calculated fixity point below the seabed

Figure 5.26 presents maximum top deck displacement for considered cases. Displacements of top deck of breasting dolphin are noticeable. For piles fixed at seabed, maximum displacements calculated for varying tsunami flow velocity are: 20.3mm, 43.9mm and 83.1mm respectively. For piles fixed at the point of fixity below the seabed these values change to 55.3mm, 158.0mm and 250.8mm. In this case uplift pressure acting on the batter piles creates additional displacement in Y direction. Due to this displacements along Y axis are increased and the correlation between forces and velocity is distorted. Battered piles are angled at 8:1 ratio and employed in partial symmetry. Due to that displacements along axis X and along axis Y are different, as discussed further in this chapter.

5.4.3. Loading Platform

For the structure of loading platform, calculated point of fixity is 8.5m below the seabed. This leads to piles fixed at -22.0mMSL and the total length of the pile equal to 26.25m. For the piles fixed at seabed, length is equal to 17.75m.

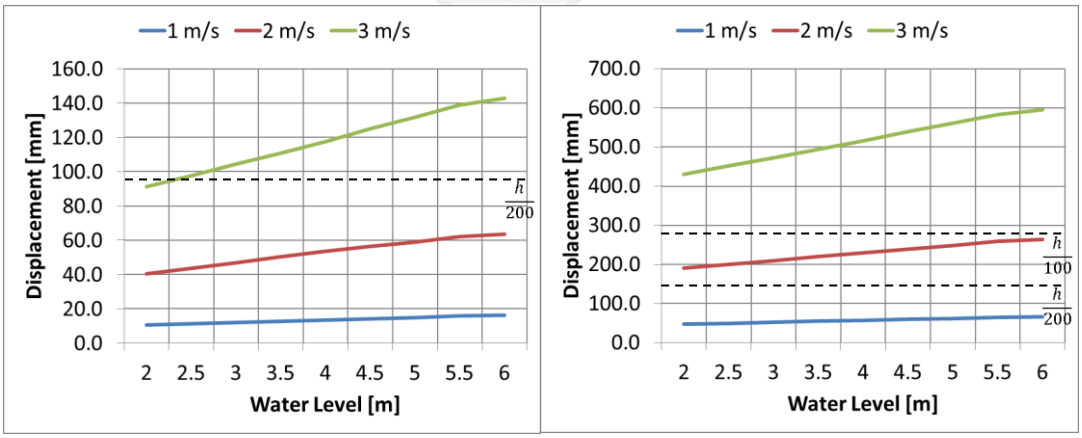

Figure 5.27 Loading platform - Maximum top deck displacement along axis Y for different velocities. Left: for piles fixed at seabed, Right: for piles fixed at calculated fixity point below the seabed

Figure 5.27 shows top deck displacements of loading platform. Loading platform is supported only on vertical piles. Due to that it does not have additional lateral resistance in any direction .Table 5.1 presents calculated values. Because of the lack of batter

piles lateral loads causes relatively big displacements. By changing the configuration of piles one can reduce the displacement in any direction.

Table 5.4- Top deck displacements along axis Y for loading platform

Water Level [m]	Tsunami flow velocity [m/s]	Displacement [mm]	
		Fixed at seabed	Fixed below seabed
6.00	1.00	16.1	65.9
	2.00	63.7	264.6
	3.00	142.9	595.2

5.5. Comparison of maximum top deck displacement between structures

In order to better understand different behavior of marine structures top deck displacements between mooring dolphin, breasting dolphin and loading platform are compared and discussed. Presented results were calculated for the tsunami of flow direction along axis X. Maximum displacements along axis X is taken as representative values. Due to negligible values of displacements along other axes, they are not presented. Similarly to previous paragraph two cases of pile length were studied.

Figure 5.28 presents comparison between top deck displacements for all analyzed structures. Left side of the figure is reserved for piles fixed at seabed, while right side shows displacement for structures with piles fixed below the seabed at the previously calculated point of fixity. From the top, results are presented for tsunami flow velocity of 1m /s, 2m/s and 3m/s respectively.

It can be observed that displacements of mooring dolphin are negligible when compared to deck displacements of other structures. In all cases displacement of deck of mooring dolphin caused by tsunami forces is small enough to don't treat it as decisive during design process.

For the case of breasting dolphin displacements start from small for low water levels and tsunami flow velocities and gradually increase to noticeable for water level equal to 6.0m above MSL and tsunami flow velocity equal to 3m/s. These values are additionally multiplied by increase of pile length. Maximum calculated value is equal to 165.4mm.

Top deck displacements of loading platform are relatively high for all cases. These values start from low numbers but rapidly increase with the worsening of condition. In the extreme case of analyzed loadings it is equal to 567.4mm, which is equal to $\frac{h}{51}$. Due to the magnitude of this value it is advised to change the pile configuration in order to reduce the displacement.

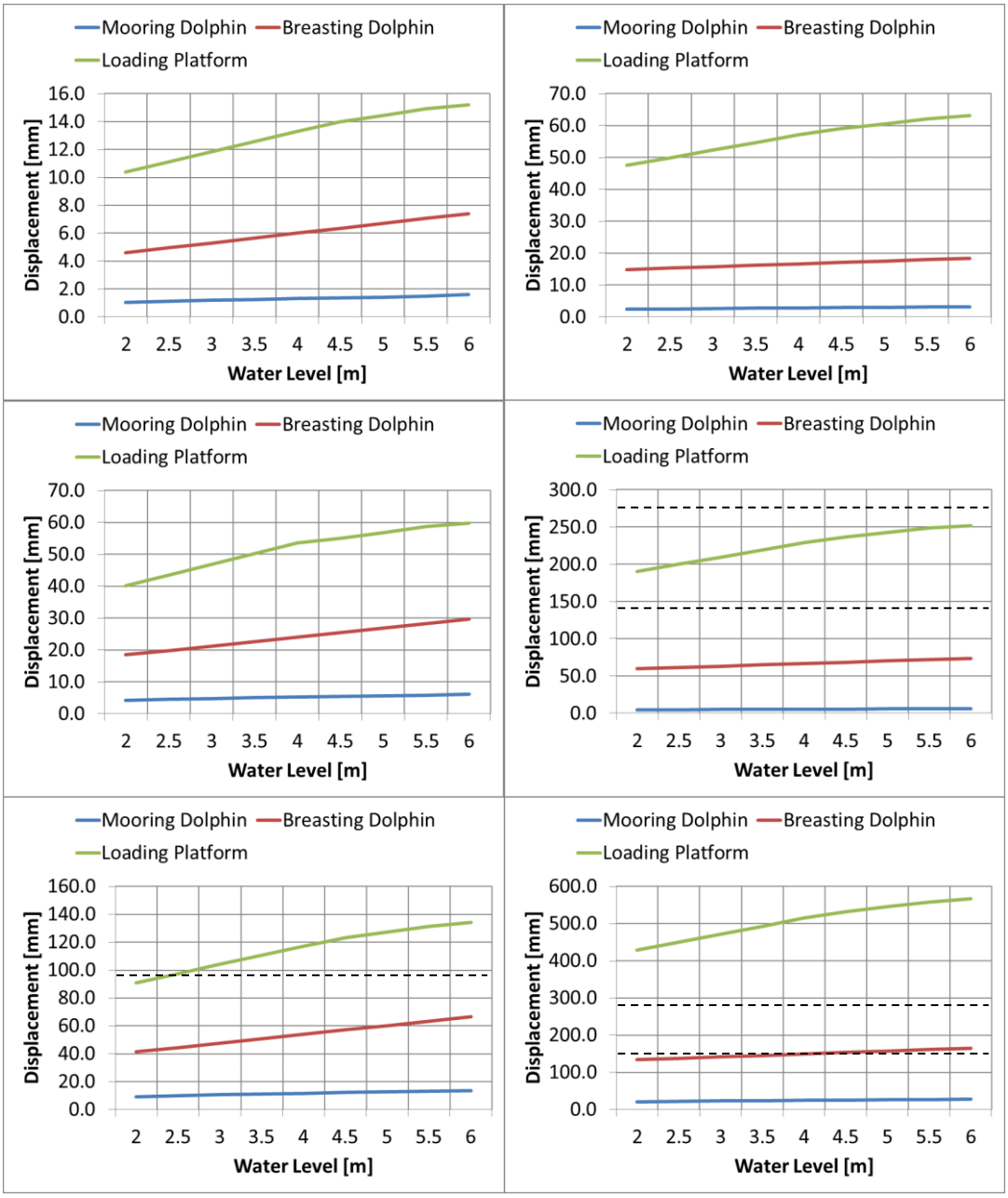

Figure 5.28 - Maximum top deck displacement along axis X for different structures for velocity equal to 1m/s, 2m/s, 3m/s respectively from the top. Left: for piles fixed at seabed, Right: for piles below the seabed

5.6. Comparison of maximum top deck displacement along both axes

Tsunami wave are unexpected events, which may be created in various processes. Due to that flow direction of such a wave is often unpredictable. This study analyzes displacement along both axes, X and Y. By comparing results in perpendicular directions one can tell which kind of tsunami would cause more devastating forces.

5.6.1. Mooring dolphin

Due to pile configuration of mooring dolphin results are identical in every direction, because of that these results are not showed in this chapter.

5.6.2. Loading platform

It can be observed that displacements along both directions are similar for both short and longer piles. This can be explained by the utilization of only vertical piles. The differences come from the geometry of the structure. For tsunami wave along axis X drag forces acting on the beams and slabs are smaller than in Y direction. Due to that and piles configuration, displacements along Y axis are bigger.

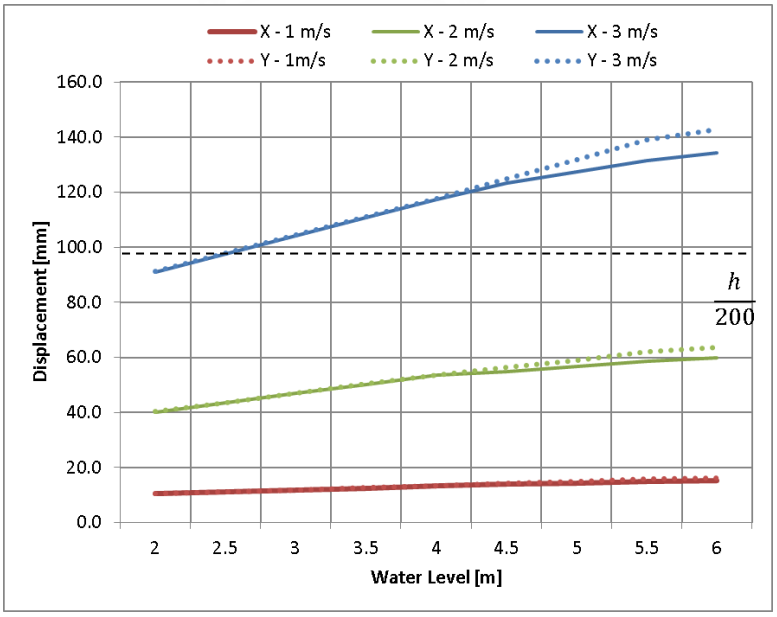

Figure 5.29 - Top deck displacement along axis X and Y for loading platform with piles fixed at seabed

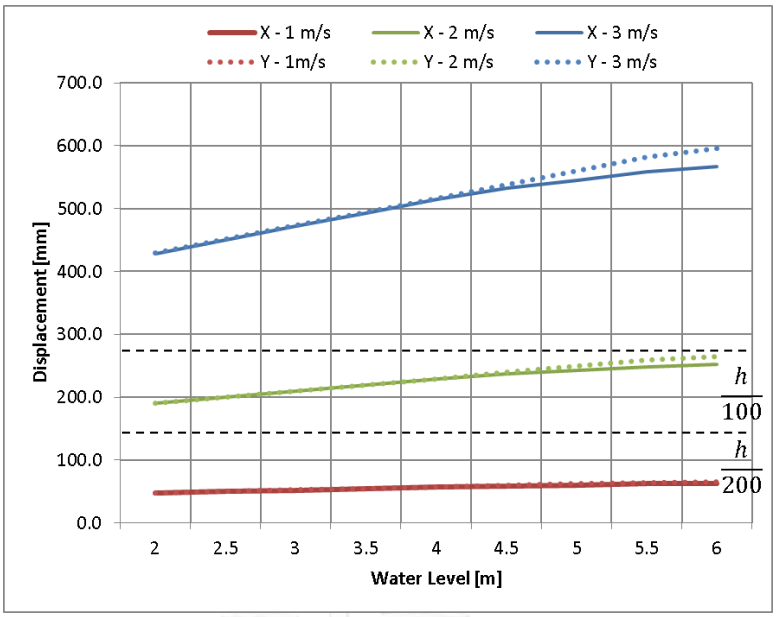

Figure 5.30 - Top deck displacement along axis X and Y for loading platform with piles fixed below seabed

5.6.3. Breasting dolphin

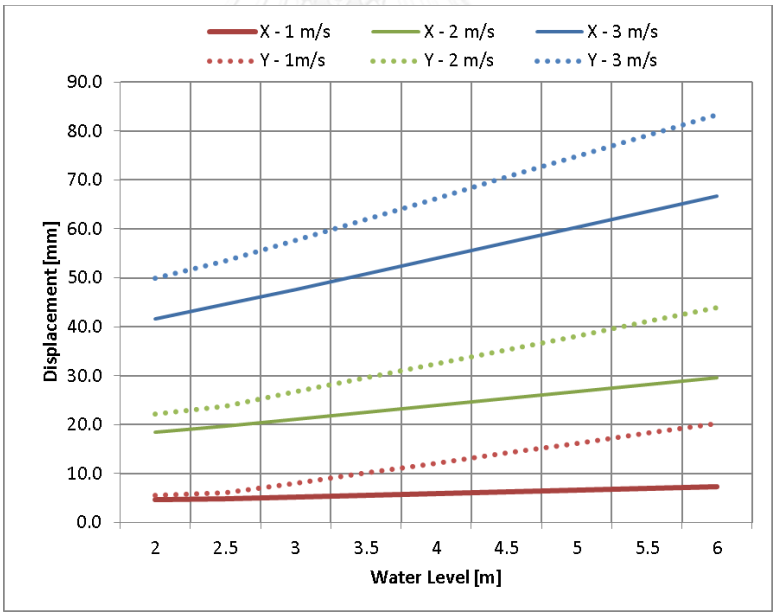

Figure 5.31 - Top deck displacement along axis X and Y for breasting dolphin with piles fixed at seabed

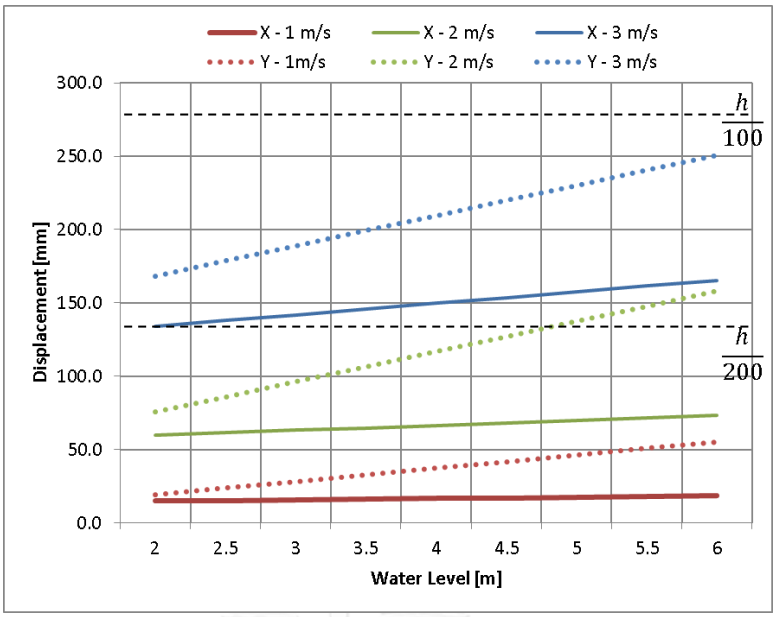

Figure 5.32 - Top deck displacement along axis X and Y for breasting dolphin with piles fixed at seabed

The differences in displacements along both axes are more visible than for other structures. Since piles are not employed symmetrically, tsunami wave along axis Y causes bigger displacements in this direction. Additionally, utilization of batter piles causes different responses than in other structures. Uplift pressure acting on the decks and piles causes displacement along Y direction, which increases displacements caused by drag forces. Due to that, relation between displacement and velocity is distorted and scaling of the values cannot be observed.

6. Conclusion

This study was conducted to investigate tsunami forces on port structures. Models of loading platform, breasting dolphin and mooring dolphin were simulated using SAP2000 software. Tsunami conditions, pile lengths and pile configurations were varied during the analysis. Displacements and forces were calculated for varying tsunami parameters. The dynamic effect of the wave was not taken into consideration. Due to that inertia forces were not taken into account. Although assumptions were made in order to simplify difficult nature of tsunami, forces and displacements caused by tsunami loading obtained in this research are little underestimated, however remained in the same order of magnitude. Since the goal of this research was to find the influence of piles configuration and tsunami parameters on response of port structures. Tsunami forces were calculated following guidelines by FEMA P-646 and British Standard. In addition, experiments by Iemura H. et al. (2007), Robertson L.H. et al. (2008) and Lau T.L. et al. (2010) were studied in order to better understand nature of tsunami forces.

Research showed that tsunami has complicated interaction with the pile-deck structures and pile configuration is a significant factor in behavior of the structure. Significance of pile configuration can be concluded:

1. Using batter piles dramatically reduces displacements and maximum bending moment values. For mooring dolphin, structure supported only by batter piles with rake 1:4, reduction of displacement was equal to 82% and reduction of maximum bending moment value equal to 60%. For structure of loading platform, supported by configuration of vertical and batter piles with rake 1:4 these values were equal to 53% and 26% respectively.
2. Structures with batter piles experience higher axial forces than structures with vertical piles. In all studied cases, increase in maximum axial force was over

30%. The overall sum of axial forces also increases. For rake 1:4, mooring dolphin experienced increase equal to 5%.

3. Increasing rake makes structure more rigid. For rake 1:6 bending moment starts to resemble bending moment of beam fixed at both ends. By further increasing this ratio to 1:4 and 1:3, it can be observed that moments in support and deck are similar. It can be assumed that further increasing this ratio would lead to "locking" of the structure, where displacement would be negligible and moments in support and deck identical.
4. Effective pile length is a significant factor, which effects maximum displacement and bending moment distribution. In studied case, by increasing effective pile from 16m to 24.5m all displacement increased by approximately 200-300%. Effective pile length depended on the point of fixity of the pile.

In addition, influence of tsunami parameters was investigated.

Tsunami amplitude changes the height of the structure subjected to tsunami forces and which forces should be taken into consideration. Once the height is close to the deck, uplift and additional forces should be simulated in order to obtain accurate results.

Tsunami flow velocity is a factor which has an effect on the magnitude of tsunami forces. In the analyzed models this parameter affected significantly the value of exerted tsunami drag force.

Tsunami flow direction has an impact on the response of the structure if the piles are not employed in radial symmetry. It changes which piles act in tension and compression, and influences values of bending moments.

It has been showed that tsunami waves exert forces which result in significant lateral movement of port structures. Even tsunami of low amplitude and flow velocity

may cause big displacement of the decks if structure has low lateral stiffness in the direction of tsunami flow. Although deck displacements caused by tsunami flow of 1 m/s can be negligible, those caused by 3 m/s and higher velocities are significant. In the analyzed cases, the biggest calculated displacement was equal to 567.4mm, for a structure of loading platform with a total height of 28m. In order to visualize the magnitude of this displacement one can compare it to seismic limit drift equal to h/200, where h is total height of the structure. In analyzed case displacement of the deck of loading platform exceeded this limit. It should be noted, that tsunami waves analyzed in this study were not extreme as those which happened in the recent years such as 2011 Tohoku earthquake and tsunami.

REFERENCES

1. Tsutsumi, A., et al., *Nearshore flow velocity of Southwest Hokkaido earthquake tsunami.* Journal of waterway, port, coastal, and ocean engineering, 2000. 126(3): p. 136-143.
2. Thoresen, C.A., *Port Designer's Handbook: Recommendations and Guidelines*. 2003: Thomas Telford.
3. Saatcioglu, M., A. Ghobarah, and I. Nistor, *Performance of structures in Indonesia during the December 2004 great Sumatra earthquake and Indian Ocean tsunami.* Earthquake Spectra, 2006. 22(S3): p. 295-319.
4. Tobita, T., et al., *Reconnaissance report of the 2004 great sumatra-andaman, Indonesia, Earthquake: Damage to geotechnical works in Banda Aceh and Meulaboh.* 2006.
5. Tomita, T., et al., *Damage caused by the 2004 Indian Ocean tsunami on the southwestern coast of Sri Lanka.* Coastal Engineering Journal, 2006. 48(02): p. 99-116.
6. IEMURA, H., et al., *Experiments of tsunami force acting on bridge models.* 地震工学論文集, 2007. 29(0): p. 902-911.
7. Gerolymos, N., et al., *Evidence of beneficial role of inclined piles: observations and summary of numerical analyses.* Bulletin of Earthquake Engineering, 2008. 6(4): p. 705-722.
8. Robertson, I., H. Riggs, and A. Mohamed. *Experimental results of tsunami bore forces on structures*. in *ASME 2008 27th International Conference on Offshore Mechanics and Arctic Engineering*. 2008. American Society of Mechanical Engineers.
9. Mondal, G. and D.C. Rai, *Performance of harbour structures in Andaman Islands during 2004 Sumatra earthquake.* Engineering Structures, 2008. 30(1): p. 174-182.

10. Lukkunaprasit, P. and A. Ruangrassamee, *Building damage in Thailand in the 2004 Indian Ocean tsunami and clues for tsunami-resistant design.* The IES Journal Part A: Civil & Structural Engineering, 2008. 1(1): p. 17-30.

11. Ruangrassamee, A. and N. Saelem, *Effect of Tsunamis generated in the Manila Trench on the Gulf of Thailand.* Journal of Asian Earth Sciences, 2009. 36(1): p. 56-66.

12. Dao, M.H., et al., *Tsunami propagation scenarios in the South China Sea.* Journal of Asian Earth Sciences, 2009. 36(1): p. 67-73.

13. Matsutomi, H. and K. Okamoto, *Inundation flow velocity of tsunami on land.* Island Arc, 2010. 19(3): p. 443-457.

14. Lau, T.L., et al., *Performance of bridges with solid and perforated parapets in resisting tsunami attacks.* Journal of Earthquake and Tsunami, 2010. 4(02): p. 95-104.

15. Giannakou, A., et al., *Seismic behavior of batter piles: elastic response.* Journal of Geotechnical and Geoenvironmental Engineering, 2010. 136(9): p. 1187-1199.

16. Honda, K. and T. Tomita. *Damage to Port Facilities by the 2011 off the Pacific Coast of Tohoku Earthquake Tsunami*. in *The Twenty-fourth International Ocean and Polar Engineering Conference*. 2014. International Society of Offshore and Polar Engineers.

17. Mikami, T. and T. Takabatake. *Evaluating Tsunami Risk and Vulnerability Along the Vietnamese Coast*. in *Elsevier Inc.* 2014.

18. Lynett, P.J., et al., *Assessment of the tsunami - induced current hazard.* Geophysical Research Letters, 2014. 41(6): p. 2048-2055.

19. Muhari, A., et al., *Assessment of tsunami hazards in ports and their impact on marine vessels derived from tsunami models and the observed damage data.* Natural Hazards, 2015. 78(2): p. 1309-1328.

20. *FEMA P-646: Guidelines for Design of Structures for vertical Evacuation from Tsunamis*. April 2012

APPENDIX

VITA